DISSERTATION

OPIOID MODULATION OF INTRINSICALLY PHOTOSENSITIVE RETINAL GANGLION CELLS

Submitted by

Allison Marie Cleymaet

Department of Clinical Sciences

In partial fulfillment of the requirements

For the Degree of Doctor of Philosophy

Colorado State University

Fort Collins, Colorado

Summer 2019

Doctoral Committee:

Advisor: Cynthia Powell
Co-Advisor: Jozsef Vigh

Michala de Linde Henriksen
Shane Hentges

ABSTRACT

OPIOID MODULATION OF INTRINSICALLY PHOTOSENSITIVE RETINAL GANGLION CELLS

Widespread opioid use and abuse has resulted in an opioid epidemic in the United States and worldwide. Among several adverse effects of this drug class, opioids disrupt the sleep/wake cycle. While sleep induction and regulation is complex, and opioid receptors are known to be located in central sleep regulatory nuclei, it has not been specifically studied if opioids affect photoentrainment of circadian rhythm and thus the sleep/wake cycle. Intrinsically photosensitive retinal ganglion cells (ipRGCs) are the exclusive conduits for non-image forming visual functions, such as the aforementioned photoentrainment of systemic circadian rhythms, including the drive to sleep, and the pupillary light reflex (PLR). Systemically applied opioids cross the tight blood/retina barrier and thereby might alter the activity of retinal neurons. It has been recently shown that ipRGCs express μ-opioid receptors (MORs) and exogenously applied opioids inhibit the firing of ipRGCs. The current work aimed to identify the mechanism by which opioids inhibit ipRGC firing as well as downstream behavioral consequence of such inhibition at the organism level, specifically as manifested by modulation of PLR.

Through the use of transgenic mice, electrophysiology including multi-electrode array recordings and patch clamp in whole and dissociated retinas, and immunohistochemistry, we have documented the following: (1) In the rodent retina M1-M3 types of intrinsically photosensitive ganglion cells (ipRGCs) express μ-opioid receptors (MORs). (2) Light-evoked firing of ipRGCs is attenuated by the MOR-specific agonist DAMGO in a dose-dependent

manner. (3) MOR activation reduces ipRGC excitability by modulating I_K and reducing the amplitude of non-inactivating I_{Ca}.

Additionally, we explored the effect of modulation of ipRGC signaling via MORs on the murine PLR using transgenic mice and pupillometry. Our main findings were: (1) In WT mice but not in systemic μ-opioid receptor knockout mice (MKO) or mice in which μ-opioid receptors were selectively knocked out of ipRGCs alone (McKO), intraocular application of the MOR selective agonist DAMGO strongly inhibited rod/cone driven PLR and slowed melanopsin-driven PLR. (2) Intraocular application of a MOR selective antagonist CTAP enhanced rod/cone driven PLR in the dark-adapted retina and melanopsin driven PLR under photopic conditions in WT mice.

In summary, these results identify both a novel site of action, MORs on ipRGCs, and a mechanistic description of a novel neural pathway by which exogenous and potentially endogenous opioids might alter light driven behavior, including the PLR, which may serve as a biomarker of systemic opioid effect.

ACKNOWLEDGEMENTS

I thank my mentors, friends, and family for their support during this work.

TABLE OF CONTENTS

CHAPTER 1. INTRODUCTION

1.1 Overview

Widespread opioid use and abuse has resulted in an opioid epidemic in the United States and worldwide. Over fifty-eight percent of Americans were prescribed opioids in 2017 (Centers for Disease Control and Prevention, 2018). In 2016, 11.8 million people misused prescription opioids and/or heroin (Substance Abuse and Mental Health Services Administration, 2017). Among several adverse effects of this drug class, opioids disrupt the sleep/wake cycle (Angarita et al., 2016).

An organism's sleep/wake cycle is set in part by its circadian clock. The circadian clock is a biological clock, located in the brain's suprachiasmatic nucleus (SCN), which controls the body's homeostatic functions. These functions, which include sleep drive, are synchronized with environmental day-night cycles through a process called photoentrainment. Without external environmental cues, an organism's clock will free run, and the cycle of sleep/wake will run longer or shorter than a 24 hour period, depending on the species (Purves et al., 2001). A specific class of retinal cells, the intrinsically photosensitive retinal ganglion cells (ipRGCs), project to the SCN and are exclusively responsible for photoentrainment of circadian rhythms (Foster et al., 1991; Güler et al., 2008; Hatori et al., 2008; Tsai et al., 2009). Projections downstream of the SCN promote the production of melatonin from the pineal gland, which in turn modulates brainstem circuits that determine the sleep/wake state (Moore, 1995; Purves et al., 2001).

While sleep induction and regulation is complex, and opioid receptors are known to be located in central sleep regulatory nuclei (Korf et al., 1974; Pert et al., 1976; Aghajanian et al., 1977; Bird and Kuhar, 1977; Pivik et al., 1977; Simantov et al., 1977; Aghajanian, 1978; Young

et al., 1978; Lydic et al., 1993; Cronin et al., 1995; Nelson et al., 2009), it has not been specifically studied if opioids affect photoentrainment of circadian rhythm and thus the sleep/wake cycle. However, it has been recently shown that ipRGCs express μ-opioid receptors (MORs) and exogenously applied opioids inhibit the firing of ipRGCs (Gallagher, 2013). The current work aimed to identify the mechanism by which opioids inhibit ipRGC firing as well as the downstream simple behavioral consequences of such inhibition at the organism level, specifically as manifested by modulation of the pupillary light response (PLR).

This section reviews: (1) intrinsically photosensitive retinal ganglion cells; (2) ipRGCs and their roles in non-image forming vision; and (3) opioids and the retina.

1.2 Intrinsically photosensitive retinal ganglion cells

Light is processed by two functionally distinct systems within the mammalian CNS: (1) an image forming visual system and (2) a non-image forming visual system, which detects environmental irradiance (Foster, 1998). Intrinsically photosensitive retinal ganglion cells (ipRGCs) are a subset of the general retinal ganglion cell (RGC) population, comprising 1-5% of the murine RGC population (Sand et al., 2012). These cells are so named because they serve as photoreceptors, capable of responding to light using an intrinsic phototransduction cascade mediated by the photopigment melanopsin without synaptic input from classical photoreceptors, i.e. rods and cones (Takahashi et al., 1984; Lucas et al., 2001; Berson et al., 2002; Hattar et al., 2002).

ipRGCs critically mediate non-image forming visual functions. ipRGCs project to the olivary pretectal nucleus (OPN) (Hattar et al., 2002, 2006; Baver et al., 2008) and as such are responsible for the PLR, with PLR maintained in mice lacking rods and cones (Lucas et al., 2001). ipRGCs also project to brain regions implicated in circadian photoentrainment, namely

the suprachiasmatic nucleus (SCN), intergeniculate leaflet (IGL), and ventral lateral geniculate nucleus (vLGN) (Harrington, 1997; Hattar et al., 2002; Baver et al., 2008). ipRGCs are exclusively responsible for photoentrainment of circadian rhythms, i.e. the synchronization of an organism's internal circadian time with the solar day. Phase adjustment of circadian rhythms represents a mechanism by which light can indirectly affect sleep. Loss of classical photoreceptors has no negative impact on photoentrainment (Foster et al., 1991; Freedman et al., 1999), while bilateral enucleation of such rodless / coneless mice eliminates circadian response to light (Foster et al., 1991). Ablation of ipRGCs using diphtheria toxin permits maintenance of image forming visual functions but not non-image forming visual functions including photoentrainment of circadian rhythms and PLR (Altimus et al., 2008; Güler et al., 2008; Hatori et al., 2008).

However, in melanopsin knock out (KO) mice where the ipRGCs' intrinsic phototransduction cascade is absent, the ipRGCs themselves continue to serve as conduits for classical photoreceptor mediated photoentrainment of circadian rhythms (Altimus et al., 2008). Does this render intrinsic melanopsin signaling in ipRGCs an unnecessary redundancy? No. The intrinsic melanopsin mediated phototransduction cascade makes specific contributions to sleep / wake induction, sleep modulation, and the PLR.

In addition to indirect mechanisms of sleep state modulation, light can directly modulate sleep state through circadian independent nonvisual mechanisms. Acute pulses of light and dark respectively induce sleep and wakefulness in the nocturnal mouse; this is referred to as negative vs. positive masking. In mice lacking ipRGCs, negative and positive masking were absent. In melanopsin KO mice, negative masking was present but less than in wild type (WT) mice and positive masking was entirely absent. In mice lacking functional rods/cones, negative and

positive masking were present but less than in WT mice. This indicates that both classical and melanopsin-mediated photoreception is required for light levels to have their full modulatory effect on the sleep/wake state, and that this effect is mediated via the conduit of ipRGCs. Further, that positive masking requires the ipRGC as conduit as well melanopsin-mediated phototransduction suggests that dark pulse mediated waking requires a reduction of ipRGC signaling and not an OFF signal from classical photoreceptors (Altimus et al., 2008). Similar findings in melanopsin KO mice were reported by Tsai et. al. in 2009; light-induced c-fos immunoreactivity, which serves as a marker for neuronal activity (Bullitt, 1990), is increased in the ipRGC target areas of the SCN and the VLPO in WT but reduced in melanopsin KOs, confirming both sleep-regulatory structures as central targets for melanopsin-mediated effects on sleep. In addition to altered acute effects of light on sleep, melanopsin KOs also demonstrated decreased total sleep time and a paradoxical decrease in sleep need, supporting an additional role for melanopsin in regulation of sleep homeostasis and thereby both sleep quality and initiation (Tsai et al., 2009).

Melanopsin is also important for achieving the PLR in response to a full range of lighting conditions. Full miosis at high irradiances is lost in melanopsin KO mice (Lucas et al., 2003). Furthermore, very few ipRGCs are necessary for this reflex, with only 17% of ipRGCs necessary for maximal miosis in response to high irradiances subsequent to partial ablation of ipRGCs with diphtheria toxin. Similarly, < 1% of ipRGCs are necessary to evoke some degree of PLR (Güler et al., 2008).

In addition to non-image forming vision, ipRGCs are also known to have distinct roles in image forming vision, such as contrast sensitivity (Schmidt et al., 2014a) and light avoidance

behavior (Johnson et al., 2010); however, a detailed description of such functions are beyond the scope of this dissertation.

1.2.1 ipRGC subtypes

There are 6 major ipRGC subtypes, M1-M6, which are morphologically classified by their dendritic ramification in specific layers of the inner plexiform layer (IPL), Fig. 1.1. The IPL

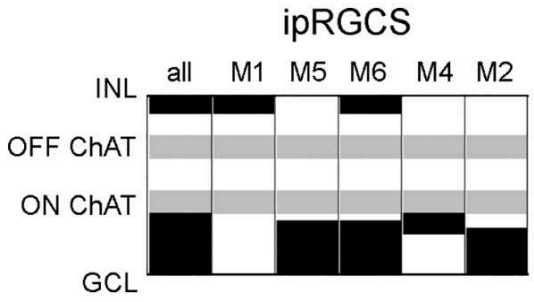

Figure 1.1 Dendritic stratification of the six ipRGC subtypes in the inner plexiform layer (IPL). The sublaminae of the IPL are delineated by the OFF and ON choline acetyltransferase (ChAT) immunoreactive bands, respectively corresponding to the OFF and ON sublaminae in which the ipRGC dendrites stratify. M1 ipRGCs stratify distal to / above the OFF ChAT band; M2, M4, and M5s stratify proximal to / below the ON ChAT band; and M6 stratify in both sublaminae. Of note is that the M3 ipRGCs mimic M6 stratification and as such are not listed in the above figure. INL: inner nuclear layer. GCL: ganglion cell layer. (adapted from Quattrochi 2019, with permission from John Wiley and Sons, License 4574910504365).

contains the synapses of the second and third order neurons of the visual pathway, i.e. bipolar cells (BCs) and retinal ganglion cells (RGCs), and is divided into functionally distinct sublaminae, the ON (inner three) and OFF (outer two) sublaminae. These are so named because those BCs which depolarize in response to light, the ON BCs, and those which hyperpolarize in response to light, the OFF BCs, synapse accordingly with ON and OFF RGCs in the respectively named sublaminae of the IPL, the ON BCs with shorts axons and the OFF BCs with long axons. ON and OFF RGCs are those ganglion cells which fire when the stimulus is brighter or darker than background, respectively (Wässle, 2004; Kolb et al., 2007).

M1 ipRGCs stratify in the OFF sublamina and M2s in the ON sublamina. The M2s have large soma, which at 15 μm on average are slightly larger than those of the M1s, with a mean of 13 μm. Similarly, the dendritic arborizations of the M1s are slightly smaller and less branched

than those of the M2s, averaging 275 μm and 310 μm respectively (Berson et al., 2002, 2010). Functionally, M1 cells demonstrate ~ 10 fold higher light sensitivity and higher maximal light responses than M2s, with M1s having a more depolarized V_m, higher input resistance, and lower spike frequencies (Schmidt and Kofuji, 2009). Such findings are unsurprising given the increased anti-melanopsin antibody staining in M1s vs. M2s, with melanopsin being the photopigment responsible for the phototransduction cascade in ipRGCs (Takahashi et al., 1984; Lucas et al., 2001; Hattar et al., 2002; Baver et al., 2008).

M3 ipRGCs are bistratified, with dendrites terminating in both the ON and OFF sublamina, though there is heterogeneity in this stratification with some M3s confining a greater or lesser proportion of their dendrites to one sublamina or the other. Their dendritic field size exceeds those of M1 but not those of M2 ipRGCs, and the complexity of branching of the M3 ipRGC dendrites was similar to that of M2s, with both M2 and M3 ipRGCs manifesting highly branches arborizations (Schmidt and Kofuji, 2009, 2011). There is some debate as to whether these cells truly constitute a distinct ipRGC subtype, given their sparse distribution and consequent lack of retinal tiling (Berson et al., 2010).

Like M2s, M4 and M5 ipRGCs are monostratified within the ON sublamina of the IPL, although M4 dendrites are located distal to those of M2 ipRGCs and proximal to the ON CHAT or cholinergic band (i.e one of two bands of choline acetyltransferase (ChAT)-like immunonopositivity within the IPL, the other band being localized to the OFF sublamina). M4 cells have the largest somata of the ipRGC subtypes and manifest wide, radiating dendritic arbors; in contrast, M5 somata are smaller and more spherical than those of the M4 ipRGCs and the M5 ipRGCs have compact bushy dendritic profiles with a higher number of dendritic branchpoints. While poorly melanopsin immunoreactive, they do exhibit intrinsic light responses

typical for ipRGCs and thus have functional photopigment / melanopsin based phototransduction. However, these light responses are even smaller and less sensitive than those of M2 ipRGCs (Ecker et al., 2010; Estevez et al., 2012; Stabio et al., 2018).

M6 ipRGCs are the most recently identified subtype of ipRGCs. Their spiny dendrites are, like M3 ipRGCs, bistratified but are the most densely branched and contribute to the smallest dendritic fields of all the subtypes. They are also poorly melanopsin immunoreactive with correspondingly weak intrinsic light responses similar in maximal amplitude to those of M4 and M5 ipRGCs (Quattrochi et al., 2019).

1.2.2 ipRGC central projections

In terms of central projections, ipRGCs as a whole were originally known to project to the SCN, IGL, OPN, vLGN, and preoptic area as well as to the lateral nucleus, peri-supraoptic nucleus, and subparaventricular zone of the hypothalamus, posterior limitans nucleus, medial amygdala, margin of the lateral habenula, and periaqueductal gray with sparse projections to the ventral lateral geniculate nucleus (dLGN) and superior colliculus (SC) (Hattar et al., 2002, 2006). M1 cells form the primary population projecting to the SCN, with SCN ipRGC innervation consisting of 80% M1 axons and 20% M2 axons. And, while M1 and M2 populations project roughly equally to the OPN, 45% and 55% respectively, M1 cells predominantly project to the OPN shell, largely considered to be the major link between the pupillomotor output and the retina, and M2 cells to the core (Baver et al., 2008). The OPN core may make a small contribution to the PLR. M1 ipRGCs can be distinguished by differential expression of the Brn3b transcription factor into functionally distinct populations, with Brn3b negative ipRGCs innervating the SCN, driving photoentrainment, and Brn3b positive ipRGCs

innervating the remaining brain targets, including the OPN, which is responsible for mediating the PLR (Chen et al., 2011).

Later work using a cre-lox system that more sensitively labeled an expanded spectrum of ipRGCs as compared to early work with *Opn4*$^{tau\text{-}LacZ}$ mice, which predominantly labeled M1 ipRGCs (Hattar et al., 2002, 2006), revealed additional ipRGC terminal projections. ipRGCs as a class are now known to additionally project to the posterior prectectal nucleus (PPN) and demonstrate more extensive projections to the SC and dLGN than previously reported. Non M1 axons project to the dLGN as well as the OPN core and demonstrated convergence with M1 projections in the SCN, IGL, and vLGN. While ipRGCs are predominantly known for their contributions to non-image forming vision, as is consistent with innervation of the SCN, IGL and OPN, non-M1 ipRGCs dominate projections to nuclei which mediate spatial/discriminative visual functions such as the dLGN and SC nuclei, indicating a role for ipRGCs in pattern forming vision, as supported by *Gnat1*$^{-/-}$; *Cnga3*$^{-/-}$ double KO mice which maintain spatial visual discrimination but not optokinetic tracking (OKT) despite the lack of rod/cone phototransduction (Ecker et al., 2010). The absence of OKT is not unexpected, given the paucity of ipRGC innervation of the accessory optic nuclei responsible for reflexive retinal image stabilization (Douglas et al., 2005). While all ipRGCs innervate the dLGN to some degree, most M4 ipRGCs innervate the dLGN (Estevez et al., 2012). Additional work focused on M5 and M6 subtypes revealed central projections concentrated in the OPN, IGL, vLGN, and dLGN, with a greater contribution from M6 vs. M5 ipRGCs, indicating a predominant role in pattern vision for these subtypes (Estevez et al., 2012; Quattrochi et al., 2019). A summary table of ipRGC central projections is given in Fig. 1.2, from (Quattrochi et al., 2019). Of note is that M3 ipRGCs are not

depicted as they match the IPL stratification of M6 cells and very little is known of their central axonal projections.

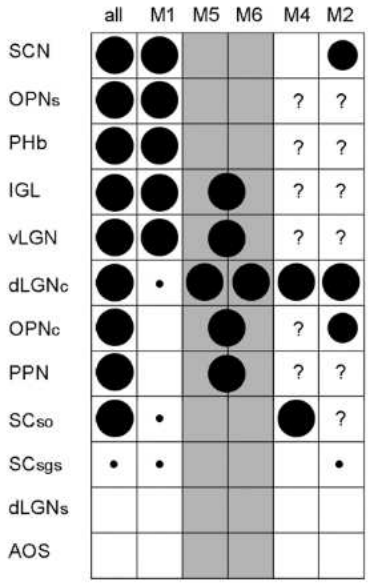

Figure 1.2 Central projections of ipRGCs. The circles indicate confirmed central projections of a given ipRGC subtype, with diameter corresponding to the strength of the projection. SCN: suprachiasmatic nucleus, OPNs: shell of the olivary pretectal nucleus, PHb: perihabenular nucleus of the thalamus; IGL: intergeniculate nucleus, vLGN: ventral division of the lateral geniculate nucleus, dLGNc: core of the dorsal division of the LGN, OPNc: core of the olivary pretectal nucleus, PPN: posterior pretectal nucleus, SCso: stratum opticum of the superior colliculus, SCsgs: superficial gray layer of the superior colliculus, dLGNs: shell of the dLGN, AOS: accessory optic system (adapted from Quattrochi 2019 with permission from John Wiley and Sons, License 4574910504365).

1.2.3 ipRGC signaling

IpRGCs respond to light via extrinsic (synaptically mediated) and intrinsic (melanopsin-mediated cascades). Developmentally, ipRGCS are the first functional photosensitive cells. Prior to eye opening and classical photoreceptor development, ipRGCs utilize intrinsic phototransduction and at the time of eye opening, as the retina matures and coincident with ipRGC dendritic architectural maturation and stratification within the IPL, integrate outer retinal signals from rods and cones (Schmidt et al., 2008).

Similar to other RGCs, all ipRGCs are the downstream recipients of photic information from classical photoreceptors, Fig. 1.3 (Wong et al., 2007; Güler et al., 2008; Hatori et al., 2008).

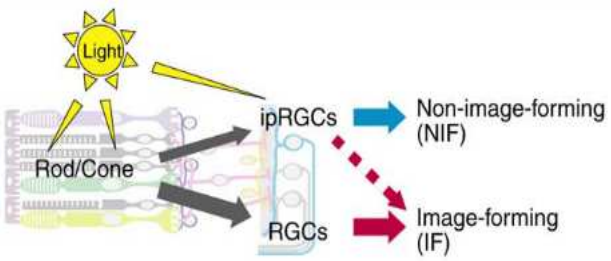

Figure 1.3 ipRGC roles in both image and non-image forming vision. ipRGC integrate light signals from the rods and cones and their own intrinsic phototransduction cascades to contribute to both image and non-image forming vision (adapted from Hatori 2010 with permission from Elsevier, License 4574910361206).

Despite M1 dendritic stratification in the OFF sublamina of the IPL, the ON-pathway is primarily responsible for excitatory input to both the M1 and M2 ipRGCs (Schmidt and Kofuji, 2010), though M1 cells do receive some OFF pathway input (Wong et al., 2007). Structurally, this may be a consequence of ON BCs that provide atypical synaptic input prior to terminal specialization via en pessant ectopic ribbon synapses that contact M1 dendrites within the OFF sublamina (Dumitrescu et al., 2009; Hoshi et al., 2009). However, in mice in which the intrinsic phototransduction cascade is absent (i.e. melanopsin null or *Opn4*$^{-/-}$ mice), M1 cells responded to light with significantly smaller and shorter duration inward current vs. the typical slow, large, sustained inward current typical of M1 cells in WT mice. In contrast, M2 light responses were preserved in the KO mice, and, in conditions of synaptic blockade of ON pathway inputs, both kinetics and magnitude of M2 light responses were reduced in WT mice while those of M1 ipRGCs were not reduced. Thus, despite the unusual ON pathway input, the M1 response to photic stimuli is more reliant upon the more sensitive intrinsic phototrandsuction cascade than extrinsic synaptic input while that of M2s is dominated and modulated by synaptic input from the ON pathway (Schmidt and Kofuji, 2010). This is consistent with the high input resistance

and large, sensitive intrinsic light response of M1s vs. the low input resistance and small, relatively insensitive photocurrents of M2s (Schmidt and Kofuji, 2009). Thus, M1 and M2 cells may have discreet influences on non-image forming vision, with M1 cells serving as conduits for rod and melanopsin-mediated and M2s for cone-mediated signaling (Schmidt and Kofuji, 2010).

The predominant synaptic input to the M3 ipRGCs is the ON pathway, despite the bistratifying nature of this subtype. As M3 OFF arborizations costratify with those of M1s, the predominant ON pathway input may be also be mediated by ectopic synapses with ON BCs, akin to M1 ipRGC dendrites (Dumitrescu et al., 2009; Hoshi et al., 2009; Schmidt and Kofuji, 2011). With regard to intrinsic membrane and spiking properties, M3s are more physiologically similar to the M2s in terms of their maximal light evoked intrinsic depolarization, resting V_m, spike frequencies, and input resistance. However, their sensitivity to 480 nm light is greater than that of M2s but less than that of M1s (Schmidt and Kofuji, 2011). Similar to M3 ipRGCs, M6 ipRGCs are bistratified and yet their synaptically driven light responses are ON-dominant, suggesting another instance of ectopic ON BC input in the OFF sublamina. Their intrinsic responses mimic those of M4 and M5 ipRGCs, and they have correspondingly low melanopsin levels (Quattrochi et al., 2019).

M4 ipRGCs have ON center receptive fields and antagonistic surrounds, which is not surprising given their dendritic arborization within the ON sublamina of the IPL, and as such are suited for contrast encoding and enhancement. They have brisk extrinsic light responses. However, their melanopsin levels are modest and given the accordingly decreased probability of photon capture, they have weak and insensitive intrinsic photoresponses (Estevez et al., 2012). Akin to M4 ipRGCs, M5s have low melanopsin immunoreactivity and weak intrinsic light responses. M5 ipRGCs manifest sustained ON responses, again as expected given their arboral

stratification within the IPL, but unique amongst other ipRGC subtypes, the synaptically driven light responses of M5 ipRGCs have chromatic opponency and as such, with their projections to the dLGN, M5s contribute to geniculo-cortical color vision. Full field UV light exposure triggers sustained ON responses while that of green light is suppressive. Such chromatic information could augment cues provided by ambient light levels alone and thereby influence photoentrainment of circadian rhythms, with the IGN projecting from the greater LGN complex to the SCN (Harrington, 1997; Stabio et al., 2018).

The different physiological properties displayed by distinct ipRGC subtypes pairs well with the organization of those subtypes within the sublaminae of the IPL, given that M1 ipRGCs that stratify in the OFF sublamina are largely responsible for non-image formatting vision and non-M1 ipRGCs, which predominantly stratify in the ON sublamina, are largely responsible for contributions to image forming vision, consistent with the notion that ipRGC subtypes contribute differentially to visual function (Hattar et al., 2002, 2006; Ecker and Hattar, 2010; Ecker et al., 2010; Estevez et al., 2012; Quattrochi et al., 2019).

The photopigment melanopsin, with a peak wavelength sensitivity of ~ 479 nm, is necessary for the intrinsic light sensitivity of ipRGCs (Takahashi et al., 1984; Lucas et al., 2001; Hattar et al., 2002). In *Opn4*$^{-/-}$ mice in which synaptic input to ipRGCs is pharmacologically blocked, ipRGCs fail to demonstrate intrinsic light responses or light-evoked inward currents (Schmidt and Kofuji, 2010). On a behavioral scale, *Opn4*$^{-/-}$*; rd/rd* mice (i.e. those that lack both melanopsin and classical photoreceptor function), demonstrate complete loss of nonvisual photic responses including photoentrainment of the SCN, PLRs, and negative masking (again, bright light suppression of locomotor activity) (Panda et al., 2003).

Photopigments consist of a non-protein light sensitive moiety (the chromophore) and an associated protein-moiety (the opsin) that spectrally tunes the molecule's absorbance of light. In general, phototransduction cascades start with the absorption of a photon of light by the chromophore; the resultant photoisomerization of the chromophore releases the opsin from its binding pocket. The opsin is a G-protein-coupled receptor (GPCR). The GPCR then activates a multimeric G-protein, the alpha subunit (G_α) of which then triggers a subsequent downstream signaling cascade that alters the photoreceptor's membrane potential. Phototransduction in rods and cones is mediated via the chromophore retinal and the release of the opsin from its pocket allows for interaction with transducin ($G_{\alpha t}$, a $G_{i/o}$ family G protein), which activates phosphodiesterase (PDE), which hydrolyzes cyclic guanosine monophosphate (cGMP) to 5'-guanosine monophosphate (5'GMP) that in turn closes a cyclic nucleotide gated channel (CNG),

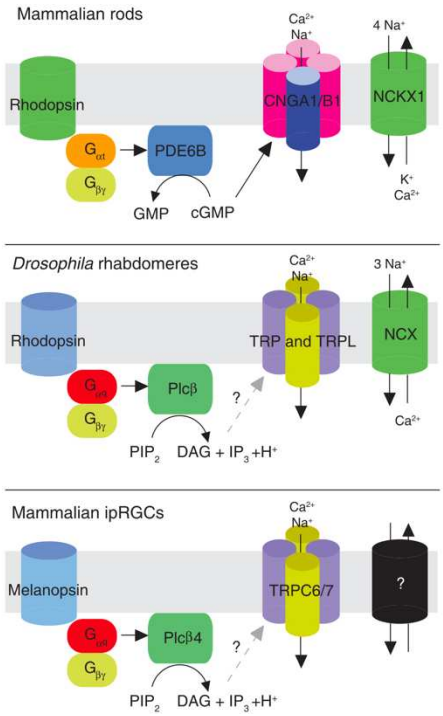

Figure 1.4 Comparison of phototransduction in mammalian rods vs. *Drosophila* rhabdomeres and mammalian ipRGCs. Key differences: in rods, a G_i pathway is used and the photoreceptor hyperpolarizes in response to light. Key similarities: in rhadomeres and ipRGCs, a G_q signaling pathway is used in conjunction with a TRP channel and the photoreceptor depolarizes in response to light. (adapted from Rupp 2014 with permission from Springer Nature, License 4574910426415)

resulting in hyperpolarization of the photoreceptor. Melanopsin, a rhodopsin-like GPCR with a seven-pass transmembrane domain, resembles invertebrate rhodopsins more closely than vertebrate opsins. In contrast to classical photoreceptors, in ipRGCs phototransduction leads to depolarization of the cell via a $G_{\alpha q}/G_{\alpha 11}$-mediated cascade and opening of a transient receptor potential (TRP) channel, Fig. 1.4 (Peirson and Foster, 2006).

In greater detail, in ipRGCs light activated melanopsin interacts with $G_{\alpha q}/G_{\alpha 11}$, activating phospholipase C-β (PLC-β), the obligate effector enzyme of that G protein class. Of the four known subtypes of PLC-β, this is most likely PLC-β4, as *Plcb4*$^{-/-}$ mice lack intrinsic light responses in M1 ipRGCs (Xue et al., 2011). In PLC mediated second messenger cascades, PLC generates from phosphatidylinositol 4,5-bisphosphate [PtdIns(4,5)P_2 or PI(4,5)P_2] (PIP_2) two primary second messengers (1) Ins(1,4,5)P3 (IP3) and (2) diacylglycerol (DAG). IP_3 represents the cytosolic branch of this cascade, as it binds to IP_3 receptors to trigger release of intracellular Ca^{2+}. However, this release of Ca^{2+} from IP_3 sensitive stores has proven unnecessary for phototransduction given that the intrinsic light responses of ipRGCs persist in the face of indirect pharmacologic blockage of Ca^{2+} release from IP_3 dependent stores or direct blockade or occupation of IP_3 receptors (with heparin or IP_3 itself). Additionally, inward currents are not detected upon intracellular injection of IP_3. However, intracellular [Ca^{2+}] increases are apparently involved in phototransduction as application of a rapid and readily diffusible Ca^{2+} chelator (BAPTA), which chelates all available intracellular free Ca^{2+} derived from any source including cell membrane associated channels, abolishes the intrinsic light response after 20 minutes. That this required a time scale of such magnitude suggests that Ca^{2+}'s role as a second messenger is largely modulatory and not requisite for phototransduction. Given that excised patches of ipRGCs are still capable of exhibiting photoresponses, the most likely candidate for

the critical second messenger would seem to be DAG, which is membrane associated. However, application of DAG analogues have failed to induce inward current in isolated ipRGC membrane patches. Diffusible cytosolic cascade components and DAG, while apparently not required for basic intrinsic light responses in ipRGCs, nonetheless may one day prove to serve *in situ* modulatory roles (Graham et al., 2008).

Regarding basic phototransduction, there may exist an interaction between PIP_2 and the light gated channel in ipGRCs that, in darkness, maintains the channel in a closed state. Light mediated PIP_2 hydrolysis via PLC-β4 could decrease intracellular [PIP_2] to the point that the channels would open. Indeed, alterations in PIP_2 levels have been shown to open channels even in the face of static IP_3, DAG, or Ca^{2+} levels (Suh et al., 2006). Pharmacologic blockade of PIP_2 synthesis in ipRGCs does slow termination of photocurrent, increase latency to peak, and reduce the changes of a second light response, indicating that phototransduction in ipRGCs is dependent upon a phosphoinositide signaling cascade localized to the plasma membrane (Graham et al., 2008). PIP_2 may then via a PKC modulate a TRPC6 or TRPC7 channel. Evidence for TRPC6/7 involvement lies in the loss of ~99% of photocurrent in M1 ipRGCs in *Trpc6*$^{-/-}$ *Trpc7*$^{-/-}$ mice. Single KOs of either TRPC failed to abolish the light responses, though kinetics were altered. As such, TRPC6/7 heteromers or redundant homomers appears to be the most likely candidates for light activated channels in ipRGCs (Xue et al., 2011). Protein kinase C zeta (Prkcz / PKCz) may also contribute to the phototransduction cascade as *Prkcz*$^{-/-}$ mice behaviorally mimic melanopsin null mice; PKCz may participate via a signaling complex composed of PLC and PKC as PKCz has been localized to the plasma membrane of ipRGCs (Hankins et al., 2007; Peirson et al., 2007).

The membrane depolarization secondary to the TRP channel activation in turn activates TTX sensitive voltage gated sodium channels (Na_V); the subsequent Na^+ flux and membrane depolarization activates verapamil sensitive L-type voltage gated calcium channels (Ca_V), which are responsible for the sustained firing of ipRGCs. The Ca_V channels are responsible for 90% of the somatic Ca^{2+} increase; however, there is a minor contribution of Ca2+ influx via the TRP channel, Fig. 1.5 (Hartwick et al., 2007). A set of voltage-gated and Ca^{2+}-dependent K^+ currents (I_K and $I_{K(Ca)}$, respectively) are also critical for repolarization of the membrane potential of ipRGCs after each spike (Hu et al., 2013).

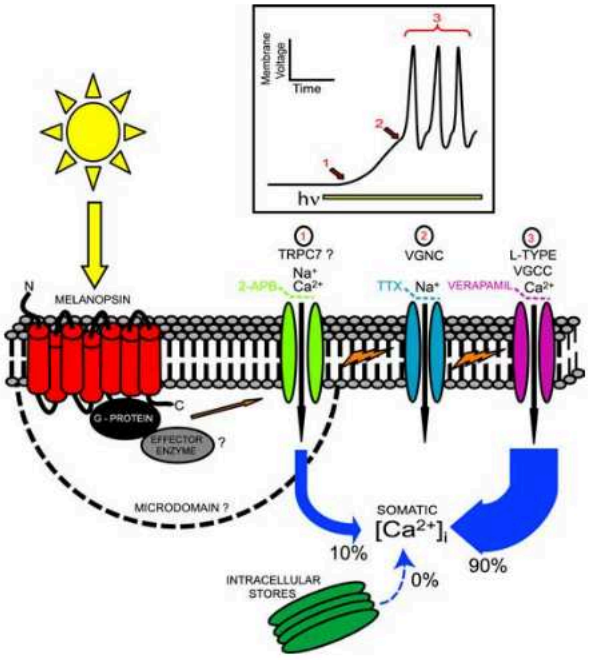

Figure 1.5 Intrinsic light-mediated signaling cascade in ipRGCs. Following melanopsin-mediate phototransduction, the membrane potential is depolarized (1) which allow for sodium influx through voltage gated sodium channels / VGNC (2) and action potential firing, which are sustained by calcium influx through voltage gated calcium channels / VGCC. (adapted from Hartwick 2007 with permission from Journal of Neuroscience).

Another difference between classical photoreceptors and iPRGCs is the mechanism of chromophore regeneration, Fig. 1.6. Following photoisomerization from *11-cis retinal* to *all-trans retinal*, *all-trans retinal* is recycled back to *11-cis retinal* via esterification by

lecithin:retinol acyltransferase (LRAT) and isomerization by RPE65 in the retinal pigmented epithelium (RPE), as is the case for the retinoid cycle between the RPE and both rods and cones. In cones, Müller cells (MCs) also contribute to the regeneration process (Wang and Kefalov, 2011). In contrast, while ipRGCs utilize retinal akin to classical photoreceptors, chromophore regeneration is an intrinsic property of ipRGCs. Melanopsin is a bistable or bireactive photopigment, meaning that it can use *all-trans-retinal* as a chromophore due to intrinsic photoisomerase activity conferred by melanopsin itself in response to absorption of long wavelength light. Again, melanopsin functions in a fashion more akin to invertebrate opsins that remain tightly bound to their chromophores, consistent with melanopsin's resistance to light bleaching. Pharmacologic blockade of the visual retinoid cycle in *rd/rd* mice (mice with loss of all rod and nearly all cone function) does not impair PLR photosensitivity, and ipRGCs from *rpe65*$^{-/-}$ and *lrat*$^{-/-}$ retinas maintain ex vivo photosensitivity, consistent with the notion that the ipRGC photocycle functions independently. Anatomically this would be of benefit for the ipRGCs, given their relatively far distance from the RPE as compared to classical photoreceptors (Panda et al., 2005; Tu et al., 2006; Sexton et al., 2012). Despite these findings, however, there remains some question regarding RPE65's and LRAT's role in regulation of chromophore availability for melanopsin and as to whether ipRGCs are definitively able to function entirely independently of the RPE and MCs as *rpe65*$^{-/-}$ mice are unable to phase shift. Circadian photosensitivity was restored upon ablation of lingering rod function in this line but not upon loss of melanopsin, suggesting that while ipGCs can function without RPE65, interactions exist between classical photoreceptors and ipRGCs, e.g. ipRGCs may be able to avail themselves of regenerated chromophores if not utilized locally by rods (Doyle et al., 2006). In a similar vein, *rpe65*$^{-/-}$*; rdta* mice (in which there is outer retinal degeneration secondary to diphtheria toxin

driven by a rod-specific promotor) and *lrat*$^{-/-}$*; rd/rd* mice exhibited paradoxically increased PLR photosensitivity compared to *rpe65*$^{-/-}$ and *lrat*$^{-/-}$ mice – implying that outer retinal degeneration rescued the functional ipRGC phenotype of mice mutant in visual retinoid cycle enzymes alone (Tu et al., 2006). This has implications regarding manifestations of differing photoentrainment phenotypes depending upon the degree of pathological outer retinal degeneration. Given the physical proximity of MCs and ipRGCs, the former may theoretically also contribute to chromophore maintenance in ipRGCs.

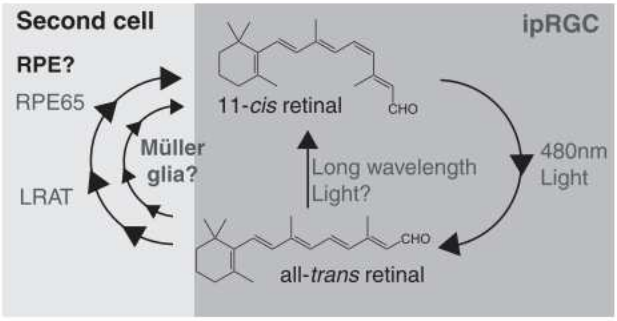

Figure 1.6 Melanopsin visual cycle. See text for description. The participation of Müller cells is not confirmed. (adapted from Rupp 2014 with permission from Springer Nature, License 4574910426415).

ipRGCs are not optimized for high spatial resolution or temporal fidelity. However their slow, insensitive signaling is excellent for the continuous transmission of average environmental irradiance levels critical to non-image forming visual processes while simultaneously excluding photic environmental "noise." With melanopsin membrane density 10^4-fold lower than that of rod and cone opsins, making the likelihood of photon capture 10^6-fold lower than for rods and cones, ipRGCs are relatively insensitive to light. As such, intrinsic phototransduction occurs only in bright light. (Of note: at lower light levels, rods and cones remain capable of synaptically driving the ipRGCs.) While this might seem insufficient for melanopsin mediated signaling, in fact a single photon is sufficient for triggering the analog signaling of ipRGCs, making ipRGC efficient though insensitive photic sentinels. This is accomplished through several mechanisms. ipRGC resting membrane potential is close to that of their action potential threshold and fire

spontaneously in dark at a low rate; a single 1 mV depolarization from one photon thus dramatically increases the rate of action potential firing. ipRGCs also have prolonged integration times on the order of seconds so that, should additional photon absorption occur as is the case in prolonged ambient light exposure, further depolarization remains possible. ipRGCs can transmit the average amount of environmental light continuously, spiking for up to minutes after stimulus offset. (Nelson and Takahashi, 1991; Berson et al., 2002; Do et al., 2009; Schmidt and Kofuji, 2009). The function of ipRGCs as irradiance detectors is reflected in the extensive dendritic arborization of the ipRGCs which provides an expansive net for light detection (Sollars et al., 2003). Further, retinohypothalamic tract (RHT) neurons do not demonstrate precise retinopathic mapping to the SCN (Provencio et al., 1998).

1.3 ipRGCs and their roles in non-image forming vision

The downstream output of ipRGCs is critical for non-image forming vision and its behavioral outputs, e.g. the PLR and photoentrainment (Hattar et al., 2003; Güler et al., 2008). While modulation of ipRGC signaling and its effect on the PLR is the subject of the third chapter of this work, photoentrainment will be subsequently discussed in this introduction as it represents both a key role for ipRGCs, which is relevant from a holistic perspective, as well as an avenue for future translational / clinical research.

1.3.1 ipRGCs and the pupillary light reflex

Given that tolerance of the PLR to a light flash develops at a different rate than that of pupil diameter (Pickworth et al., 1990), it is generally held that different mechanisms control resting pupil size and the constriction phase of the PLR (Nisida and Okada, 1959; Adler et al., 1981; Pickworth et al., 1989, 1990; Sharpe, 1991). These mechanisms diverge at the level of the midbrain. Resting pupil diameter is controlled by tonic firing of the Edinger-Westphal nucleus /

EWN (aka the oculomotor nucleus / OMN), which is spontaneous and persistent in the face of deafferenation. The PLR, however, is determined by retinal illumination and subsequent light-evoked EWN excitation and an increase in the firing rate of parasympathetic neurons arising from the EWN and innervating the iris via the short ciliary nerve (Nisida and Okada, 1959).

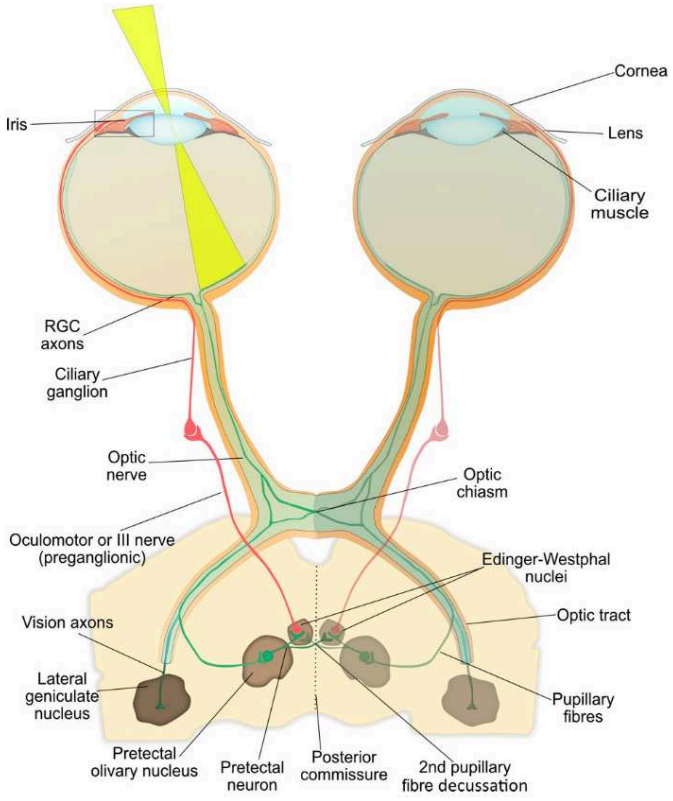

Figure 1.7 The pupillary light reflex. See text for description. (adapted from Hall 2018 – open access).

The afferent arm of the pupillary light reflex (PLR) is mediated by ipRGCS, which again are most sensitive to intense, short wavelength (blue) light (Lucas et al., 2001, 2003; Berson et al., 2002). The axons of Brn3b+ ipRGC course through the optic nerve to the optic chiasm, where nerves from the nasal retina project to the contralateral side and those from the temporal retina maintain an ipsilateral orientation along the optic tracts. The first synapse occurs at the olivary pretectal nucleus (OPN) of the dorsal midbrain. The percentage of axons which decussate to the opposite optic tract is species dependent, with 50% decussation in man. From there, pretectal neurons continue ipsilaterally or cross the posterior commissure to EWN. At that

juncture, the efferent arm of the PLR begins with pre-ganglionic parasympathetic fibers integrating with cranial nerve III or the oculomotor nerve to synapse at the ciliary ganglion. Post-ganglionic parasympathetic fibers travel via the short ciliary nerves to innervate the muscles of the iris sphincter, where acetylcholine is released to mediate pupil constriction, Fig. 1.7 (Young and Lund, 1994; Hattar et al., 2002, 2006; Gooley et al., 2003; Baver et al., 2008; Chen et al., 2011; Hall et al., 2018).

Both classical photoreceptors, i.e. rods and cones, and the ipRGCs contribute to the PLR. Rodless, coneless mice maintain normal PLRs in response to high irradiance stimuli (Lucas et al., 2001; Panda et al., 2003). Melanopsin KO mice maintain normal PLRs in response to low irradiance stimuli but not high, with melanopsin being requisite for maximal constriction (Lucas et al., 2003; Panda et al., 2003), and treatment with opsinamides slowing pupil constriction starting 1 second after onset of high irradiance stimuli (Jones et al., 2013). Triple KO mice, i.e. mice lacking both classical photoreceptor transduction mechanisms and melanopsin, do not manifest a PLR, supporting the complementary nature of both systems (Hattar et al., 2003; Panda et al., 2003). However, outer retinal signals contribute to the PLR via the conduit of ipRGCs, as genetic ablation of ipRGCs eliminates rod-cone mediated miosis in response to all light intensities (Güler et al., 2008).

The PLR consists of both sustained and transient components that are determined by the contribution of specific photoresponses. In addition to promoting maximal miosis in response to high irradiance stimuli as well as late PLR constriction velocity, melanopsin phototransduction is responsible for the post illumination pupillary response (PIPR), i.e. sustained miosis after light offset (Gamlin et al., 2007; Adhikari et al., 2015) as well as maintenance of miosis under long term low-irradiance photopic conditions (McDougal and Gamlin, 2010). This sustained

component of the PLR as well as stable daytime pupil diameter is mediated by the central release of the neuropeptide pituitary adenylyl cyclase-activating polypeptide (PACAP) by ipRGCs into the brain (Keenan et al., 2016). The synaptic input generated by classical photoresponses that impinge upon the ipRGCs extends the dynamic range of the PLR in both the temporal frequency and intensity domains. Blockade of rod-cone signaling increases PLR response latency by ~ 1 second (Gamlin et al., 2007), and the pupils of patients with outer retinal blindness cannot track high-frequency intermittent light (Gooley et al., 2012). In mice without classical photoreceptor input to ipRGCs, the PLR is ~ 4 log units less sensitive than WT (Lucas et al., 2001, 2003). It is of note that the photoresponses of both rods, cones, and ipRGCs are not linearly additive, as the melanopsin photoresponse exclusively drives the PLR given stimuli above the threshold of the melanopsin photoresponse (480 nm, $10^{11.5}$ photons/cm^2/s) (Lucas et al., 2001), effectively shunting rod-cone mediated outer retinal signals that feed into the ipRGCs. Below this threshold, after a brief period of adaptation, tonic rod signaling synergistically drives the PLR via central ipRGC glutamatergic output, maintaining miosis at irradiances below the melanopsin threshold and enhancing sensitivity to long-wavelength light (McDougal and Gamlin, 2010; Keenan et al., 2016). In contrast, cones minimally contribute to maintaining miosis at either high or low irradiances (McDougal and Gamlin, 2010), unless they are permitted to dark adapt with short, intermittent dark pulses (Gooley et al., 2012).

1.3.2 ipRGCs and the hypothalamic regulation of sleep and circadian rhythms

Sleep is integral to physical and mental well-being; inadequate or poor quality sleep can have both short and long term consequences for both health and performance (NHLBI, 2018). Given the importance of sleep, the architecture and timing of sleep / wake states are closely regulated. This is achieved via two processes that work in concert with each other (1) the

homeostatic process, or the drive to sleep and (2) the circadian process, or the sleep-independent timing of the sleep/wake cycle that, if properly synchronized with environmental cues, provides an arousal signal in antiphase to the sleep drive (Borbély, 1982). The processes are integrated by the SCN, which (in a diurnal primate) actively facilitates wakefulness during the subjective day and opposes the homeostatic drive to sleep in order to regulate daily total sleep/wake time and rhythms (Edgar et al., 1993). As previously mentioned, light (via ipRGCs) can impact sleep both indirectly (through phase adjustments of sleep independent circadian rhythms) and directly (through nonvisual mechanisms that impact the homeostatic drive to sleep), though these mechanisms are not entirely independent of each other.

The SCN is the master biological clock, with lesioning of the SCN resulting in elimination of the capacity for photoentrainment and the loss of endogenous circadian rhythms of multiple homeostatic functions (Moore and Eichler, 1972; Stephan and Zucker, 1972). Free running rhythms, though not the ability to photoentrain, in an SCN-lesioned animal can be restored with brain grafts containing fetal SCN (Lehman et al., 1987). The axons of the ipRGCs project to the SCN (Berson et al., 2002; Hattar et al., 2002) and are exclusively responsible for its photoentrainment and thus that of endogenous circadian rhythms, such as the sleep wake cycle. ipRGCs are capable of photoentrainment in the absence of rods and cones, utilizing their melanopsin mediated intrinsic phototransduction cascade (Provencio et al., 2000; Hattar et al., 2003); in the absence of melanopsin, ipRGCs convey upstream rod and cone signals to the SCN

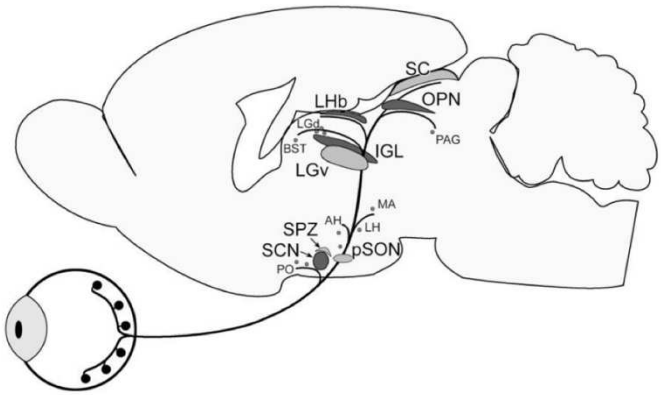

Figure 1.8 M1 ipRGC central projections, lateral view. PO: preoptic area, SCN: suprachiasmatic nucleus, pSON: peri-supraoptic nucleus, SPZ: subparaventricular zone, AH: anterior hypothalamic nucleus, LH: lateral hypothalamus, MA: medial amygdaloid nucleus, LGv: lateral geniculate nucleus - ventral division, IGL: intergeniculate leaflet, BST: bed nucleus of the stria terminalis, LGd: lateral geniculate nucleus - dorsal division, LHb: lateral habenula, PAG: periaqueductal grey, OPN: olivary prectecal nucleus, SC: superior colliculus. (adapted from Hattar 2006 with permission from John Wiley and Sons, License 4574910025338).

as long as the ipRGCs remain in the retinal circuit (Güler et al., 2008). ipRGCs reach the SCN via the monosynaptic retinohypothalamic tract (RHT) (Hattar et al., 2002, 2006), Fig. 1.8, and there release both the excitatory neurotransmitter glutamate and pituitary adenylate cyclase-activating polypeptide (PACAP), triggering slow and sustained EPSCs that mimic the light responses of ipRGCs (Berson et al., 2002; Meijer and Schwartz, 2003; Hannibal, 2006; Engelund et al., 2010). The exact mechanism linking the rhythm of SCN neuronal firing and alteration of oscillation of clock gene transcription, and therefore activity of descending circuits, remains to be fully elucidated, though glutamate and PACAP are thought to regulate mPer1 gene expression in the SCN, which in turn may modulate SCN neuronal excitability and thus firing rate (Pennartz et al., 2002; Reppert and Weaver, 2002). The rhythmic firing of the SCN is required for the circadian rhythmicity of homeostatic functions, and it is the light signals mediated by the RHT that are critical for the daily resetting of the SCN, with a single pulse of short wavelength light mediated by ipRGCs capable of phase advancing circadian rhythms in man (Warman et al., 2003). Other factors, e.g. locomotor activity, sleep-wake cycles, and food / reward systems, are capable of circadian clock resetting or, as is the case with serotinergic signaling, modulation of

photic input to the SCN, but photic signals remains the strongest zeitgeber for the SCN (reviewed in: Fuller et al., 2006; Sollars and Pickard, 2015).

The circadian clock of the SCN sets the rhythm of melatonin secretion from the pineal gland, with melatonin levels being elevated ~10 fold at night relative to daytime levels. It is melatonin's feedback as an endogenous zeitgeber on the SCN in a homologous loop that reciprocally resets the central pacemaker at night to consolidate the sleep-wake cycle (Cassone et al., 1986). Melatonin is also capable of antagonizing light induced phase advances in circadian rhythms when contemporaneously administered with light pulses (Cagnacci et al., 2017). Further a single light pulse at night is capable of depressing melatonin levels to daytime values (Reiter, 2003), and physiologic doses of melatonin shift human circadian rhythms according to a phase-response curve (Lewy et al., 1992). Such light pulses are mediated by the ipRGCs, which monosynaptically project along the RHT to the SCN which in turn projects via GABAergic neurons to the parvocellular autonomic subdivision of the paraventricular nucleus (PVN),

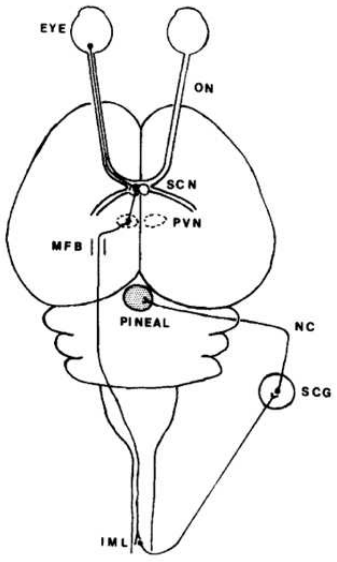

Figure 1.9 Neural pathway for melatonin production. See text for description. ON: optic nerve, MFB: medial forebrain bundle, IML: intermediolateral cell column, PVN: paraventricular nucleus, SGC: superior cervical ganglion, SCN: suprachiasmatic nucleus. (adapted from Moore 1995 with permission from Elsevier, License 4574910131886).

relaying the circadian signals of the SCN through the medial forebrain bundle and brainstem reticular formation to the intermediolateral (IML) cell column of the T1-T3 segments of spinal cord; the preganglionic cholingergic IML projections extend to superior cervical ganglion and finally the melatonin-synthesizing pineal gland via sympathetic noradrenergic postganglionic fibers, Fig. 1.9 (Moore, 1995). Indeed, nighttime melatonin suppression tests were one of the earlier studies to suggest a novel circadian photoreceptor and opsin photopigment, with 446-477 nm identified as the most potent λ range responsible for melatonin suppression (Brainard et al., 2001). Further, individuals blind from rod/cone degeneration maintain the ipRGC mediated decrease in melatonin production upon bright light exposure (Czeisler et al., 1995). As a consequence of central excitatory glutamatergic ipRGC signaling (Engelund et al., 2010), the SCN tonically inhibits the pineal gland's production of melatonin, with daytime GABA release from the SCN eliminating the PVN's excitatory glutamatergic input to downstream sympathetic preganglionic neurons (Kalsbeek et al., 2000). And, while the SCN is in general less active at night, a subpopulation of glutamatergic SCN neurons stimulates the PVN at night and therefore melatonin secretion (Perreau-Lenz et al., 2004).

There is anatomic and physiologic evidence that melatonin levels are regulated by environmental light levels via the ipRGCs and capable of phase shifting circadian rhythms; however, does melatonin in fact impact the sleep/wake homeostat and promote sleep? Yes; in addition to its chronobiotic effects, melatonin has hypnotic / sleep-promoting effects. Exogenous melatonin administration prior to nocturnal sleep advances sleep timing in man without altering the duration of sleep stages and additionally facilitated sleep for 3 hours post-administration, suggesting that in addition to its phase-shifting effects, melatonin directly facilitates sleep but does not induce it akin to classic hypnotics (Rajaratnam et al., 2004). While the circadian effects

of melatonin are mediated by melatonin receptors in the SCN (Vaněček et al., 1987), the mechanism for sleep-promoting effects are less clear. One possible mechanism may be that melatonin increases sleep drive, as measured by latency to sleep onset and sleep consolidation, by inducing a drop in body temperature (Cagnacci et al., 1997; Dijk and Cajochen, 1997; Kräuchi et al., 1997). It is of note that in lower mammals, even nocturnal ones, melatonin levels are highest during the day and lowest at night. Thus, the link between melatonin and sleep in such species must still be further explored (Fuller et al., 2006).

Murine studies detailing ipRGC and melanopsin mediated direct and indirect photic effects on sleep have been detailed in *Section 1.2*. In man, ipRGC dysfunction has been clinically shown to contribute to reduced sleep quality. Might the PLR be useful as a metric of sleep impairment? In advanced age related macular degeneration (AMD), ipRGC dysfunction as quantified by the melanopsin-mediated post-illumination pupil response (PIPR), a test that provides a direct measure of the intrinsic melanopsin photoresponse (Adhikari et al., 2015), accounted for 13% of the total reduction in sleep efficacy in AMD patients (Maynard et al., 2017). Given that a single M1 ipRGC send can send bilateral output to the SCN as well as collateral outputs to multiple brain regions relevant to non-image forming vision (Fernandez et al., 2016), dysfunctional ipRGC projections to both the SCN and OPN may account for the correlation between reduced sleep efficacy and PIPR. There is similar reduced PIPR in glaucoma patients (Kankipati et al., 2011), a patient population wherein impaired ipRGC function contributes to daytime sleepiness as well as lower total sleep time and efficiency (Gracitelli et al., 2015, 2016).

1.4 Opioids and the retina

Opioids are a drug class that includes pain relievers such as codeine, morphine, hydrocodone (Vicodin ®), and oxycodone as well as synthetic drugs, e.g. fentanyl, and illegal drugs of abuse, e.g. heroin (NIH: National Institute on Drug Abuse (NIDA), 2019). Opioids are a mainstay of chronic pain therapy, and while chronic pain can intrinsically cause insomnia and worsen it (Ohayon, 2005), opioid administration alone in healthy, pain free opioid-naïve adults has been shown to disrupt sleep and cause insomnia (Lewis et al., 1970; Shaw et al., 2005; Dimsdale et al., 2007). While opioids may have centrally mediated effects on the sleep/wake state, no consensus has been reached on which specific CNS sites therapeutic or abused opioids act upon to trigger sleep abnormalities nor have targeted pharmacotherapeutics been developed to alleviate such side effects (Angarita et al., 2016). As discussed above, ipRGC dysfunction can negatively modulate the PLR. In chronic opioid users, the PLR evoked by bright blue light has reduced velocity (Grace et al., 2010). Thus, given the notion that light can both directly and indirectly impact the sleep/wake state and the PLR, it is of interest to understand if and how opioids might modulate photically induced ipRGC signaling.

1.4.1 Endogenous opioids and their receptors

In addition to exogenous opioid modification of the sleep wake state and potentially the PLR, endogenous opioids might serve a physiologic role in ipRGC signaling. There are four prohormone peptides from which the endogenous opioid peptides are derived by the action of endo and carboxypeptidases and post-translation modification: (1) proenkephalin (ProEnk) (2) prodynorphin (ProDyn) (3) proopiomelanocortin (POMC) and (4) pronociceptin/orphanin FQ (Pasternak, 2010). Further, all opioid peptides contain the amino acid sequences Tyr-Gly-Gly-Phe-Met or Leu, known as the YGGF motif, that enables binding to the opioid receptors (Kakidani et al., 1982; Yoshikawa et al., 1984). The classical opioid receptors are μ-, κ-, and δ-

opioid receptors; or, MOR, KOR, and DOR respectively. There is also a non-classical opioid receptor, or NOP receptor. All the receptors are G-protein coupled and consistent of 7 transmembrane spanning linked domains with an intracellular C-terminal tail and extracellular N-terminus. Overall homology between receptor types is ~ 60%. Various splice variant and SNPs exist (McDonald and Lambert, 2016). While there is no absolute receptor ligand pair specificity, in general, a Tyr-Gly-Gly-Phe-Met or Leu core is necessary and sufficient for binding to MORs and DORs while a Tyr-Gly-Gly-Phe-Met or Leu with an Arg-X extension is necessary and sufficient for binding to KORs (Mansour et al., 1995).

ProEnk carries six copies of Met-enkephalin and subsequent to processing gives rise to the pentapeptides Leu-enkephalin and Met-enkephalin (Hughes et al., 1975), as well as heptapeptide, octapeptide, metorphamide, and bovine adrenal medulla peptides of 18 residues (BAM18) (Pasternak, 2010). The pentapeptides are selective for DORs but the extended peptides share affinity for all three classical receptor subtypes (Mansour et al., 1995).

Dynorphins A and B and α- and β-neoendorphin are derived from ProDyn (Kangawa et al., 1979; Minamino et al., 1980, 1981; Goldstein et al., 1981) and preferentially bind KORs but also bind MORs and DORs (Mansour et al., 1995; Pasternak, 2010).

POMC predominantly gives rise to the β-endorphins (Li and Chung, 1976), α-, β-, and γ-melanocyte stimulating hormones (MSH), adrenocorticotropic hormone (ACTH), corticotropin-like intermediate lobe peptide (CLIP), γ-lipoprotein / lipotropic hormones (LPH), γ- and α-endorphin (also known as β-LPH variants), and J-peptide; aside from the endorphins, the majority of POMC products are non-opioid peptides (De Wied and Jolles, 1982; Krieger, 1983; Pasternak, 2010). It is interesting to note that α-MSH and CLIP have been shown to increase

SWS and REM sleep, respectively (Chastrette et al., 1990). β-endorphin serves as the endogenous ligand for MORs and DORs, with preferential binding to MORs (Pasternak, 2010).

Pronociceptin/orphanin FQ gives rise to nocistatin and nociceptin/orphanin FQ (N/OFQ). The actions of the heptadecapeptide N/OFQ are mediated through the nociceptin opioid peptide receptor (NOP) which is also referred to as ORL-1 in man and LC12 in rat and MOR-3 in mouse. Activation of NORs results in decreased locomotor activity and hyperalgesia, suggesting that this opioid may have pro-nociceptive properties (Meunier et al., 1995; Reinscheid et al., 1995; Pasternak, 2010; McDonald and Lambert, 2016). However, an alternative notion is that N/OFQ does not in fact intrinsically cause hyperalegisa but has anti-analgesic action via reversal of stress-induced analgesia derived from the release of endogenous opioids (McDonald and Lambert, 2016). $NOR^{-/-}$ (NOP KO) mice demonstrate reduced analgesic tolerance to chronic morphine administration as well as reduced morphine-induced dependence. However, acute morphine analgesia is not impacted in the NOP KO vs. WT. As such, the NOP system may play a role in the neuroplasticity seen with opioid tolerance and dependence; NOP antagonism may represent an avenue for reducing the dose required for opioid mediated analgesia and the development of tolerance and dependence (Ueda et al., 2000). Nocistatin, unlike N/OFQ, does not bind NOP but does bind brain and spinal cord membranes and attenuates allodynia and hyperalgesia and reverses N/OFQ inhibition of morphine-induced analgesia (Okuda–Ashitaka and Ito, 2000).

Two additional endogenous opioids exist; these are endomorphin 1 and 2; their precursors are unknown, however, they have been shown to preferentially bind to MORs (McDonald and Lambert, 2016).

1.4.2 Opioids in the retina

Enkephalins (Jackson et al., 1980; Altschuler et al., 1982; Isayama and Zagon, 1991; Britto and Hamassaki-Britto, 1992; Pan et al., 2008) and β-endorphin (Jackson et al., 1980; Gallagher et al., 2010) have been detected in the avian, amphibian, and mammalian retina. Retinal opiate binding sites have been demonstrated in several species, including chick, rabbit, goldfish, rat, mouse, cow, toad, and skate (Medzihradsky, 1976; Howells et al., 1980; Djamgoz et al., 1981; Borbe et al., 1982; Slaughter et al., 1985; Gallagher et al., 2012; Cleymaet et al., 2019). Indeed, opioid receptors (most likely MORs given dihydromorphine's preferential MOR binding) were localized to the IPL, GCL, and the optic nerve of rats, non-human primates, and humans (Wamsley et al., 1981). DOR (and possibly MOR and KOR) activation has been shown to be neuroprotective in times of ischemic and/or hypoxic stress in the rat (Peng et al., 2008; Husain et al., 2009, 2012), and morphine has also been shown to mediate its protective effects against ischemia-reperfusion injury via opioid receptors in a rabbit model of ischemic retinopathy (Riazi-Esfahani et al., 2009). DOR activation is neuroprotective in the rat in the face of glaucomatous injury (Abdul et al., 2013).

Converging lines of evidence suggest that systemically applied opioids could act on (MORs) expressed by ipRGCs in the retina. Novel MOR immunolabeling of ipRGCs has been demonstrated (Gallagher, 2013). Opioids, including morphine and methadone, cross the tight retina/blood barrier (Hosoya et al., 2011) and accumulate in the vitreous humor of the eye (Wyman and Bultman, 2004; Fernández et al., 2013) at concentrations high enough to trigger cellular effects via activation of MORs (Selley et al., 2001; Lee et al., 2011). Morphine (0.30 μg/ml) and methadone (0.11 μg/ml) have been detected in the vitreous of opioid-dependent individuals (Fernández et al., 2013). Topical application of 1% morphine in the equine eye is sufficient to achieve vitreal concentrations on the order of ng/mL (Gordon et al., 2018). Drugs

administered via intravitreal injection are known to alter the activity of retinal neurons (Saszik et al., 2002), thus intravitreal opioids are expected to activate opioid receptors in the retina. Modulatory processes that are capable of inhibiting ipRGC activity have been proposed to inhibit ipRGC-mediated, light-driven behavior (Jones et al., 2013). Indeed, preliminary data has shown that the synthetic MOR agonist [D-Ala^2, N-MePhe^4, Gly-ol]-enkephalin (DAMGO) inhibits ipRGC spiking in responses to light recorded on multi-electrode arrays (MEA) in a dose dependent fashion; this effect is reversed by naloxone, confirming opioid-receptor mediated negative modulation of ipRGC light responses (Gallagher, 2013).

1.4.3 Opioid signaling

Opioids, via opioid-receptors expressed on ipRGCs, may exert their inhibitory effect on ipRGC firing via ion channels that are critical for photosignaling of ipRGCs. Opioid signaling is overwhelmingly inhibitory at the cellular level. Activation of opioid receptors has been shown to increase neuronal potassium currents (I_K), decrease calcium currents (I_{Ca}) via closure of voltage sensitive calcium channels (VSCC), and inhibit adenylate cyclase (AC), depending on the studied cell type (Kieffer, 1995; Minami and Satoh, 1995; Pasternak, 2010; Al-Hasani and Bruchas, 2011; McDonald and Lambert, 2016). All subtypes of opioid receptors are coupled to inhibitory pertussis toxin-sensitive G-proteins ($G_{i/o}$) that are sensitive to pertussis toxin (Hsia et al., 1984). Binding of the ligand promotes the exchanges of GDP for GTP and the G_α and $G_{\beta\gamma}$ dimer dissociates, triggering a downstream signal cascade. Eventually, the G_α subunit's intrinsic GTPase activity converts GTP to GDP, terminating the signal. In general, G_α modulates AC activity and I_K and $G_{\beta\gamma}$ modulates the activity of VSCCs (Kieffer, 1995; Minami and Satoh, 1995; Pasternak, 2010; Al-Hasani and Bruchas, 2011; McDonald and Lambert, 2016). Given the coupling of the GPCR to a similar set of signaling pathways, opioids achieve their specific

effects via biased agonism. Also known as ligand-directed signaling, this reflects a specific opioid agonist's ability to direct the receptor to preferentially favor a particular set of signaling events (Kanakin, 2009).

Documented opioid inhibition of VSCC include the following types of calcium channels: N- and P/Q-type as well as L-, R- and T-types. In light of N- and P/Q-type VSCC's location at the synaptic terminal, opioid inhibition of their function leads to a reduction of transmitter release (Bourinet et al., 1996; Rusin et al., 1997; Zamponi and Snutch, 1998). Opioids also stimulate the opening of G-protein-coupled inwardly rectifying potassium channels (GIRK or Kir3); the resultant membrane hyperpolarization reduces neuronal excitability and transmitter release (Torrecilla et al., 2002, 2008). (Note: GIRK has not been described in ipRGCs.) AC inhibition results in a decrease in cyclic adenosine 3',5'-monophosphate (cAMP). Typically, cAMP positively regulates the hyperpolarization-activation cation current, I_h, a membrane K^+ current, akin to prostaglandins and other inflammatory mediators that shift the voltage dependence of I_h to more depolarized potentials. I_h reduces neuronal refractory periods; by reducing cAMP levels, neuronal excitability and thus nocicipetive transmission is reduced by opioids. cAMP dependent Ca^{+2} influx is also reduced by opioid inhibition of AC (Yatani et al., 1987; Ingram and Williams, 1994). After prolonged opioid agonist treatment, however, AC activity levels and cAMP increased above baseline when the agonist is withdrawn, a phenomenon known as AC superactivation, which is thought to contribute to tolerance (Nestler et al., 1988; Avidor-Reiss et al., 1996). While opioid signaling is complex, the above represent potential avenues by which opioids may modulate ipRGC firing.

1.5 Hypothesis and aims of this study

Our overall hypothesis is that opioids alter light-evoked activity of ipRGCs and this has behavioral consequences detectable at the reflex level i.e. in the pupillary light reflex. The specific aims are as follows: (1) Analyze the molecular mechanism by which opioids modulate light-evoked signaling of ipRGCs; (2) Determine if acute inhibition of ipRGC signaling via MORs reduces pupillary light reflex (PLR) and (3) alters circadian rhythm of wheel running and the sleep/wake cycle. The following two chapters will discuss aims 1 and 2. Future directions targeting aim 3 and the translational potential / clinical relevance for this work will be discussed in the final chapter.

CHAPTER 2. μ-OPIOID RECEPTOR ACTIVATION DIRECTLY MODULATES INTRINSICALLY PHOTOSENSITIVE RETINAL GANGLION CELLS

This chapter includes the complete published manuscript for this aim, μ-opioid receptor activation directly modulates intrinsically photosensitive retinal ganglion cells (Allison M. Cleymaet, Shannon K. Gallagher, Ryan E. Tooker, Mikhail Y. Lipin, Jordan M. Renna, Puneet Sodhi, Daniel Berg, Andrew T.E. Hartwick, David M. Berson and Jozsef Vigh, Neuroscience, 2019). My contributions to this publication included generating retinal cultures, performing the whole cell electrophysiology experiments, data analysis and drafting of the relevant sections of the paper. This paper is reproduced with minimal modification beyond those necessary to meet the formatting requirements. As author of this Elsevier article, I retain the right to include it in a thesis or dissertation.

2.1 Summary

The aim of the present study was to investigate how μ-opioid receptor activation modulates intrinsically photosensitive retinal ganglion cell signaling. The main findings of this study were: (1) In the rodent retina M1-M3 types of intrinsically photosensitive ganglion cells (ipRGCs) express μ-opioid receptors (MORs). (2) Light-evoked firing of ipRGCs is attenuated by the MOR-specific agonist DAMGO in a dose-dependent manner. (3) MOR activation reduces ipRGC excitability by modulating I_K and reducing the amplitude of non-inactivating I_{Ca}. These findings suggest a potential new role for endogenous opioids in the mammalian retina.

Abbreviations:

adenylate cyclase (AC); 4-Aminopyridine (4-AP); basolateral amygdala (BLA); calcium-dependent potassium currents ($I_{K(Ca)}$); [S-(R*,R*)]-[3-[[1-(3,4-Dichlorophenyl)ethyl]amino-2-hydroxypropyl] (cyclohexylmethyl) phosphinic acid (CGP54626); H-D-Phe-Cys-Tyr-D-Trp-

Orn-Thr-Pen-Thr-NH_2 CTAP, H-D-Phe-Cys-Tyr-D-Trp-Arg-Thr-Pen-Thr-NH_2 (CTOP); [D-Ala^2, MePhe^4, Gly-ol^5]-enkephalin (DAMGO); D-(-)-2-Amino-5-phosphonopentanoic acid (D-AP5);, D-(-)-2-Amino-7-phosphonoheptanoic acid (D-AP7); enhanced green fluorescent protein (EGFP); ganglion cell layer (GCL); G-protein-activated inwardly rectifying K^+ channels (GIRK); half-blocking concentration (IC_{50}); half-activation potential ($V_{0.5}$); 4-(2-Hydroxyethyl)piperazine-1-ethanesulfonic acid (HEPES); inner nuclear layer (INL); inner plexiform layer (IPL); intrinsically photosensitive retinal ganglion cells (ipRGCs); L-(+)-2-Amino-4-phosphonobutyric acid (L-AP4); liquid junction potential (LJP); membrane potential (V_m); multielectrode array (MEA); μ-opioid receptor (MOR); 2,3-Dioxo-6-nitro-1,2,3,4-tetrahydrobenzo[*f*]quinoxaline-7-sulfonamide (NBQX); outer nuclear layer (ONL); outer plexiform layer (OPL); series resistance (R_s); (1,2,5,6-Tetrahydropyridin-4-yl) methylphosphinic acid (TPMPA); tetrodotoxin (TTX); voltage-gated calcium channel (Ca_v); voltage-gated calcium current (I_{Ca}); voltage-gated potassium channel (K_v); voltage-gated potassium current (I_K); voltage-gated sodium current (I_{Na}); command voltage at which the resulting I_K was 5% of the peak ($V_{0.05}$).

2.2 Introduction

The discovery of melanopsin-containing intrinsically photosensitive retinal ganglion cells (ipRGCs) has fundamentally altered our understanding of how light influences mammalian physiology and behavior. These ganglion cells were initially identified as a third photoreceptor type that respond to environmental light cues and help synchronize circadian rhythms to external day/night cycles (Berson et al., 2002; Hattar et al., 2002). Since their discovery, intense research has broadened our understanding of morphology and function of ipRGCs. These photosensitive cells are now classified into several distinct subtypes (M1-M6 cells) that, as a group, send axons

to diverse brain areas that participate in both image-forming and non-image-forming vision (Baver et al., 2008; Schmidt and Kofuji, 2009; Ecker et al., 2010; Schmidt et al., 2011; Lee and Schmidt, 2018; Quattrochi et al., 2108). In addition, ipRGCs have been implicated in light-mediated pathological processes such as light-evoked exacerbation of migraine headache (photophobia) (Noseda et al., 2010) and altered mood and cognitive function associated with irregular light schedules (LeGates et al., 2012).

Although capable of producing light responses intrinsically (Berson et al., 2002; Hartwick et al., 2007), ipRGCs receive rod/cone-mediated light information through synapses employing fast excitatory and inhibitory transmitters (Perez-Leon et al. 2006; Wong et al. 2007; Schmidt et al. 2008). IpRGCs are also subject to neuromodulatory influences that tune their signaling to physiological needs. For example, dopamine acts through D1 receptors to directly modify ipRGC signaling (van Hook et al., 2012). Adenosine inhibits light-stimulated responses in ipRGCs via A1 receptor activation (Sodhi and Hartwick, 2014), and somatostatin has been implicated in parallel inhibition of dopaminergic amacrine cells and ipRGCs (Vuong et al., 2015). Acetylcholine stimulates ipRGC spiking even in the absence of light through a muscarinic receptor-mediated mechanism (Sodhi and Hartwick, 2016).

We have previously confirmed the expression of the endogenous opioid, β-endorphin, and its preferred receptor, the μ-opioid receptor (MOR), in the mouse retina (Gallagher et al., 2010, 2012). Specifically, we have shown that besides dopaminergic amacrine cells, other GAD-67-expressing amacrine cells and some Brn3a-positive ganglion cells also express MORs (Gallagher et al., 2012). Here we show that the M1-M3 types of ipRGCs express MORs in both rats and mice. Further, we show that exogenously applied opioids acting on MORs inhibit light-evoked ipRGC signaling two ways: by delaying the onset of light-evoked firing and by reducing

the duration of spiking. We propose that the delayed onset of light-evoked firing is caused by a shift in the activation of voltage-gated potassium currents (I_K) to hyperpolarized potentials, thereby elevating the current threshold of voltage-gated sodium currents (I_{Na}) and spike initiation. We provide evidence that the MOR-mediated reduced duration of light-evoked spiking of ipRGCs results from suppression of non-inactivating voltage-gated calcium currents. These findings outline a previously unrecognized role for endogenous opioids in the mammalian retina.

2.3 Materials and Methods

Animals

Animals were handled in compliance with the Institutional Animal Care and Use Committees of Colorado State University, Ohio State University, and Brown University, and all procedures met United States Public Health Service Guidelines. Every effort was made to minimize the number of animals used and to mitigate any possible discomfort. Experiments were performed using both rat and mouse tissue. Rats were young (postnatal day 6-11) or adult (>3 months) males and females of the Sprague Dawley strain (Harlan Laboratories, Indianapolis, IN). For multielectrode array experiments on adult rat retinas, adult (>3 months) males and females of the Long-Evans strain were utilized (Charles River, Wilmington, MA). Mice were of the transgenic Tg(*Opn4*-EGFP)ND100Gsat/Mmucd strain, generated by the GENSAT project. These mice carry a bacterial artificial chromosome (BAC) in which the melanopsin (*Opn4*) promoter drives expression of enhanced green fluorescent protein (EGFP); for simplicity, they will be referred to here as *Opn4*::EGFP mice. Animals were kept on a 12 hr light:12 hr dark cycle, with lights on at 6:00 AM, and were fed standard chow and water ad libitum. Adult rats were anesthetized with 0.2ml sodium pentobarbital (i.p. injection) or isoflurane (inhalation) and

euthanized by decapitation; postnatal day 6-11 (P6-P11) rats, and wildtype mice were anesthetized with isoflurane and euthanized via decapitation, *Opn4*::EGFP mice were euthanized with CO_2 asphyxiation or anesthetized with isoflurane and euthanized via decapitation.

Patch-clamp recording solutions

For investigation of ipRGC excitability in whole cell current-clamp experiments, a K-gluconate based internal solution was used. It contained (in mM) the following: 110 K-gluconate, 7 phosphocreatine-di(tris) salt, 10 L-ascorbic acid, 2 EGTA, 3 Mg-ATP, 0.5 Na-GTP, 20 KCl, 10 HEPES, pH 7.2 (adjusted with KOH) and osmolarity of 300 ± 5 mOsmol. For isolation of I_K in whole-cell voltage-clamp, 2 mM QX 314 was added to the above K-gluconate based internal solution to block I_{Na} with appropriate adjustments made to the solution to maintain constant osmolarity. For I_{Ca} recordings, a Cs-gluconate based internal solution was used that contained (in mM) the following: 100 Cs-gluconate, 10 phosphocreatine-di(tris) salt, 10 L-ascorbic acid, 2 EGTA, 3 Mg-ATP, 0.5 Na-GTP, 10 tetraethylammonium chloride, 0.1 $CaCl_2$, 10 NaCl, pH 7.2 (adjusted with CsOH) and osmolarity of 300 ± 5 mOsmol, and the extracellular solution was supplemented with 5 mM $CaCl_2$ (Hu et al., 2013). The standard extracellular / bathing solution was Ames' medium (US Biological), with osmolarity of 300 ± 10 mOsmol constantly gassed with 95% O_2 / 5% CO_2. [D-Ala^2, MePhe^4, Gly-ol^5]-enkephalin (DAMGO), H-D-Phe-Cys-Tyr-D-Trp-Arg-Thr-Pen-Thr-NH_2 (CTAP), H-D-Phe-Cys-Tyr-D-Trp-Orn-Thr-Pen-Thr-NH_2 (CTOP), QX 314 and 4-Aminopyridine (4-AP) were obtained from Tocris Bioscience (Bristol, UK). Tetrodotoxin (TTX) obtained from Alomone Labs (Jerusalem, Israel). Other salts or chemicals were purchased from Sigma (St. Louis, MO).

Dissociated ipRGC preparation for loose patch recording

Eyes were enucleated and hemisected posterior to the limbus; the lens and vitreous humor were removed. Retinal neurons from *Opn4*::EGFP mice were dissociated using enzymatic digestion for 30 min at 37°C with 20 U/mL papain (Worthington, Lakewood, NJ), 1mM L-Cysteine, B-27 (Invitrogen, Grand Island, NY), 0.5 mM GlutaMAX (Gibco, Grand Island, NY), and 0.004% DNase in Hibernate-A without calcium (BrainBits, Springfield, IL). The cells were centrifuged (3 min at 200g) then washed and gently triturated with Hibernate-A (with calcium) containing 10% (vol/vol) heat-inactivated fetal calf serum, 0.004% DNAse and 0.5 mM GlutaMAX. Retinal ganglion cells (RGCs) were enriched by incubating with magnetic nanoparticles conjugated to antibodies towards the pan-RGC surface marker Thy1.2 and filtering the suspension through a 30μm Pre-Separation Filter and magnetic columns (Miltenyi Biotec, Auburn, CA). The eluted RGCs were then plated and cultured on coverslips for 18-64 hr as previously described (Van Hook et al., 2012) with culturing additives (Chen et al., 2008).

Dissociated ipRGC preparation for whole cell recording

IpRGCs were enzymatically dissociated from *Opn4*::EGFP mouse retina as previously described (Meyer-Franke et al., 1995; Van Hook and Berson, 2010). In brief, eyes were enucleated and hemisected posterior to the limbus; the lens and vitreous humor were removed. Retinas were detached in dark from the retinal pigmented epithelium and incubated for 15 min at 37˚C in a papain solution (10 U/ml, Worthington; Lakewood, NJ). After rinsing in a papain free solution, manual trituration was performed with a large-bore Pasteur pipette and dissociated cells were plated on poly-d-lysine/laminin coated coverslips (Corning™BioCoat™; Bedford, MA) followed by overnight incubation in MACS® NeuroMedium without L-Glutamine (Miltenyi Biotech; Auburn, CA). The medium was supplemented with MACS® NeuroBrew-21 as per the manufacturer's instructions, antibiotics (100 u/ml penicillin and 100 μg/ml streptomycin), ciliary

neurotrophic factor (10 ng/ml; Sigma), brain-derived neurotrophic factor (25 ng/ml; Sigma), and forskolin (5 mM; Tocris; Ellisville, MO). Coverslips were transferred to a perfusion chamber mounted on an upright microscope (Akioskop 2 FS plus, Zeiss) and superfused at 2-5 ml/min with 300 ± 10 mOsmol bicarbonate buffered Ames' medium (US Biological; Swampscott, MA) constantly gassed with 95% O_2 / 5% CO_2. Coverslips were viewed through a 40X water immersion objective, infrared differential contrast, and an infrared CCD camera with 2.5 pre-magnification (XC-75; Sony, Japan) connected to a Camera Controller C2741–62 (Hamamatsu; Japan), which directed output to a 19" monitor (Westinghouse; Santa Fe Springs, CA). Dissociation yielded a mixture of retinal neurons from which M1 ipRGCs were identified based on their large size (~ 10 μm) and bright green fluorescence.

Multielectrode array recordings of opioid effects on ipRGC photoresponses

Retinas of P6-P10 rats were isolated from eye cups in bicarbonate buffered Ames' medium (A1372-25; US Biological, Swampscott, MA) supplemented with 0.1 mM EGTA (Sigma) and bubbled with 95% O_2 /5% CO_2. A flat portion of the central retina not including the optic nerve head was placed with the ganglion cell layer down on a multielectrode array (60MEA200/30iR-ITO; Multi Channel Systems, Reutlingen, Germany) and was secured with nylon mesh and a wire weight. For all recordings, retinas were superfused with Ames' medium constantly gassed with 95% O_2 /5% CO_2 at 37 °C. Synaptic inputs to ipRGCs were blocked by bath application of a cocktail of pharmacological agents in Ames' medium as previously described (Wong et al., 2007; Perez-Leighton et al., 2011). The cocktail contained 100 μM L-(+)-2-Amino-4-phosphonobutyric acid (L-AP4), 30 μM D-(-)-2-Amino-5-phosphonopentanoic acid (D-AP5) or 100 μM D-(-)-2-Amino-7-phosphonoheptanoic acid (D-AP7), 25 μM 2,3-Dioxo-6-nitro-1,2,3,4-tetrahydrobenzo[f]quinoxaline-7-sulfonamide (NBQX), 50 μM picrotoxin,

5 μM [S-(R*,R*)]-[3-[[1-(3,4-Dichlorophenyl)ethyl]amino]-2-hydroxypropyl](cyclohexylmethyl) phosphinic acid (CGP54626), 50 μM (1,2,5,6-Tetrahydropyridin-4-yl) methylphosphinic acid (TPMPA), 10 μM strychnine, 10 μM atropine and 100 μM (+)-Tubocurarine chloride. Apart from the experiment shown in Fig 3Ai-Aiv, single doses (1 nM-10 μM) of DAMGO were bath applied with the synaptic blockers. Results were considered for further processing only if DAMGO-mediated (inhibitory) effects were reversed with 1μM-10μM of D-Phe-Cys-Tyr-D-Trp-Orn-Thr-Pen-Thr-NH_2 (CTOP, a MOR-selective antagonist). Apart from atropine and strychnine (Sigma), all pharmacological agents were obtained from Tocris (Ellisville, MO).

Full-field light stimuli were generated using a light-emitting diode (470 nm; Digikey, Thief River Falls, MN). The intensity of light pulses was set to 7.5 x 10^{14} photons cm^{-2} s^{-1} by a function generator (Berkley Nucleonics, CA) and calibrated by an optical power meter (Newport, model 1918-C). Retinas were dark adapted for at least one hour prior to initial light stimulation. Responses to 20 s flashes presented every 15 min were recorded, amplified, band-pass filtered between 500 Hz and 1.5 kHz, and digitized at 25 kHz using MCRack software (Multi Channel Systems). Spikes were isolated using a -4.5 standard deviation of noise threshold filter (MCRack software, MCS).

Adult rats were dark adapted for 1 h prior to enucleation, and the retinas were dissected under dim red light. Retinas were placed RGC-side down on multielectrode arrays as described above for the neonatal retinas. Prior to recordings, array-mounted retinas were stored in Hibernate-A medium plus 2% B-27 supplements (Life Technologies), and during recordings, the superfusing Ames' medium was buffered with 10 mM HEPES (pH 7.4) and constantly gassed with 100% O_2. The light stimulus (20 s duration) was generated by a blue LED source (470 nm,

Colibri system, Zeiss, Germany) and delivered through a 40x objective on an upright microscope (Axio Examiner, Zeiss) in previous work (Sodhi and Hartwick, 2014). The irradiance of the 20 s light stimulus was 3.9×10^{15} photons cm^{-2} s^{-1} at 470 nm. After an initial light pulse to confirm retina viability, the array-mounted adult rat retinas were superfused with a cocktail of glutamatergic antagonists (100 μM L-AP4, 25 μM NBQX, 10 μM MK-801) to block rod/cone-driven excitatory signaling.

Cluster analysis of the isolated spike data (obtained from both neonatal and adult rat retinas) was performed using Offline Sorter (Plexon Inc., Dallas, TX) in two consecutive steps (first using a T-distribution Expectation-Maximization algorithm followed by iterative K-means sorting) and then the number of spikes in 1 s bins were separated and counted using Neuroexplorer (Plexon Inc. Dallas, TX). Only cells with robust intrinsic light responses were used for further analysis; specifically, all analyzed cells produced at least twice as many spikes during the first 10 seconds of light stimulation as during the 10 seconds immediately preceding the light stimulation (i.e., in darkness). Due to these relatively strict criteria, the cell sample was likely biased towards the selection of M1-type ipRGCs. Further information on the spike sorting and ipRGC identification criteria can be found in previous work (Sodhi and Hartwick, 2014, 2016).

Peristimulus time histograms for each channel (1 ms binwidth) were normalized to their maximum spike frequency, then pooled and averaged across channels to yield a light response for a given retina. The duration of the light response was defined as the time (in seconds) from light onset to the time when binned spike frequency fell below the prestimulus baseline. Using Graphpad Prism software, best-fit dose response curves were generated for DAMGO concentrations of 1 nM-10 μM. We used the following two alternative output measures: the

duration of light response and the average number of spikes during the 20 s light stimulus. Both measures were normalized to their control value, assessed under synaptic blocker cocktail (presented as mean ± SEM).

When testing the effect of DAMGO on ipRGC photoresponses, individual retinas were exposed to only a single concentration; concentrations across experiments ranged from 1 nM-10 μM. Only ipRGCs showing recovery of photoresponses in the MOR antagonist CTOP were included in the analysis. We assessed the magnitude of the opioid effect from the duration of the light-evoked spike train spiking and the number of spikes fired during the light stimulation, both normalized to pre-drug control responses. Normalized data were then averaged across all recorded ipRGCs exposed to a given DAMGO dose to generate dose-response curves.

Whole cell voltage- and current-clamp recording from dissociated, solitary ipRGCs.

A horizontal puller (model p-97, Sutter; Novato, CA) was used to pull patch pipettes of 5–15 MΩ from 1.5-mm-diameter, thick-walled borosilicate glass (World Precision Instruments; Sarasota, FL). The pipettes were subsequently coated with dental wax (Cavex; Netherlands) to minimize stray pipette capacitance. Whole-cell voltage- and current-clamp recordings were made from dissociated ipRGC somas using an EPC-10 USB patch-clamp amplifier and Patchmaster software (version 2.3; HEKA) at room temperature during daytime. Membrane current and voltage data were filtered at 3 kHz. Recordings with leak >50 pA at -70 mV holding potential and/or series resistance (R_s) >30 MΩ at any time during the recording were terminated and excluded from analysis. Similarly, if the leak or R_s changed more than 44% and 13%, respectively during the recording, data was not considered for further analysis (see Results for details). The holding current to set the holding potential at -70 mV at break in was determined in voltage-clamp mode and maintained via Patchmaster's "Gentle CC-switch" function in current-

clamp mode. Membrane potential spikes were evoked from ipRGCs using a current-clamp ramp protocol that lasted 2 seconds and extended from -20 to 25 pA relative to the holding current injection required to introduce -70 mV membrane potential; the sampling rate was 20 kHz. Voltage-gated potassium current (I_K) was evoked by a voltage-clamp ramp protocol that lasted 2 seconds and extended from -100 to 50 mV (sampled at 5 kHz) or with 500 ms voltage-clamp steps between -120 mV and 50 mV in 5 mV increments, with a 5 second interval between each step (sampled at 50 kHz). Inactivating and non-inactivating portions of the total I_{Ca} were determined as previously described (Hu et al., 2013). In brief, ipRGCs were held at -80 mV and subjected to a voltage-clamp step protocol consisting of 150 ms steps, from - 90 mV to 30 mV in 10 mV increments, with 2 seconds between steps and a sampling rate of 50 kHz to obtain total I_{Ca}. To reveal the non-inactivating portion of I_{Ca}, cells were then held at - 40 mV to apply steps from -40 mV to 30 mV in 10 mV increments, with 2 seconds between steps.

Loose patch recording of light responses of dissociated, solitary ipRGCs.

Following identification of an ipRGC by EGFP fluorescence, the cell was dark adapted for 10-30 minutes, and drugs were bath-applied 1-2 minutes prior to a 10 s light stimulus. White light stimuli (2.7×10^{15} photons cm^{-2} s^{-1} at 500 nm) were generated by a 100 W tungsten-halogen lamp and blue light stimuli (10^{14} photons /cm^2/s at 470 nm) by a LED (Digikey, Thief River Falls, MN). To record light-evoked spiking of single ipRGCs at room temperature pipettes made of borosilicate glass were filled with extracellular solution.

Recording light-evoked responses from ipRGCs in whole-mount preparation.

Euthanasia of *Opn4*::EGFP mice and tissue preparation for whole-mount preparation were performed under infrared illumination. Both eyes were enucleated and retinas were detached from the retinal pigment epithelium and placed in Ames' medium gassed with 95%

O_2/5% CO_2 at room temperature. A piece of retina was secured with a tissue anchor (harp) to the glass bottom of a superfusion chamber with the ganglion cell layer up. The retinas were visualized with an upright microscope (Axioskop; Zeiss) with a custom-built infrared LED (940 nm; Osram) light source through a 40x water-immersion objective coupled to a 2.5x magnification Optovar (Zeiss) and camera (AxioCam; Zeiss). The chamber sat in a light-tight Faraday cage and except during brief epifluorescence viewing (470±20 nm) to locate EGFP-positive large, putative M1 type ipRGCs, the retina was maintained in darkness. In the presence of synaptic blocking cocktail (see Multielectrode array recordings) retinas were stimulated with full-field blue light (10^{14} photons cm^{-2} s^{-1} at 470 nm) stimuli with an LED (Digikey, Thief River Falls, MN) positioned 3 cm above the preparation at a 30° angle. The LED voltage was controlled by the EPC-10 (HEKA Electronik) through D/A output. Whole cell voltage- and current-clamp recordings were made from ipRGCs using an EPC-10 USB patch-clamp amplifier and Patchmaster software (version 2.3; HEKA) at room temperature as described for solitary ipRGCs above.

Data analysis

Data was analyzed off-line using IgorPro software (version 5.03; Wavemetrics), SigmaPlot (version 11; Systat Software), and Excel (Microsoft). Current ramp evoked spike threshold was defined as the membrane potential value at which the sharpest phase of the voltage-gated Na^+ influx-mediated depolarization started, and current threshold was defined as the injected current which correlated with the spike threshold (Hu et al., 2013). Current-clamp recordings were neither baseline-subtracted nor normalized. For I_K analysis, voltage-clamp ramp and step evoked I-V curves were leak subtracted and normalized to the peak (Tooker et al., 2013). Briefly, leak current, estimated from extrapolation of the slope of the line between -100 to

-60 mV in voltage-clamp ramp experiments or the first 13 points i.e. from - 120 to -60 mV in voltage-clamp step experiments, was subtracted from the raw recording to determine the actual I_K. The normalized, leak-subtracted ramp and step evoked I-V curves were then fit using SigmaPlot with the following third order sigmoidal equation:

$$I = a/(1+\exp(-(V-V_{0.5})/b))$$

where $V_{0.5}$ is the half-activation potential, b is the slope of the voltage dependency, and a is the maximal I_K (constrained to 1 for normalized traces). I-V kinetic analysis was performed using SigmaPlot. Activation was defined as the voltage at which the resulting I_K was 5% of the peak ($V_{0.05}$) and half-activation as the voltage at which the resulting current was 50% of the peak ($V_{0.5}$). For I_{Ca} analysis, voltage-clamp step evoked I-V curves were generated from leak subtracted data (Hu et al., 2013; Tooker et al., 2013), with the first three points (-90, -80, -70 mV) used to estimate the leak current for extrapolation. The total I_{Ca} ($I_{Ca,total}$) was considered to be the I_{Ca} elicited by the step protocol applied to the cell held at -80 mV. The non-inactivating component of I_{Ca} ($I_{Ca,non\text{-}inact}$) was considered to be the I_{Ca} elicited by the step protocol applied to the cell held at -40 mV. The inactivating component of I_{Ca} ($I_{Ca,inact}$) was calculated as the difference between the total and the non-inactivating component ($I_{Ca,total} - I_{Ca,non\text{-}inact} = I_{Ca,inact}$).

Liquid junction potential (LJP) was calculated as 13.05 mV for I_K and 13.1 mV for I_{Ca} recordings. All voltage-clamp recordings were a posteriori corrected for LJP.

Statistics were performed with SigmaPlot (version 11; Systat Software) and Excel (Microsoft). Paired and unpaired Student t-tests, Mann-Whitney Rank Sum tests, and one way ANOVA were used for comparisons between groups of paired traces. Data are presented as mean ± SEM and $p < 0.05$ considered significant.

Immunohistochemistry.

Immunohistochemical procedures were conducted as previously described for retinal sections (Gallagher et al., 2010). In brief, animals were deeply anesthetized with isoflurane and decapitated before both eyes were enucleated. A small incision was made anterior to the ora serrata, and the whole eye was fixed at room temperature in freshly prepared 4% paraformaldehyde in 0.1 M phosphate buffered saline (PBS; pH 7.35) for 15 min. The cornea and lens were removed and the eyecups left in the same fixative solution for an additional 5 min. Fixed eye cups were cryoprotected in 30% sucrose overnight, embedded in OCT (Ted Pella Inc.) and cut into 20 μm thick vertical sections. Sections were mounted on glass slides and stored frozen until immunostained. The melanopsin immunolabeling was done according to a previously described protocol (Van Hook et al., 2012); primary antibody: c26962, 1:50; Santa Cruz Biotechnology, Santa Cruz, CA). Methods for anti-MOR immunostaining (AOR-011, 1:200; Alomone Labs, Jerusalem, Israel) were also described previously (Gallagher et al., 2012). Retinal sections from *Opn4*::EGFP mice in some cases were also colabeled with an anti-GFP antibody (ab13970, 1:500; Abcam, Cambridge, MA). Fluorescent images were taken with a Zeiss LSM 800 confocal microscope (Carl Ziess, Oberkochen, Germany). For all acquisitions, sequential scans at the different wavelengths were performed. Z-stack images through the full thickness of immunolabeled tissues were taken at 40x, with 1 μm increments between images. Brightness and contrast of images were adjusted uniformly in Photoshop CS3 (Adobe 10.1). Images were compiled and analyzed using Zeiss LSM Image Examiner software (Carl Zeiss, Oberkochen, Germany). Subjective assessment of fluorescent signal colocalization was performed on single plane optical sections.

2.4 Results

ipRGCs express μ-opioid receptors in rat and mouse retinas.

We detected immunoreactivity for μ-opioid receptors (MORs) in ipRGCs of both rats and mice. In adult rats (n=3), substantial anti-MOR immunolabeling marked the inner retina (Fig. 2.1A). The labeling pattern resembled that observed previously in mice (Gallagher et al., 2012), but in the rat retina, labeling of the inner plexiform layer (IPL) was more robust, with discernible MOR+ processes. The anti-melanopsin antibody strongly labeled ipRGCs of the M1 type, with dendrites extending into the outermost layer of the IPL (Fig. 2.1B, white arrow). The M2/M3 types were also identified as more weakly immunolabeled cells of the ganglion-cell layer, often with dendrites extending into the innermost layer of the IPL (Fig. 2.1F, white arrow). Melanopsin+ dendrites were invariably MOR immunoreactive (Fig. 2.1, white arrow, 28/28 dendrites from 3 animals). Melanopsin+ cell bodies were also typically labeled by the MOR antibody, although usually more weakly than the dendrites (Fig. 2.1: hollow arrowhead, insets).

To evaluate MOR expression in mouse ipRGCs, we used retinas from adult *Opn4*::EGFP melanopsin reporter mice (n=3). In other melanopsin reporter mice generated by using BAC technology (Schmidt et al., 2008; Do et al., 2009), only ipRGCs of the M1, M2 and M3 types express detectable levels of the fluorescent reporter evidenced by the high coincidence of transgenic reporter protein and melanopsin immunolabeling (Lee and Schmidt, 2018); similarly, in the *Opn4*::EGFP mice we found that 173 of 182 EGFP-expressing cells were also melanopsin+. M1 cells are easily distinguished from the other types by their brighter fluorescence and dendritic arborizations in the outer IPL (Fig. 2.2B). The pattern of MOR immunolabeling resembled that previously reported in wild type mice (Gallagher et al., 2012), with heaviest MOR immunolabeling occurring in a minority of somata in the inner nuclear and ganglion-cell layers (INL and GCL), as well as puncta and some dendritic profiles in the IPL. Nearly all EGFP+ somas of ipRGCs were strongly MOR immunopositive (173/182 cells from 3

animals; Fig. 2.1E-H). The double labeled cells included M1 ipRGCs (including 'displaced' M1s, with somata in the INL), M2 cells (characterized by weak EGFP fluorescence and processes in the inner IPL), as well as M3 cells with bistratified dendrites occupying the same layers as M1 and M2 cells (Pickard et al., 2011) (Fig. 2.2H, hollow arrowhead and white arrow, respectively). Importantly, ipRGCs dissociated enzymatically from the *Opn4*::EGFP mouse retina showed positive immunolabeling with the anti-MOR antibody, suggesting MOR expression (Fig. 2.2I-M).

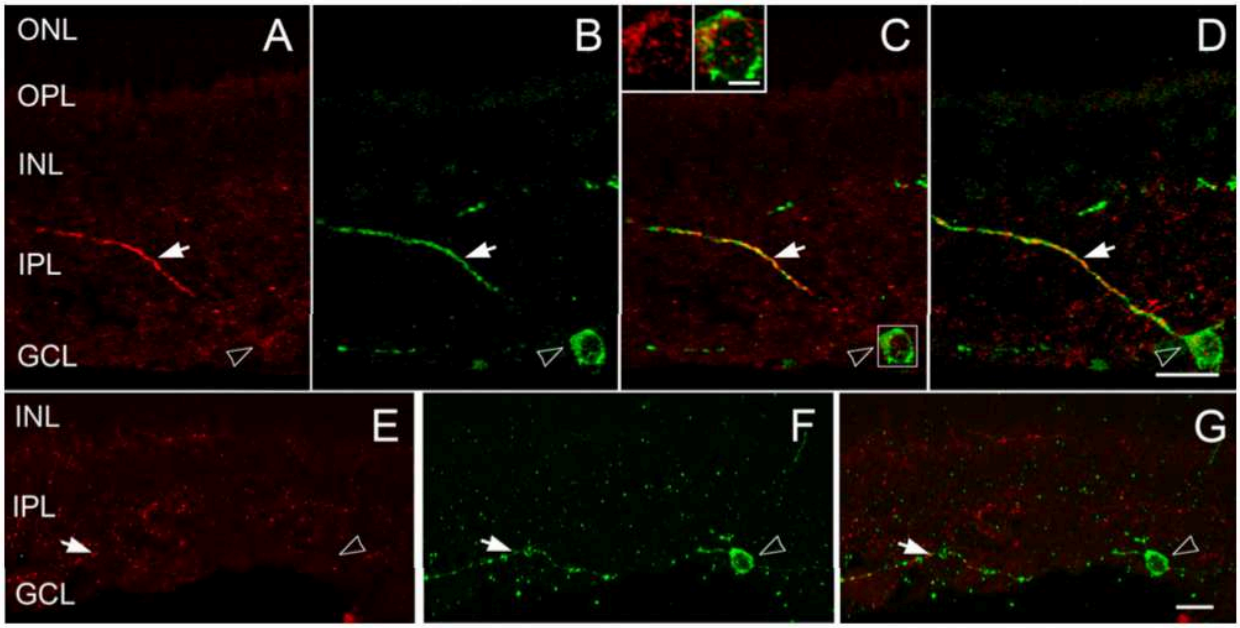

Figure 2.1. In the rat retina M1 ipRGCs are immunopositive for μ-opioid receptors (MORs). A: Single-plane confocal image of vertically sectioned adult rat retina showing a MOR+ dendrite (red) within the IPL (white arrow). Weaker MOR immunofluorescence is apparent in a ganglion cell body (hollow arrowhead). **B:** Immunolabeling for melanopsin (green) in the same optical section as in **A**, showing a single melanopsin+ ipRGC soma in the GCL (hollow arrowhead) and a well-labeled dendrite in the IPL (white arrow). **C:** A merged image of **A** and **B**, showing that the same cell is immunoreactive for MOR and melanopsin. Inset: expanded view of MOR+ labeling of melanopsin+ ipRGC soma marked by the box in C (brightness and contrast adjusted). **D:** Projected image compiled from five single-plane Z-stack confocal images of the same field of view as in A-C showing that the melanopsin immunopositive dendrite derives from the labeled soma; this appears to be an M1 cell based on its strong melanopsin staining and dendrites ascending into the outer IPL. Note that punctate MOR+ labeling decorates most of this dendrite. **E:** Single-plane confocal image of vertically sectioned adult rat retina showing a MOR+ dendrite (red) deep within the IPL (white arrow). **F:** melanopsin immunolabeling (green) in the same optical section as in **E**, showing a single melanopsin+ ipRGC soma in the GCL (hollow arrowhead) and a well-labeled dendrite deep in the IPL (white arrow). **G:** A merged image of **E** and **F**, showing that the melanopsin+ dendrite is immunoreactive for MOR (white arrow); based on its position at the border of IPL and GCL it originates from a putative M2 or M3 ipRGC. ONL: outer nuclear layer; OPL: outer plexiform layer; INL: inner nuclear layer; IPL: inner plexiform layer; GCL: ganglion cell layer; Scale bars: **D** and **G**: 20μm; **C inset**: 5μm.

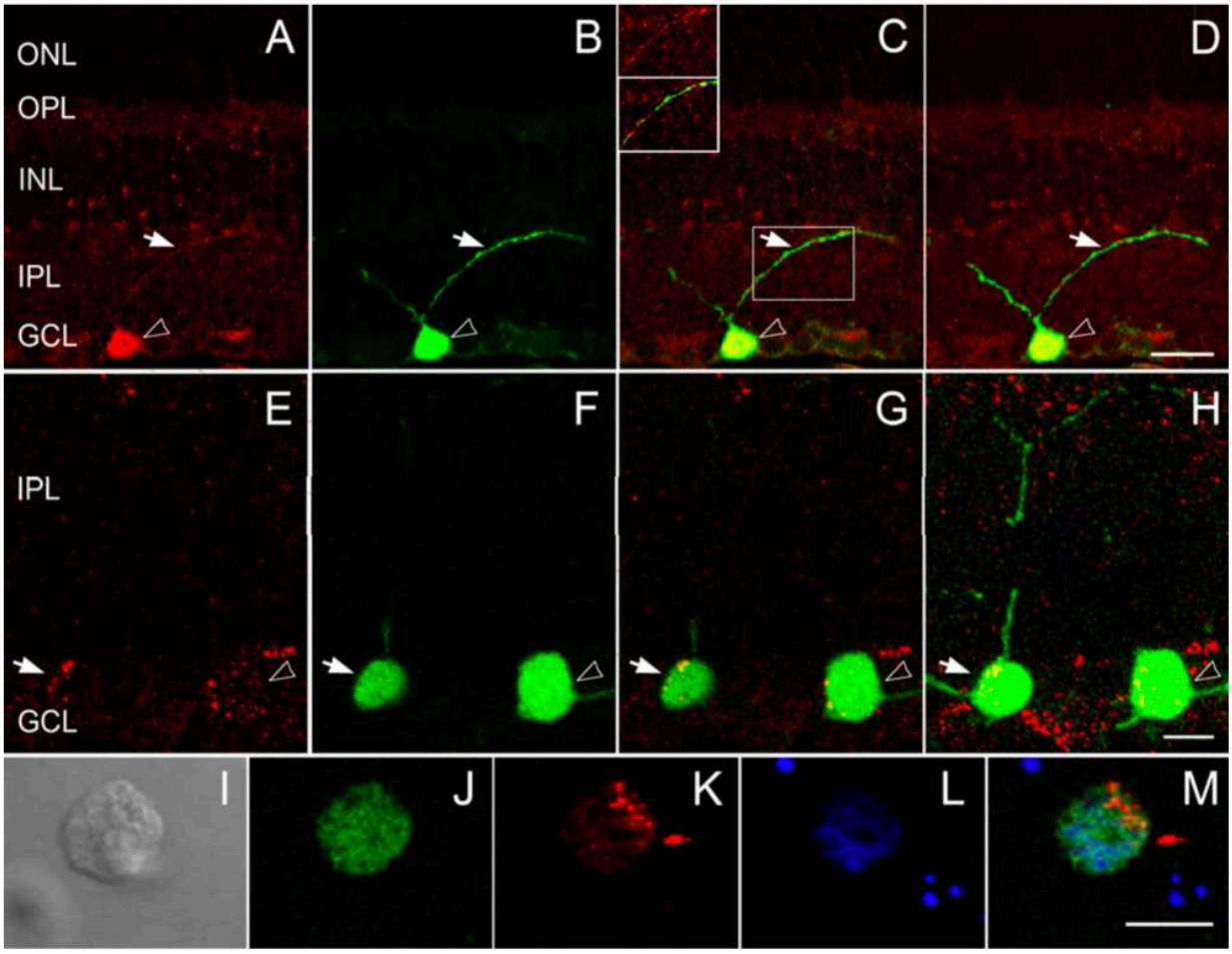

Figure 2.2. EGFP-expressing ipRGCs in the *Opn4*::EGFP mouse retina are immunopositive for μ-opioid receptors (MORs). A: Single-plane optical section of the *Opn4*::EGFP mouse retina showing red MOR immunolabeling in a soma of the GCL (hollow arrowhead) and a dendritic process in the IPL (arrow). **B:** The same optical section as in **A**, but showing a green EGFP+ ipRGC soma in the GCL (hollow arrowhead) and its processes in the IPL (white arrow). **C:** A merged image of **A** and **B**, indicating colocalization of MOR immunolabeling and EGFP in the GCL (hollow arrowhead). Weak MOR immunoreactivity also marks the dendrite (white arrow), as shown more clearly in the inset in C, represented the area marked by the rectangle in C, with brightness and contrast adjusted. **D:** Projected image of the same field of view compiled from four single-plane Z-stack confocal images. **E:** Single-plane confocal image of vertically sectioned adult *Opn4*::EGFP mouse retina showing a MOR+ puncta (red) within the GCL (white arrow, hollow arrowhead). **F:** melanopsin immunolabeling (green) in the same optical section as in **E**, showing two EGFP+ somas of putative ipRGCs in the GCL. **G:** A merged image of **E** and **F**, showing that the EGFP+ somas are immunoreactive for MOR. **H:** Projected image compiled from five single-plane Z-stack confocal images of the same field of view as in E-G revealing that EGFP+ putative ipRGCs expressing MOR+ immunolabeling are most likely M2 (hollow arrowhead) and M3 (white arrow) types based their dendritic arborization pattern. **I-M:** DIC image (**I**) of a representative EGFP-expressing (**J**), putative ipRGC enzymatically dissociated from the *Opn4*::EGFP mouse retina. The same cell shows both anti- MOR (**K**) and melanopsin immunolabeling (**L**), evident on the merged fluorescent image (**M**). ONL: outer nuclear layer; OPL: outer plexiform layer; INL: inner nuclear layer; IPL: inner plexiform layer; GCL: ganglion cell layer; Scale bars: **D**: 20μm; **H** and **M**: 10μm.

Multielectrode array recordings reveal dose-dependent μ-opioid attenuation of light responses in ipRGCs.

To test whether MOR activation affects ipRGC signaling, we recorded light-evoked spiking of ipRGCs in early postnatal rat retinas (P6-P11) on a multielectrode array (MEA). A drug cocktail blocked all major retinal neurotransmitters (GABA, glycine, acetylcholine and both ionotropic and metabotropic glutamate receptors (Wong et al., 2007; Perez-Leighton et al., 2011; Sodhi and Hartwick 2016, see *Experimental Procedures*). Synaptogenesis is incomplete in rat retinas at this young age (P6-11) (Sernagor et al., 2001), further minimizing any influence of synaptic inputs on ipRGCs in these studies.

Intrinsic photoresponses of ipRGCs were clearly modulated by bath application of the MOR-specific opioid antagonist DAMGO. Figure 2.3Ai shows the intrinsic light responses of a representative ipRGC recorded under synaptic blockade. In control medium (top), spiking remained elevated through the full stimulus duration (20 s) and persisted for many seconds after stimulus offset. This is as expected for intrinsic responses derived from melanopsin phototransduction (Emanuel and Do, 2015). The MOR-specific agonist DAMGO shortened the duration of the light response in a dose-dependent manner (Fig. 2.3Ai, 2.3Aii; doses: 10 nM, 100 nM, 1 μM and 10 μM). Even the lowest dose (10 nM) significantly reduced the number of light-evoked spikes (n=43 cells from 3 retinas, ANOVA, $p<0.05$), and the effect appeared to saturate because increasing the concentration from 1 μM to 10 μM did not further reduce the number of spikes (ANOVA, $p=0.72$). Subsequent application of the MOR- selective antagonist CTOP (10 μM) not only restored the intrinsic light responses but actually increased the number of spikes compared to the control (Fig. 2.3Ai, 2.3Aii). This increase, though slight, was significant

(ANOVA, $p<0.05$). Thus, the reduction of ipRGC in response to increasing DAMGO concentrations was not due to rundown.

A second functional effect of DAMGO application was to delay the onset of light-evoked spiking in ipRGCs (Fig. 2.3Aiii, 2.3Aiv). Group data revealed no clear dose dependence of this effect (Fig. 2.3Aiv), and dose-response curves for individual cells were highly variable (Fig. 2.3Aiii). Nonetheless, for the population of ipRGCs (n=43 cells from 3 retinas) DAMGO significantly increased the delay to the first spike (Fig. 2.3Aiv). The MOR antagonist CTOP (10 μM) reversed the opioid-induced delay to levels statistically indistinguishable from the initial control response (ANOVA, $p=0.96$).

Importantly, the robust effects on spiking of DAMGO (1μM; Fig. 2.3Ai) were abolished by simultaneous application of CTOP (10 μM) (Fig. 2.3B; n=60 from 2 retinas). Application of CTOP alone (1 μM and 10 μM) did not alter the light responses of ipRGCs (Fig. 2.3C; n=52 from 3 retinas).

These results collectively suggest a dose-dependent and MOR-specific opioid modulation of ipRGC photoresponses. Because these effects may have been distorted by opioid receptor desensitization during prolonged agonist exposures (Kelly et al., 2009; Dang and Christie, 2012; Williams et al., 2013), we constructed dose-response curves for MOR-mediated inhibition of ipRGC photoresponses (see *Experimental procedures*) (Fig. 2.3Di, Dii). The dose-response relationships revealed IC_{50} values of 23 nM for the duration index (Fig. 2.3Di) and 39 nM for the spike-count measure (Fig. 2.3Dii) with saturation occurring at ~1μM in both cases. At saturating DAMGO concentrations, the suppression of the spike-count (~70%) was greater than that for the decrease in response duration (~50%). Regardless, both outcome measures indicated that the

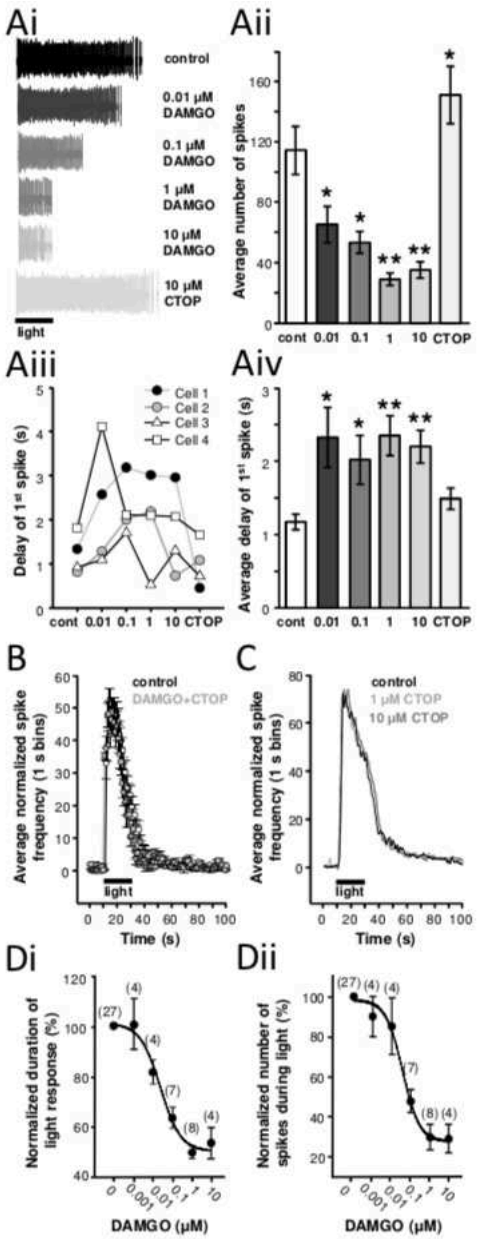

Figure 2.3. The μ-opioid-specific agonist DAMGO inhibits intrinsic light responses of ipRGCs in isolated retinas. Ai: Multielectrode array (MEA) recording of the light responses a representative ipRGC in response to a 20 s stimulation (3.9 x 10^{15} photons cm^{-2} s^{-1} at 470 nm, black bar) a P10 rat retina in the presence of increasing concentrations of MOR-selective agonist DAMGO (0.01-10 μM) followed by application of MOR-selective antagonist CTOP (10 μM). Light-evoked ipRGC spiking was greatly attenuated by DAMGO in a dose-dependent manner, and rescued by consecutive application of CTOP. **Aii**: Cumulative ipRGC light response data obtained in increasing concentrations of DAMGO (0.01-10 μM) followed by CTOP as in Ai. Data is shown as Average ± SEM, n=43 from 3 retinas. *: $p<0.05$; **: $p<0.001$. **Aiii:** Delay of the 1st light-evoked spikes of representative ipRGCs (Cell 1-4) recorded by MEA in the presence of increasing concentrations of MOR-selective agonist DAMGO (0.01-10 μM) followed by application of MOR-selective antagonist CTOP (10 μM). **Aiv:** Cumulative data summarizing 1st spike delays ipRGC light response as in Aiii. DAMGO significantly increased the 1st spike delays in all instances, whereas consecutive CTOP treatment resulted in a delay close to that observed in control. Average ± SEM, n=43 from 3 retinas. *: $p<0.05$; **: $p<0.001$. **B:** Simultaneous

application of DAMGO (1 μM) and CTOP (10 μM) did not alter light-evoked ipRGCs firing. Data is shown as Average ± SEM, n=60 from 2 retinas **C:** CTOP (1 and 10 μM) application does not alter light-evoked ipRGCs firing. Dots and error bars representing Average ± SEM were omitted for better visibility of the lines connecting the average values; n=52 from 3 retinas. **Di:** Dose-response curve of the duration of the ipRGC light responses in DAMGO (1nM-10μM). Data are plotted as a percentage of light response under control conditions (synaptic blocker cocktail without DAMGO). Parenthetical numerals indicate the number of retinas studied for each DAMGO dose. Every retina was exposed to a single DAMGO concentration. Error bars represent ± SEM. **Dii:** Dose-response curve plotting the number of spikes recorded in ipRGCs during the 20 s light stimulus as a function of the applied DAMGO concentration; data normalized as in **Di**. Parenthetical numerals indicate the number of retinas studied for each DAMGO dose.

intrinsic light response of ipRGCs in the isolated juvenile rat retina was highly sensitive to selective activation of MORs.

To determine whether similar MOR-mediated ipRGC modulation was present in more developed retinas with fully functional retinal circuit wiring, we assessed the effects of DAMGO on MEA-mounted retinas from adult (> 3 month old) rats. A saturating dose (10 μM; see Fig. 2.3Di, 2.3Dii) of DAMGO was chosen for these experiments. IpRGCs were identified by their sustained spiking responses to a bright blue light stimulus in the presence glutamate receptor antagonists (Fig. 2.4A). DAMGO significantly reduced both peak spike rate and response duration of the light response relative to control (n=6 from N=5 retinas; Fig. 2.4B; p=0.03, one way repeated measures ANOVA, Holm-Sidak post-hoc) (Fig. 2.4C). After 40 min of drug

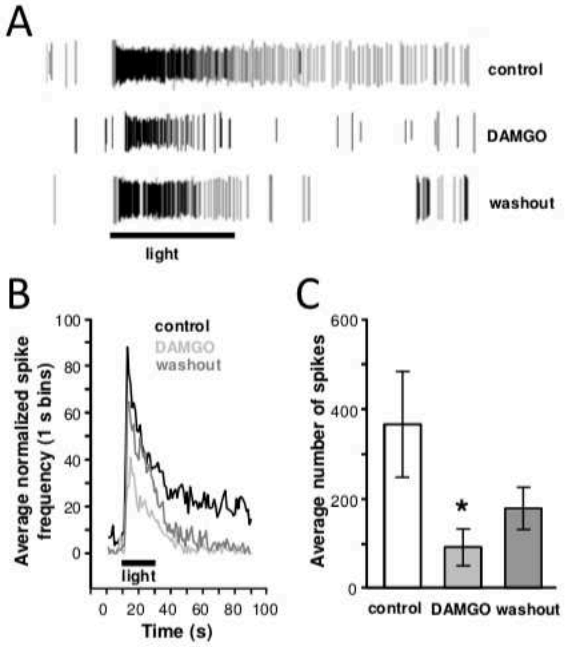

Figure 2.4. DAMGO modulates spiking activity in adult rat ipRGCs. A: Spike rasters from an example MEA recording from an ipRGC. Sustained spiking response to bright (3.9×10^{15} photons cm^{-2} s^{-1}, 10 s) blue light persisted in the presence of glutamatergic antagonists, confirming ipRGC identity. Rasters of spiking activity recorded before, during and after treatment with 10 μM DAMGO illustrates inhibitory effect of this MOR agonist on ipRGC spiking. **B:** Summary of mean spike frequency (spikes per 1 s bins) and **C:** total counts of spikes fired over 80 s period (20 s light stimulation plus 60 s post-light) by light-stimulated ipRGCs (n=6 from N=5 retinas) before during and after DAMGO treatment. *$p<0.05$, one way repeated measures ANOVA, Holm-Sidak post-hoc testing.

washout, responses exhibited partial recovery (Fig. 2.4B, 2.4C), so that the light-evoked spike count was no longer significantly different from that measured for the initial control response ($p=0.10$). Thus, the effect of DAMGO on ipRGC light responses is not restricted to early development. This is consistent with our immunohistochemical evidence demonstrating MOR localization to ipRGC dendrites in adult rat retinas (Fig. 2.1).

Loose-patch recordings from dissociated ipRGCs confirm direct modulation by μ-opioid receptors.

Though retinal cells other than ipRGCs do express MORs (Gallagher et al., 2012), the DAMGO effects on ipRGCs we observed occurred during blockade of fast neurotransmitters in our experiments. This suggests that the observed effects were likely due to direct action on MORs expressed by ipRGCs themselves. As a more stringent test of this interpretation, we made loose patch recordings from isolated ipRGCs, which have been shown to maintain their light sensitivity in primary culture (Hartwick et al., 2007; van Hook et al., 2012). We enzymatically dissociated retinas from *Opn4:*:EGFP mice and targeted the largest and brightest EGFP+ cells (presumably corresponding to M1 ipRGCs) for loose-patch single cell recordings (Fig. 2.5A). Bath application of DAMGO (1μM) diminished light-evoked spiking in isolated ipRGCs (5/5 cells), as shown for a representative cell in Fig. 2.5B. In this cell, the light response partially recovered upon long washout of DAMGO ("recovery"), but in most cases (3/5) no recovery was observed before losing the cell during the wash. It is important to note that recovery of ipRGC light responses from intact retinas recorded on the MEA, following DAMGO treatment, was not

complete after tens of minutes of wash without subsequent application of a MOR antagonist, which is consistent with the recovery paradigm used in other neural preparations following DAMGO application (Pennock and Hentges, 2011; Qu et al., 2015). Furthermore, it is important to point out that phototransduction of ipRGCs at room temperature is weaker than at 37 °C (Do et al., 2012) that might explain the more robust DAMGO-mediated inhibition of light responses in these experiments compared to the results of MEA experiments. Nonetheless, as for the earlier MEA experiments, co-application of the MOR antagonist CTOP (1μM) blocked the effects of DAMGO on the light responses of solitary, cultured ipRGCs (n=3) (Fig. 2.5C).

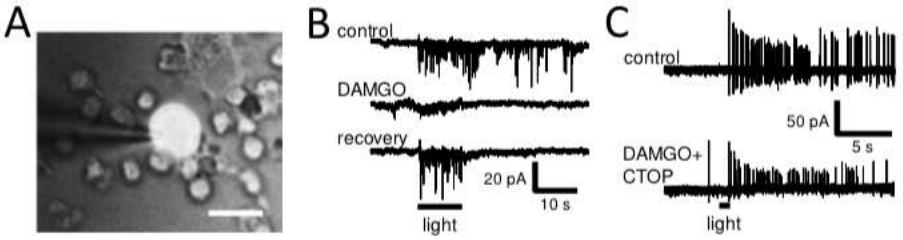

Figure 2.5. **The DAMGO modulated intrinsic light responses of dissociated ipRGCs directly, by MORs expressed by ipRGCs. A:** Direct opioid modulation of intrinsic light responses via MORs expressed by ipRGCs was revealed by loose-patch recordings of an isolated EGFP+ ipRGC dissociated from an *Opn4*::EGFP mouse retina. **B:** Representative recording showing that bath application of DAMGO (1μM) reversibly eliminated the light-evoked spikes of an enzymatically dissociated ipRGC. **C:** Simultaneous application of DAMGO (1 μM) and CTOP (10 μM) did not alter light-evoked firing of enzymatically dissociated ipRGCs.

MOR signaling reduces excitability of ipRGCs

The sequence of depolarizing events along with the ion channels that mediate the characteristically sluggish but sustained intrinsic light responses of melanopsin-expressing ipRGCs have not been fully identified, but evidence supports the involvement of TRP channels, voltage-gated sodium currents (I_{Na}), and voltage-gated calcium currents (I_{Ca}) (Warren et al., 2006; Hartwick et al., 2007; Xue et al., 2011). A set of voltage-gated and calcium-dependent potassium currents (I_K and $I_{K(Ca)}$, respectively) are also critical to repolarizing the membrane potential of ipRGCs after each spike (Hu et al., 2013).

To determine how MOR activation reduces light responses of ipRGCs, first we recorded melanopsin-driven light responses from ipRGCs in whole mount preparation, bathed in Ames' medium that was supplemented with the synaptic blocking cocktail in the presence of 2 mM Co^{2+} to block I_{Ca}; the recording pipette solution contained 2 mM QX 314 to eliminate I_{Na} (Fig. 2.6). QX 314 at this concentration is expected to slightly inhibit I_{Ca} (Talbot and Sayer, 1996), acting in concert with Co^{2+} in these experiments. Under these conditions DAMGO (1 μM)

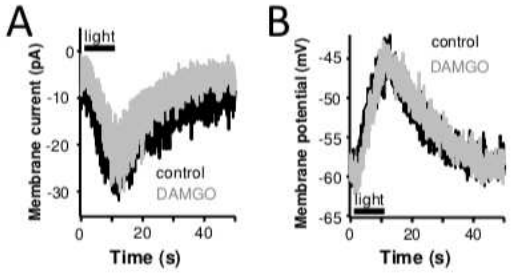

Figure 2.6. MOR agonist DAMGO did not alter the melanopsin-driven increase in light-evoked cationic conductance/depolarization in ipRGCs. Representative light responses of the same ipRGC were evoked by a 10 s light flash (10^{14} photons cm^{-2} s^{-1}, 470 nm, black bar) and recorded in voltage-clamp mode at -60 mV holding potential (**A**) or in current-clamp mode with resting potential set at -60 mV (**B**).

altered neither the light-induced inward current in voltage-clamp recordings (Fig. 2.6A; V_{hold} = -60 mV) nor the light-evoked membrane depolarization (Fig. 2.6B) of the same ipRGCs (n=3; V_m set by current injection at -60 mV). These results indicate that in ipRGCs MOR activation does not affect melanopsin-dependent phototransduction including the photocurrent flowing through TRP channels, unlike in sensory neurons where MOR activation reduces TRPV1 currents (Bao et al., 2015).

Therefore, we next tested whether MOR activation altered spiking of ipRGCs depolarized by current injections in whole mount preparations that were bathed in Ames media supplemented with the synaptic blocking cocktail. IpRGCs held at ~-70 mV resting potential in current clamp by injecting -70 pA holding current were subjected to a depolarizing current ramp from -70 pA to -20 pA over 2 s (see *Experimental procedures*). A representative recording is shown in Fig.

2.7Ai. In this cell, the depolarizing current ramp evoked the first spike with 1.68±0.04 s delay (n=15 trials) in control, but the delay increased to 1.87±0.03 s (n=15 trials) after 3 min in the presence of 1 μM DAMGO ($p<0.0004$; Student t-test). In other words, DAMGO increased the current threshold of action potential generation in this ipRGC (Fig. 2.7Aii) from 15.07 ± 0.98 pA (relative to the holding current maintaining the membrane potential at -70 mV) in control to 20.82 ± 1.08 pA (n=15; $p< 0.007$, Student t-test) but did not alter the membrane potential threshold (Fig. 2.7Aiii) for action potential generation (-54.02± 3.59 mV vs. -54.09± 3.62 mV, in

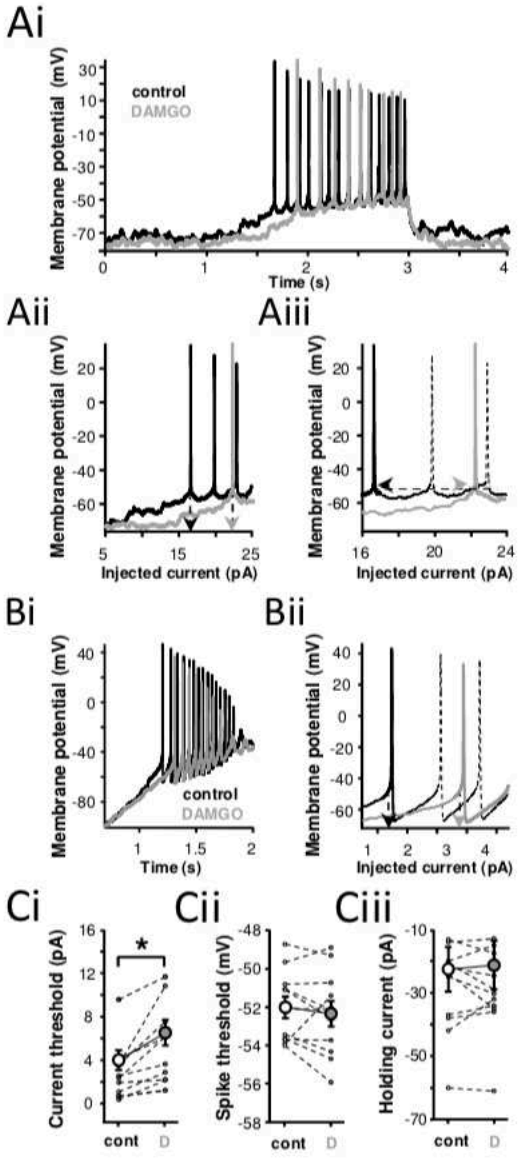

Figure 2.7. **MOR agonist DAMGO reduced excitability of ipRGCs. Ai:** Representative current clamp recording from an M1 ipRGCs made in whole mount preparation in the presence of the synaptic blocking cocktail. DAMGO (1 μM) increased delay of the 1st spike evoked by a depolarizing current ramp from -70 pA to -20 pA over 2 s, starting at 1 s. **Aii:** Replotting V_m changes shown in Ai against the injected current (relative to the holding current of -70 pA) revealed that DAMGO increased the current threshold for the 1st spike. **Aiii:** Extended timescale view of Aii shows that DAMGO did not alter the V_m threshold for spike generation in ipRGCs. **Bi:** Representative current clamp recording from an enzymatically dissociated solitary ipRGCs showing that similar to intact cells, DAMGO (1 μM) increased delay of the 1st spike evoked by a depolarizing current ramp. **Bii:** Plotting V_m changes against the injected current (relative to the holding current necessary to maintain V_m at -70 mV) from the same recordings as in Bi revealed that DAMGO increased the current threshold for the 1st spike. Note the smaller current values here, due to the higher input resistance of dissociated ipRGCs compared to the intact ones in situ (Aii). **Ci:** Summary graph showing that current threshold for spike generation is significantly increased by DAMGO (D) compared with control (cont). White circles represent control; gray circles represent DAMGO. *$p < 0.004$ (paired Student t test). n=11. **Cii:** Summary graph showing that membrane potential (V_m) threshold for spike generation was not altered by DAMGO (D) compared with control (cont). White circles represent control; gray circles represent DAMGO. $p=0.37$ (paired Student t test) n=11. **Ciii:** Summary graph showing that holding current necessary to maintain V_m at -70 mV was not altered by DAMGO (D) compared with control (cont). White circles represent control; gray circles represent DAMGO. $p= 0.51$ (paired Student t test). n=11.

control and DAMGO, respectively). Importantly, DAMGO application did not cause a significant change in the resting membrane potential measured just before the depolarizing ramp (-79.47± 1.14 mV vs. -76.76± 0.87 mV, in control and DAMGO, respectively; p=0.07, Student t-test). Similar results were obtained from two other intact ipRGCs in whole mount preparation.

To confirm that DAMGO exerted its effect on the excitability of ipRGCs directly, via MORs expressed by ipRGCs, we turned to solitary ipRGCs enzymatically dissociated from the *Opn4*::EGFP mouse retina. In solitary, dissociated ipRGCs, as in intact retina, DAMGO (1 μM) consistently increased the delay of the first spike evoked by a depolarizing current ramp (Fig. 2.7Bi) by increasing the current threshold of action potential generation (Fig. 2.7Bii) from 3.95 ± 1.05 pA (relative to the holding current injected to maintain the membrane potential at -70 mV) in control to 6.02 ± 1.20 pA (n=11, paired Student t-test, $p < 0.004$) (Fig. 2.7Ci) without affecting the membrane potential threshold for spike generation (Fig. 2.7Cii) that was -52.06 ± 0.56 mV in control and -52.39 ± 0.66 mV in DAMGO (n =11; p = 0.37, paired Student t-test). Importantly, DAMGO did not alter the holding current injected into ipRGCs to maintain their resting V_m at -70 mV (Fig. 2.7Ciii), indicating that in ipRGCs DAMGO did not activate G-protein activated

inward rectifier K^+ currents (GIRK) (Pennock and Hentges, 2011) that are widely distributed effectors of MOR signaling in the CNS (Williams et al., 2001, 2013) .

In parallel experiments, pretreatment of solitary ipRGCs with the MOR selective antagonist CTAP (1 μM) did not alter current threshold for depolarizing current ramp-evoked action potentials (2.18 ± 0.6 pA) compared to control (3.39 ± 0.86 pA) or to that seen during the consecutive application of CTAP+DAMGO (1 μM each) (2.37 ± 0.66 pA) (n=5-8, p=0.19, one way repeated measures ANOVA, data not shown). Similarly, the membrane potential threshold of depolarizing ramp-evoked action potential firing did not change in consecutive treatments with CTAP and CTAP+DAMGO (control: -50.28 ± 1.12 mV; CTAP: -50.32 ± 0.93 mV; CTAP + DAMGO: -50.61 ± 0.89 mV, n=5-8, p=0.43, one way repeated measures ANOVA, data not shown).

Effectors of MOR signaling in ipRGCs

The above results collectively suggested that MOR signaling altered the excitability of ipRGCs without interfering with the melanopsin-mediated signal transduction, TRP channel function, or by opening GIRK channels. Furthermore, the fact that DAMGO did not alter the membrane potential threshold for spike generation indicated that I_{Na} in ipRGCs is not modulated upon MOR activation; this is consistent with the lack of evidence for I_{Na} being an effector of MOR signaling-evoked neuronal responses.

To test whether MOR activation affects voltage-gated potassium currents (I_K) of enzymatically dissociated ipRGCs, I_K was isolated in the presence of 2 mM Co^{2+} in the bath solution to eliminate I_{Ca} and by using a recording pipette solution containing 2 mM QX 314 to eliminate $I_{Na.}$ I_K was then evoked in voltage-clamp using both depolarizing voltage steps and depolarizing ramp protocols (see *Experimental procedures*). DAMGO (1 μM) shifted activation

($V_{0.05}$) of I_K to more negative potentials regardless of the voltage-clamp protocol (i.e., sequential steps or continuous ramp). When depolarizing ramps were used, 6-10 minutes of DAMGO (1 μM) application reduced the activation threshold ($V_{0.05}$) of I_K (Fig. 2.8Ai) from -39.44± 2.85 mV in control to -51.43 ± 3.36 mV (n=10, p<0.001, paired Student t test) as well as the half activation potential ($V_{0.5}$) from -6.14± 2.28 mV in control to -12.30± 1.93 mV in DAMGO (n=10, p<0.001, paired Student t test) (Fig. 2.8Aii). The ramp evoked I_K activation steepness, defined as the slope of the sigmoidal fit to I-V curve (*b*), was not significantly altered by DAMGO (13.02 ± 0.95) relative to control (11.26 ± 0.67, n = 10, p = 0.101, paired t test, data not shown). Similar results were obtained when I_K was activated by a voltage step protocol (see *Experimental procedures).* Namely, the activation threshold of step-evoked I_K ($V_{0.05}$: -40.63± 0.92 mV) was significantly lowered by DAMGO ($V_{0.05}$: -48.51± 1.22 mV, n=10, p<0.001, paired Student t test, data not shown) along with the half activation potential ($V_{0.5}$ of -8.24± 1.07 mV in control to -12.16 ± 1.31 mV in DAMGO, n=10, p=0.003, data not shown). We found no statistical difference between the ramp-evoked versus step-evoked I_K parameters ($V_{0.05,}$ $V_{0.5}$ and *b*) in similar conditions (i.e. in control or in DAMGO, respectively; p=0.04-0.95, Mann-Whitney Rank Sum test).

To make sure that the shift in I_K kinetics was due to MOR activation, we again performed a parallel series of experiments in which CTAP (5 μM) was applied for at least 2 min prior to concurrent application of both DAMGO (1 μM) and CTAP (5 μM) for at least 3 min. Neither treatment with CTAP alone, nor consecutive application of CTAP+DAMGO together altered the depolarizing ramp-evoked I_K activation parameters (Fig. 2.8Bi) in ipRGCs (n=8) ($V_{0.05}$ control: -37.31± 2.28 mV, $V_{0.05}$ CTAP:-41.30± 3.27 mV, $V_{0.05}$ CTAP+DAMGO:-36.11± 4.71 mV, p=0.47; $V_{0.5}$ control: -6.57± 1.78 mV, $V_{0.5}$ CTAP:-5.32± 1.82 mV, $V_{0.5}$ CTAP+DAMGO:-6.61±

2.12 mV, p=0.28; *b* control: 10.74 ± 0.59, *b* CTAP: 12.13 ± 0.78 , *b* CTAP + DAMGO: 10.01 ± 1.63, p = 0.39; one way repeated measures ANOVA) (Fig. 2.8Bii).

In addition, we explored the possibility whether the rundown of I_K in ipRGCs could artificially cause a negative shift of the activation curve (DiFrancesco et al., 1986) although there was no appreciable loss of I_K amplitude after DAMGO application (Fig. 2.8Ai). To test this notion we held the dissociated ipRGCs in whole-cell voltage-clamp as long as the amplitude of I_K started to decay, up to 10 min; no significant difference was found for any of the measured I_K kinetic parameters between the first (control) trace obtained within seconds of patch break and the latest ("second") trace without amplitude rundown ($V_{0.05}$: -39.95 ± 1.23 mV vs. -40.35 ± 1.14 mV, p = 0.18; $V_{0.5}$: -7.76 ± 1.25 vs. -7.59 ± 1.38, p = 0.74; b: 10.38 ± 0.40 vs. 10.25 ± 1.06 mV, p = 0.72; for control and second traces, respectively, n = 8, paired Student t test, data not shown).

We also considered the possibility that small uncompensated increases in inter-trace series resistance (R_s) could result in hyperpolarizing shifts of $V_{0.05}$ and $V_{0.5}$ between control and DAMGO treated traces (Armstrong and Gilly, 1992). We tested and found that the presence or absence of automatic R_s compensation up to 54.83% ± 2.42 (n=13) did not cause a significant difference between the first, uncompensated control trace and the second, R_s compensated trace for any of the measured I_K kinetic parameters ($V_{0.05}$: -41.45 ± 1.87 mV vs. -42.17 ± 1.42 mV, p = 0.38; $V_{0.5}$: -10.71 ± 0.94 mV vs. -12.74 ± 1.12 mV, p = 0.002; b: 10.42 ± 0.43 vs. 9.91 ± 0.34, p = 0.15 for control and R_s compensated traces, respectively, paired Student t test, data not shown) for the recordings falling within the range of acceptable R_s (< 30 MΩ, see *Experimental procedures*). With the small, round, electronically compact soma of dissociated ipRGCs that lack processes and the gradual activation kinetics of I_K, it is likely that these small (< 13%), uncompensated increases in R_s did not cause significant shifts in $V_{0.05}$ and $V_{0.5}$. Notably, a leak

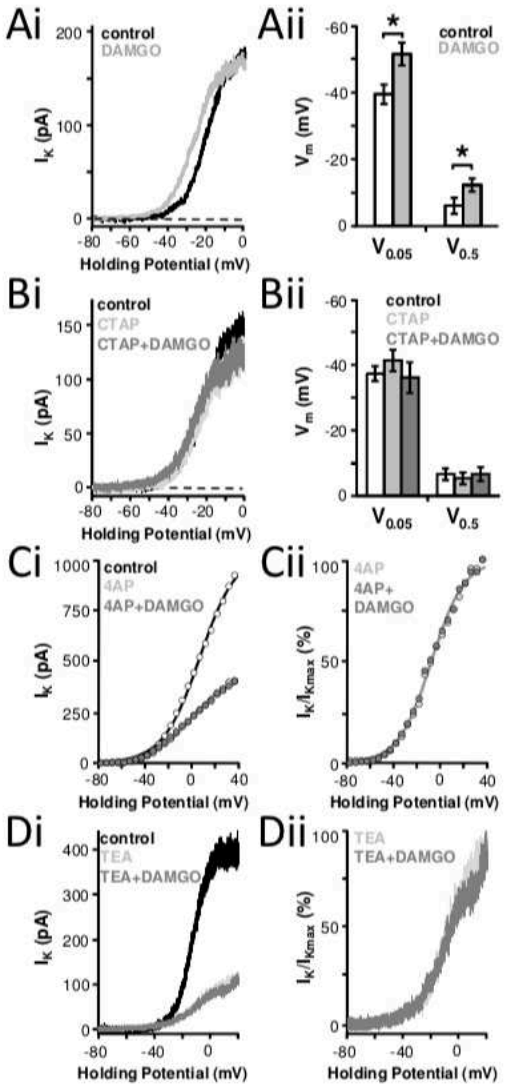

Figure 2.8. MOR agonist DAMGO alters I_K activation in ipRGCs. **Ai:** Representative leak-subtracted current traces show that DAMGO (1 μM) increased the voltage ramp-evoked I_K between -55 mV and -15 mV by shifting the activation to hyperpolarized potentials without increasing the overall I_K amplitude. **Aii:** Summary graph showing I_K activation ($V_{0.05}$) and half-activation ($V_{0.5}$) from Boltzmann fits in control and DAMGO (*: $p<0.001$, paired Student t test, n=10). **Bi:** Representative leak-subtracted current traces show that pretreatment with MOR selective antagonist CTAP (5 μM) or consecutive application of CTAP (5 μM) +DAMGO (1 μM) did not alter voltage ramp-evoked I_K. **Bii:** Summary graph showing I_K activation ($V_{0.05}$) and half-activation ($V_{0.5}$) from Boltzmann fits in control, followed by pretreatment with CTAP and with CTAP+DAMGO ($V_{0.05}$: $p=0.47$, one way repeated measures ANOVA, n=8; $V_{0.5}$: $p=0.28$, one way repeated measures ANOVA, n=8). **Ci:** Representative leak-subtracted current traces show that I_K evoked by depolarizing voltage steps in ipRGCs was markedly reduced by 4-AP (2 mM). In presence of 4-AP, DAMGO (1 μM) did not shift the activation of the remaining I_K. **Cii:** Same as in Ci, but traces obtained in 4-AP and 4-AP+DAMGO normalized to their peak showing no difference in their activation kinetics**. Di:** Representative leak-subtracted current traces show that I_K evoked by depolarizing voltage ramps in ipRGCs was markedly reduced by TEA (1 mM). In presence of TEA, DAMGO (1 μM) did not shift the activation of the remaining I_K. **Dii:** Same as in Di, but traces obtained in TEA and TEA+DAMGO normalized to their peak showing no difference in their activation kinetics.

increase of up to 44% did not affect measured IK kinetic parameters in these parallel experiments and these cut-offs were accordingly imposed on recordings chosen for analysis across experiments (see Experimental procedures).

The activation properties of IK, namely the V0.05 of ~-40 mV in control, suggested that the voltage-gated potassium channels expressed by ipRGCs might belong to the Kv1 or perhaps to the Kv4 family (Grissmer et al., 1994; Cox, 2005). To investigate the identity of Kv gene product(s) that might be responsible for mediating the DAMGO effect in ipRGCs, we exploited the differences in efficacy of IK inhibition by two broad-based K+ channel blockers, 4-aminopyridine (4-AP) and tetraethyl ammonium (TEA). Namely, Kv4 family members are inhibited by 4-AP only at 5 mM or higher concentrations, whereas Kv1 channels are blocked by 2 mM 4-AP (Grissmer et al., 1994; Cox, 2005). We found that 2 mM 4-AP not only markedly reduced IK in ipRGCs (Fig. 2.8Ci), but 4-AP prevented significant shift of the IK activation to more negative potentials by DAMGO (1 μM) (V0.05 4-AP: -37.31± 2.28 mV, V0.05 4-AP+DAMGO:-41.30± 3.27 mV, n=7, p=0.33) (Fig. 2.8Cii). The action of 4-AP in blocking the DAMGO-sensitive IK component in ipRGCs supports the premise that Kv1 family members mediate the DAMGO-sensitive IK component in ipRGCs. We also found that 10 mM TEA eliminated IK in ipRGCs (data not shown). Importantly, Kv4 channels, as well as most Kv1 channels, are resistant to TEA of ~10 mM concentration (Jerng et al., 2004), except Kv1.1, which is inhibited by TEA with an IC50 of ~0.3 mM (Grissmer et al., 1994; Gutman et al., 2005). In our hands, 1 mM TEA reduced IK in dissociated ipRGCs (Fig. 2.8Di) and also markedly reduced the potential of DAMGO (1 μM) to shift the activation to hyperpolarized potentials (V0.05 TEA: -42.60± 2.54 mV, V0.05 TEA+DAMGO: -44.45± 2.42 mV, n=5, p=0.61) (Fig. 2.8Di, 2.8Dii). Taken together, the pharmacological and biophysical data together

strongly implicate Kv1.1 channels as the effector of MOR signaling that mediate DAMGO effects in ipRGCs.

Next we tested if MOR activation affects voltage-gated Ca2+ currents (ICa) (Kieffer, 1995) in ipRGCs (Hartwick et al., 2007; Hu et al., 2013). I_{Ca} in voltage-clamped solitary ipRGCs was recorded in the presence of 5 mM extracellular Ca^{2+} (Hu et al., 2013) using cesium-based pipette solution (see *Experimental procedures*). Inactivating and non-inactivating components of I_{Ca} in ipRGCs were separated according to Hu et al. (2013): Total I_{Ca} ($I_{Ca,total}$) was obtained with depolarizing steps from -80 mV holding potentials (Fig. 2.9A). The non-inactivating I_{Ca} ($I_{Ca,non-inact}$) component was recorded in response to depolarizing voltage-steps from the holding potential of -40 mV (Fig. 2.9B). Peak $I_{Ca,non-inact}$ values were subtracted from the peak values of $I_{Ca,total}$ at corresponding step potentials to calculate the inactivating portion of I_{Ca} ($I_{Ca,inact}$) in ipRGCs (Fig. 2.9C). These were lengthy experiments, and we often found I_{Ca} run down well before the desired 3-5 min DAMGO application following the acquisition of control data. Therefore, I_{Ca} recordings in control (n=26) and DAMGO (n=6) were not performed on the same cells. Our results show that in the presence of DAMGO (1 μM) the current density of $I_{Ca,total}$ was significantly smaller than that in control (p=0.01, two way ANOVA) (Fig. 2.9A). Similarly, the non-inactivating component ($I_{Ca,non-inact}$) was significantly reduced in DAMGO (p=0.01, two way ANOVA) (Fig. 2.8B) but not the calculated $I_{Ca,inact}$ (p=0.43, two way ANOVA) (Fig. 2.7C).

Together, these results suggest that voltage-gated Ca^{2+} channels mediating the non-inactivating component of I_{Ca} in ipRGCs are also subject to opioid modulation upon MOR activation.

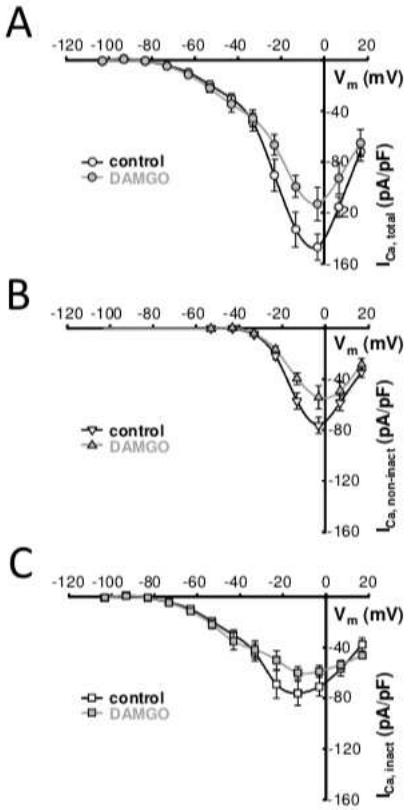

Figure 2.9. **MOR agonist DAMGO inhibits I_{Ca} in ipRGCs. Ai:** DAMGO (1 μM) inhibited the total I_{Ca} ($I_{Ca,total}$) evoked with depolarizing steps from -80 mV holding steps between -10 mV and 0 mV (p=0.01, two way ANOVA). **Aii:** The non-inactivating I_{Ca} ($I_{Ca,non\text{-}inact}$) component, recorded in response to depolarizing voltage-steps from the holding potential of -40 mV was also significantly reduced by DAMGO (p=0.01, two way ANOVA) at -10 mV and 0 mV. **Aiii:** Peak $I_{Ca,non\text{-}inact}$ values were subtracted from the peak values of $I_{Ca,total}$ at corresponding step potentials to calculate the inactivating portion of I_{Ca} ($I_{Ca,inact}$), which was not inhibited significantly (p=0.43, two way ANOVA) by DAMGO.

2.5 Discussion

We have previously shown β-endorphin and MOR expression in the mouse retina (Gallagher et al., 2010, 2012). Here we present convergent evidence that: (1) ipRGCs in both mouse and rat retinas express MORs; (2) the activation of MORs on ipRGCs results in the suppression of light responses by (3) increasing the delay of the first light-evoked spike as well as by reducing the duration of the spike train through a (4) shift in the activation of K_v1 channels to hyperpolarized membrane potentials and (5) inhibition of the non-inactivating component of

voltage-gated I_{Ca}. In addition to being observed in both mouse and rat, the MOR-mediated effect was present in young animals (P6-10 rats) as well as in adults (rats and *Opn4*::EGFP mice). Whether opioid modulation of ipRGCs has a fully conserved role at distinct time-points during development and adulthood remains to be examined. Interestingly, the MOR mediated physiological effect was shown in rat at a developmental time-point in which ipRGCs can modulate retinal wave activity and development of the visual system (Renna et al., 2011).

MOR activation and downstream modulation of Ca_v and K_v channels

Voltage-gated calcium (Ca_v) channels are activated downstream of TRP and I_{Na} in ipRGCs during light-evoked signaling (Hartwick et al., 2007), and they are thought to contribute to sustained firing of ipRGCs that characteristically outlasts the duration of stimulation: indeed, blocking I_{Ca} resulted in reduced spiking upon light stimulation (Berson et al., 2002). MOR activation in ipRGCs caused dose-dependent reduction of the duration of light-evoked ipRGC signaling (Fig. 2.3Ai, 2.3Aii) that is consistent with the observation that the non-inactivating component of I_{Ca} in ipRGCs (Hu et al., 2013) was inhibited by DAMGO (Fig. 2.9). MOR activation can result in the activation of multiple downstream pathways, including G-protein-dependent and -independent ones (reviewed by (Williams et al., 2013). Furthermore, some effectors are directly coupled to MORs, such as the G protein-gated inwardly rectifying potassium [GIRK, GIRK isoform (Kir3)] channels, in which case the amplitude of GIRK is proportional to the MOR activation by a given agonist (i.e. dose-dependent) (Pennock and Hentges, 2011). Similarly, many types of Ca_v channels have been shown to be inhibited directly by G proteins where, upon activation of various G protein–coupled receptors, in a dose-dependent manner the Gβγ dimer binds to Ca_v channels to inhibit I_{Ca} (reviewed by Proft and Weiss, 2015). It is noteworthy, however, that activation of somatic MOR in hypothalamic

proopiomelanocortin (POMC) neurons leads to inhibition of I_{Ca} and activation of GIRK, with apparently distinct MOR reserves for the separate process (Fox and Hentges, 2017). In our experiments, we isolated I_K by blocking voltage-gated I_{Ca} with Co^{2+}. This pharmacological manipulation has been shown to eliminate the calcium-dependent potassium currents ($I_{K(Ca)}$) (Solessio et al., 2002), therefore the DAMGO-mediated changes of I_K in our hands could not include a potential DAMGO-mediated increase in $I_{K(Ca)}$ at ~-50 mV. Nonetheless, the fact that MOR-mediated analgesic effects were not sensitive to $I_{K(Ca)}$ blockers such as apamin or charybdotoxin (Welch and Dunlow, 1993; Ocaña et al., 2004), suggests that a direct interaction between MOR signaling and $I_{K(Ca)}$ is unlikely.

The I_K that we identified to be modulated via MOR activation by DAMGO in ipRGCs was blocked by 1 mM TEA or by 2 mM 4-AP, making $K_v1.1$ the most plausible candidate (Grissmer et al., 1994; Cox, 2005; Gutman et al., 2005). However, it has been shown that $K_v1.1$ channels are capable of heterotetramerization *in vivo*, often with $K_v1.2$ and that TEA sensitivities as well as half activation values of these $K_v1.1$ and $K_v1.2$ heterotetramers can vary depending on both subunit composition and arrangement (Wang et al., 1993). The IC_{50} of TEA for a $K_v1.1$ homotetramer ranges from 0.47 mM to 0.67 mM, for a $K_v1.2$ homotetramer ranges from 47 mM to 50 mM, and for a $K_v1.1$ and $K_v1.2$ heterotetramer ranges from 0.8 mM to10 mM, depending on subunit arrangement. As well, while the activation threshold of $K_v1.1$ homotetramers has been reported near -50 mV and that of $K_v1.2$ near -40 mV, varying spatial arrangements of 2:2 $K_v1.1$:$K_v1.2$ heterotetramers in heterologous systems can alter measured half activation of I_K by ~ 5 mV (Al-Sabi et al. 2010; Kew and Davis, 2010) . Given our pharmacological data, it seems most likely that the DAMGO sensitive channel in ipRGCs is a $K_v1.1$ and $K_v1.2$ heterotetramer. While a $K_v1.1$ homotetramer cannot be entirely ruled out based

strictly upon TEA affinity, it would seem less likely given the reported activation threshold of near -50 mV (Kew and Davis, 2010).

Of particular relevance to this study, $K_v1.1$ and $K_v1.2$ have been shown to form heterotetramers *in vivo* (Wang et al., 1993; Shamotienko et al., 1997; Coleman et al., 1999), and opioid induced negative regulation of GABAergic tone of basolateral amygdala (BLA) output neurons occurs through modulation of pre-synaptic $K_v1.1$ and $K_v1.2$ channels (Finnegan et al., 2006). Dendrotoxin-K and tityustoxin-Kα, purported to be $K_v1.1$ and $K_v1.2$ specific blockers, respectively, each blocked the inhibitory effects of 1 μM DAMGO on miniature inhibitory postsynaptic currents (mIPSCs) in the BLA, leading the authors to suspect that BLA $K_v1.1$ and $K_v1.2$ form heteromeric complexes. $K_v1.1$ and $K_v1.2$ are important determinants of cellular excitability (Smart et al., 1998; Glazebrook et al., 2002; Brew et al., 2003, 2007) and as such are key players in nociceptive pathways and their modulation by opioid signaling (Clark and Tempel, 1998; Galeotti et al., 1999; Finnegan et al., 2006). For example, mice with an antisense oligonucleotide on the $K_v1.1$ gene lack morphine and baclofen-induced antinociception (Galeotti et al., 1997), and $K_v1.1$ null mice have reduced morphine-induced antinociception (Clark and Tempel, 1998). In a sense, $K_v1.2$ provides for increased neuronal excitability, and $K_v1.1$ provides for negative regulation of that excitability; adjustments of the $K_v1.1$:$K_v1.2$ stoichiometric balance may represent a precise, real-time method for down-regulation of neuronal excitability (Brew et al., 2007). Another mechanism of $K_v1.2$ subunit containing channel modulation by opioids could involve $K_v\beta$ subunit modulation of I_K activation. Coexpression of $K_v1.5$ and $K_v\beta2.1$ in heterologous systems results in a 10 mV hyperpolarizing shift in $V_{0.05}$ without alteration of I_K amplitude as seen in our experiments (Fig. 2.7Ai), with phosphorylation of $K_v\beta2.1$ postulated to rapidly regulate its interaction with the α subunit (Uebele et al., 1996). $K_v\beta2$ is the predominant

subunit isoform present in the brain, and it has additionally been shown to positively regulate $K_v\beta2/K_v1.2$ complex stability and $K_v1.2$ surface expression (Shi et al., 1996).

MOR activation and consequent $G_{\alpha i/o}$ signaling might be coupled to the effectors through enzymatic steps: for example, in pyramidal neurons of the lateral amygdala, activation of the PLA2/arachidonic acid/12-lipoxygenase cascade with morphine and DAMGO enhances spike frequency adaptation, which involves shifting the voltage dependence of K_v channels containing $K_v1.2$ subunits to more negative potentials by ~ 14 mV (Faber and Sah, 2004). Furthermore, extensive literature documents G protein coupled receptor - mediated changes in $K_v1.1$ and $K_v1.2$ surface expression via clathrin-dependent endocytotic mechanisms (Bosma et al. 1993; Cachero et al. 1998; Connors et al. 2008; Hattan et al. 2002; Huang et al. 1993; Nesti et al. 2004; Stirling et al. 2009; Williams et al. 2007, 2012). In addition, MOR activation results in decreased adenylyl cyclase (AC) activity and thus cAMP levels and PKA activity; to that end, $K_v1.2$ is affected by cAMP levels, with elevation of cAMP increasing $K_v1.2$ surface expression and low cAMP decreasing it. Thus, through its effects on $K_v1.2$ surface levels, cAMP homeostasis also functions as buffer for cellular excitability (Connors et al., 2008).

Integration of opioid signaling with the retinal-ipRGC circuit

What might be the retinal circuit that leads to a rise in endogenous retinal opioid levels and what are the functional consequences of the effect of these opioids on ipRGC excitability? Similar to how MOR activation in the lateral amygdala serves to attenuate neuronal spiking in depolarizing conditions (Faber and Sah, 2004), modulation of K_v and Ca_v channels in ipRGCs by MOR activation may serve to limit ipRGC output in response to depolarizing stimuli. When might ipRGC output need to be suppressed? The biological clock is located in the suprachiasmatic nucleus in the hypothalamus, and it receives photic information through

ipRGCs. As clock neurons are active during the day / light cycle and its output accordingly integrated by central sleep-regulatory systems, there would be advantages to mechanisms of ipRGC output suppression during the dark cycle that are capable of modulating the cells sensitivity to depolarizing input (Saper et al., 2005).

IpRGCs exhibit both intrinsic (melanopsin-driven) and extrinsic (synaptically-driven) light responses (Wong et al., 2007; Schmidt et al., 2011), and these responses have a powerful impact on ipRGC-mediated central processes. The intrinsic phototransduction cascade has very high gain, with ipRGCs capable of signaling single photon absorption to the brain via spiking, as a 1 mV depolarization results in a several-fold increase in the spike rate of ipRGCs. Such high efficiency signaling of ipRGCs could be achieved by the ipRGCs operating near spike threshold. Furthermore, at the organism level, only a few hundred melanopsin molecules need to undergo photoisomerization in order to trigger the pupillary light reflex (PLR) (Do et al., 2009). Selective elimination of ≥ 99% of ipRGCs does not eliminate the PLR completely (Güler et al., 2008), confirming that signaling from even a very limited number of ipRGCs has significant downstream behavioral consequence. These findings suggest that relatively small shifts in ipRGC spiking could be expected to have discernable impact on behaviors and reflexes regulated by these photoreceptors. Opioid signaling could serve to modulate the efficiency of ipRGC signaling in darkness when such high gain is both unnecessary and counter-productive. As even a slight rise in the spike threshold would decrease ipRGC light signaling by orders of magnitude, the spike threshold of ipRGCs has previously been postulated to be a regulatory point for ipRGC sensitivity (Do et al., 2009). We have shown that the spike threshold is indeed a regulatory point, although MOR activation in ipRGCs reduces ipRGC excitability not by increasing the spike

threshold itself but by increasing I_K at the threshold of voltage-gated Na^+ channels, thereby delaying the Na^+-mediated depolarization of ipRGCs.

Negative regulation of ipRGCs by opioids during darkness could serve as an effective nighttime counterpart to the known regulation by dopamine (DA) of ipRGCs during daylight (van Hook et al., 2012). DA, via D1-receptor activation, has been shown to affect light-evoked spiking in ipRGCs by both attenuating the photocurrent and depolarizing ipRGC resting membrane potentials (van Hook et al., 2012). While cAMP's effects on light evoked spiking were not directly investigated in the study by van Hook et al. (2012), a subsequent study showed that elevated cAMP increased light evoked spiking via a PKA-dependent pathway (Sodhi and Hartwick, 2014). Given that opioids are known to decrease cAMP (Kieffer, 1995), in ipRGCs DA and opioids might act to promote the transition between daytime and nighttime, respectively, as it was proposed for avian retinas (Morgan and Boelen, 1996). In support of this notion in the rabbit retina, exogenous opioids were shown to inhibit the release of dopamine (Dubocovich and Weiner, 1983). The increased number of light-evoked spikes after application of CTOP (Fig. 2.3Ai, 2.3Aii) suggests the presence of a weak inhibitory tone mediated by endogenous opioids in dark-adapted retinas (Morgan and Boelen, 1996). With our experimental paradigm, however, this effect of CTOP could instead be the result of a homeostatic sensitization of AC triggered by the long exposure to multiple concentrations of DAMGO, resulting in an overshoot of cAMP production upon the addition of a competitive MOR antagonist (Watts, 2002; Levitt et al., 2010). The fact that CTOP alone did not increase light-evoked signaling (Fig. 2.3C) suggests that the CTOP-mediated increase of ipRGC light responses seen in our experiments, which were performed during the day following long DAMGO exposures (Fig. 2.3Ai, 2.3Aii), was most likely caused by MOR antagonist-induced cAMP overshoot (Watts, 2002). In the mouse retina β-

endorphin, the endogenous opioid that is preferentially bound by MORs, is expressed by a subpopulation of ON and OFF cholinergic amacrine cells (Gallagher et al., 2010): the OFF types somas are located at the INL/IPL border and their processes arborize in a thin layer between sublaminae 1 and 2 of the IPL, whereas the ON types somas are displaced to the GCL and whose processes arborize between IPL sublaminae 3 and 4 (Haverkamp and Wassle, 2000). In essence, this close spatial apposition of putative β-endorphin release sites to M1 and M3 ipRGC processes that cross the inner retina might support either direct synaptic or paracrine opioid regulation of ipRGCs, whereas a paracrine opioid regulation of M2 type ipRGCs with processes running along in sublamina 5 is more likely. Although it is not known whether the expression and release of β-endorphin follows a circadian rhythmicity in the retina, it is tempting to speculate that endogenous opioid levels, akin to those of adenosine, rise at night to likewise co-regulate nighttime signals from ipRGCs to the brain. A1 adenosine receptor activation in ipRGCs, like MOR activation, decreases AC activity, cAMP levels, and PKA activity, with the consequence of decreased light evoked spiking. While not yet explicitly investigated, postulated downstream targets of A1 receptor signaling include Ca_v channels, TRPCs, and (less likely) hyperpolarization-activated cyclic nucleotide-gated channels (Sodhi and Hartwick, 2014). It would appear that opioids and adenosine are poised to work synergistically to inhibit light-evoked spiking in ipRGCs. While in the basal forebrain increases in adenosine promote sleep and increases in opioids promote insomnia (as reviewed by Nelson et al. 2009), the effects of adenosine and opioids in the spinal cord are not in opposition but are instead additive (Sawynok, 1998), and this is consistent with how they appear to function in the retina.

CHAPTER 3. OPIOID SIGNALING IN THE MOUSE RETINA MODULATES PUPILLARY LIGHT REFLEX

3.1 Summary

The aim of the present study was to determine the effect of modulation of ipRGC signaling via MORs on the murine PLR. The main findings of this study were: (1) In WT mice but not in systemic μ-opioid receptor knockout mice (MKO) or mice in which μ-opioid receptors were selectively knocked out of ipRGCs alone (McKO), intraocular application of the MOR selective agonist DAMGO strongly inhibited rod/cone driven PLR and slowed melanopsin-driven PLR. (2) Intraocular application of a MOR selective antagonist CTAP enhanced rod/cone driven PLR in the dark-adapted retina and melanopsin driven PLR under photopic conditions in WT mice. These results identify a novel site of action for exogenous and potentially endogenous opioids in the retina, i.e. MORs on ipRGCs, that has significant impact on a behavioral measure of opioid effect, the PLR.

3.2 Introduction

Over the past 25 years, the liberalization of laws governing opioid prescription for the treatment of chronic non-cancer pain has led to dramatic increases in opioid use, often referred to as an opioid epidemic in the United States (Manchikanti et al., 2012; Cobaugh et al., 2014; Poon and Greenwood-Ericksen, 2014). While there exist several biomarkers for opioid effect, in man the development of resting miosis is used as an indicator of systemic opioid effect (Murray et al., 1983; Pickworth et al., 1989, 1991; Zacny and Goldman, 2004; Verster et al., 2006; Grace et al., 2010).

The effect of opioids on resting pupil diameter is highly variable and species dependent, in some species causing resting mydriasis and in others resting miosis (Murray et al., 1983). The exact mechanism by which opioids regulate resting pupil diameter is not definitively understood, though both central (midbrain) and local regulatory sites have been postulated, with likely species-specific differences (Lee and Wang, 1975; Korczyn and Maor, 1982; Murray et al., 1983). There is evidence that central opioid receptors that modulate resting pupil size are located in the EWN (Sharpe and Pickworth, 1985), and their activation may decrease EWN tonic firing in species where opioids cause resting mydriasis (Pickworth et al., 1989). In species in which opioids cause resting miosis, pupil constriction may be secondary to opioid induced inhibition of cholinergic neurons that otherwise tonically inhibit the EWN (disinhibition), given that injections of opioids into the EWN caused miosis (Lee and Wang, 1975) and injections of cholinergic (specifically muscarinic) agonists into the EWN induced mydriasis in sympathectomized and decerebrated dogs (Sharpe and Pickworth, 1981). There are likely species specific variations in neurocircuitry and chemistry which account for the different direct effects of opioids on the EWN (Sharpe and Pickworth, 1985). Outside of the EWN, opioid receptors located in the reticular formation may also serve to link respiration to pupil changes, though the species-dependent effects of opioids on respiration often preclude a direct link between opioid-RAS interactions and resting pupil diameter (Lynch et al., 1985, 1990). There also exists support for local ocular effects of opioids, as topical morphine results in mydriasis in rats and in miosis in man, and both topical and intraocular opiates induce miosis in rabbits; the intraocular site of action has previously been postulated to be at iris though definitive proof of iridial opioid receptors has not been shown (Drago et al., 1980; Fanciullacci et al., 1981; Korczyn and Maor, 1982; Bonfiglio et al., 2006).

Given the variability of opioid effect on resting pupil diameter, the PLR may prove a more consistent reflexive read-out of opioid effect. Indeed, while opioids also exert species-specific effects on the PLR, there is less variability as opioids retard the PLR in most species including the cat (Pickworth and Sharpe, 1985; Sharpe, 1991) and man (Pickworth et al., 1989, 1991) yet enhance it in the rabbit (Murray and Loughnane, 1981). It is noteworthy that the PLR evoked by bright blue light in chronic human opioid users has reduced velocity (Grace et al., 2010).

How might opioids modulate the PLR? Prior work demonstrated that opioids, via μ-opioid receptors (MORs), strongly attenuate the light-evoked firing of ipRGCs. As well, in *Opn4*::EGFP mouse retinas, 54% of the EGFP+/ MOR+ ipRGCs (93/173) were also Brn3b+ (Cleymaet et al., 2019). As previously discussed in section 1.4.2, systemically applied opioids could act on the MORs expressed by ipRGCs (Selley et al., 2001; Saszik et al., 2002; Wyman and Bultman, 2004; Hosoya et al., 2011; Lee et al., 2011; Fernández et al., 2013). This suggests that PLR might be influenced by opioids acting on Brn3b+ M1 ipRGCs. In the present study, we test the hypothesis that inhibition of ipRGC signaling via MORs negatively modulates the murine PLR, and we determine the relative impact of opioids on classical photoreceptor vs. ipRGC contributions to the PLR utilizing cell specific knock-outs.

3.3 Materials and Methods

Animals

All animals used in these studies with handled in compliance with the Institutional Animal Care and Use Committees of Colorado State University and in accordance with the ARVO Statement for the Use of Animals in Ophthalmic and Vision Research. Animals were housed under a 12:12 light dark (LD) cycle. Food and water were made available *ad libitum*.

Four strains of mice were used. C57BL/6J (stock # 000664, Jackson Labs) mice, in which opioid dependence-relevant behaviors are robust, were used as wild-type (WT) controls (Kirkpatrick and Bryant, 2015). Mice lacking functional MORs globally (B6.129S2-Oprm1tm1Kff/J, MKO for short, stock# 007559, Jackson Labs) were used. We generated a conditional KO mouse line in which only ipRGCs were lacking MORs (McKO) by crossing a well-characterized mouse line expressing Cre recombinase upstream of the melanopsin coding sequence (*Opn4*) (Tg(*Opn4*-cre)SA9Gsat/Mmucd or *Opn4*::Cre for short, stock # 036544-UCD, MMRRC) with mice where exon 2 and 3 of the MOR gene (Oprm1) are flanked by a loxP site ("floxed μ" or Oprm1fl/fl2). Primary anti-melanopsin antibody verification was carried out using the previously described *Opn4*::EGFP mouse line (Cleymaet et al., 2019).

In vivo pupillometry

Control series:

Mice were dark adapted for 15 minutes. PLR was tested on mice that were either awake or maintained on a very light plane of anesthesia with isoflurane (Hattar et al., 2003; Lucas et al., 2003; Panda et al., 2003; Mohan et al., 2012; Kostic et al., 2016). There was limited bias due to handling stress or anesthetic plane as reproducible control pupil sizes were obtained prior to each stimulus. Dark adapted PLR mediated by classical photoreceptors was evoked by stimulating the right eye with green light at an intensity below the melanopsin activation threshold i.e. rod and green cone opsin saturating green light (10^{11} photons/cm^2/s at 525 nm) (Lucas et al., 2001, 2003). The second stimulus (10^{14} photons/cm^2/s at 470 nm) was well above melanopsin threshold to activate ipRGCs, which has been reported be as low as $10^{11.5}$/photons/cm^2/s at 480 nm (Berson et al., 2002; Lucas et al., 2003). Photopic PLR was tested with the blue stimuli superimposed on the rod and green cone opsin saturating green intensity. Intermittent light

enhances pupillary constriction responses and prevents adaptation (Gooley et al., 2012); accordingly, we delivered the 1 min long light stimulation at 2 Hz to the right eye, while recording PLR in the left eye at 30 frames/sec. Control stationary pupil measurements were taken 1-10s before the stimulation was begun. Stationary PLR was recorded after 1 min of intermittent light stimulation. Stationary recovery values of the pupil size were recorded ~ 2 min after the termination of light stimulation protocol. Pupil area was measured off-line at 1s intervals using NIH ImageJ. Similar to prior studies (Lucas et al., 2001), to correct for individual variation in dark adapted pupil area, pupil sizes during illumination were calculated as percentage of the average of the stationary control and recovery pupil sizes.

It is of note that recent work with dynamic pupillometry comparing WT vs. rodless or coneless mice has demonstrated that rods contribute to blue light PLR and low and medium intensity red light PLRs while cones drive the initial rapid dilation of low intensity blue light PLR (Kostic et al., 2016). However, the focused goal of this study is to clearly delineate MOR mediation of classical photoreceptor vs. ipRGC input on the (stationary) PLR, without subdividing the classical photoreceptor inputs into those of rods vs. cones. As previously discussed by (McDougal and Gamlin, 2010), it is difficult to chromatically make a distinction between the relative contributions of rod and cone input to ipRGCs, given that the wavelength sensitivity of rods and green cones in mice closely overlap at λ_{max} 498 nm and 508 nm, respectively (Lucas et al., 2001). Also of note is that photoresponses of both rods, cones, and ipRGCs are not linearly additive, as the melanopsin photoresponse exclusively drives the PLR given stimuli above the threshold of the melanopsin photoresponse (480 nm, $10^{11.5}$ photons/cm^2/s) (Lucas et al., 2001), effectively shunting rod-cone mediated outer retinal signals that feed into the ipRGCs. Below this threshold, after a brief period of adaptation, tonic rod

signaling synergistically drives the PLR via central ipRGC glutamatergic output, maintaining miosis at irradiances below the melanopsin threshold and enhancing sensitivity to long-wavelength light (McDougal and Gamlin, 2010; Keenan et al., 2016). In contrast, cones minimally contribute to maintaining miosis at either high or low irradiances (McDougal and Gamlin, 2010), unless they are permitted to dark adapt with short, intermittent dark pulses (Gooley et al., 2012). For these reasons, most landmark studies assessing the relative contribution of classical photoreceptor and melanopsin photoresponses to ipRGC physiology pool rod and cone inputs together as a collective outer retinal input, utilizing high vs. low intensity light stimulus protocols (Hattar et al., 2003; Lucas et al., 2003; Panda et al., 2003; Güler et al., 2008; Jones et al., 2013). Additional laboratories have utilized red light (630 nm, luminance 200 kcd/m^2) to elicit PLRs in mice; however, without the benefit of genetic KO mice, the resultant PLR was still considered to be a combined, rod-cone-mediated PLR (Mohan et al., 2012). Given the above considerations, we elected to use rod and green cone opsin saturating green light in our study.

Sham/opioid injection series:

Different mice were used in the sham/opioid injection series vs. the control series mice. MOR selective agonist [D-Ala^2, $MePhe^4$, Gly-ol^5]-enkephalin (DAMGO) or the MOR selective antagonist CTAP (2 mg/ml each) were administered via unilateral intravitreal injection (2 µl/eye) under isoflurane anesthesia following application of topical 0.5% proparacaine (Mojumder et al., 2009). Controls received saline (2 µl/eye). Mice were dark adapted for 15 minutes. PLR was tested on mice maintained on a light plane of anesthesia with isoflurane, in the same fashion as for the control series, with the light stimulus being delivered to the sham/opioid treated right eye and PLR recorded from the contralateral left eye.

Previous MEA data (Cleymaet et al., 2019) shows that maximal effect of DAMGO for reducing ipRGC response was reached at ~1 μM. Intravitreal injection of 2 μl of 2 mg/ml DAMGO will result in ~100 M DAMGO concentration in the vitreous, assuming equal distribution in the estimated total vitreous volume (~20 μl) of the mouse eye (Saszik et al., 2002). Thus, even if some drug reflux took place during and following the injection (Rappoport et al., 2013), the intravitreal concentration of DAMGO is expected to produce maximal inhibition of light-evoked ipRGC spiking, and in turn, inhibition of PLR. Existing evidence supports this: pharmacological inhibition of melanopsin with opsinamides inhibited ipRGC firing by about 50%, and reduced bright light-triggered PLR in rodless/coneless mice by about 50%, without affecting PLR evoked by dim intensities (i.e. rod-cone mediated PLR) in wild-type mice (Jones et al., 2013).

Verification of MKO / McKO mouse strains via retinal immunohistochemistry

Following the pupillometry experiments, the mice were immediately euthanized via cervical dislocation following establishment of a deep plane of anesthesia with isoflurane. The eyes were subsequently enucleated and eye cups were prepared for cryosectioning. Validation of transgenic mice was performed via immunohistochemistry proving lack of MOR immunolabeling in ipRGCs in McKOs. Tissue preparation, IHC, and confocal laser microscopy were performed as previously described (Gallagher et al., 2012).

Statistical analysis

All data were analyzed using SigmaPlot11 (version 11; Systat Software) and Excel (Microsoft). Specific statistical comparisons are described in text. Data are presented as mean ± SEM, and $p < 0.05$ considered significant.

3.4 Results

MOR specific agonist DAMGO inhibited dark adapted pupillary light reflex (PLR) in WT mice

In dark adapted WT mice, unilateral, intraocular injection of DAMGO (1 µl of 2 mg/ml) strongly inhibited contralateral rod/cone driven PLR. The normalized pupil area of green light evoked stationary PLR was significantly greater after DAMGO injection compared to control, Fig. 3.1 (control: 41.78±3.16%, n=16, DAMGO: 107.77±5.56%, n=9, $p<0.001$, Student's t-test).

The stationary PLR evoked by bright blue irradiance that can activate melanopsin signaling directly was inhibited by DAMGO, but not significantly - see Fig. 3.1, (normalized pupil area of control: 8.67±3.02%, n=5, DAMGO: 14.18±2.67%, n=5, $p=0.82$, Student's t-test).

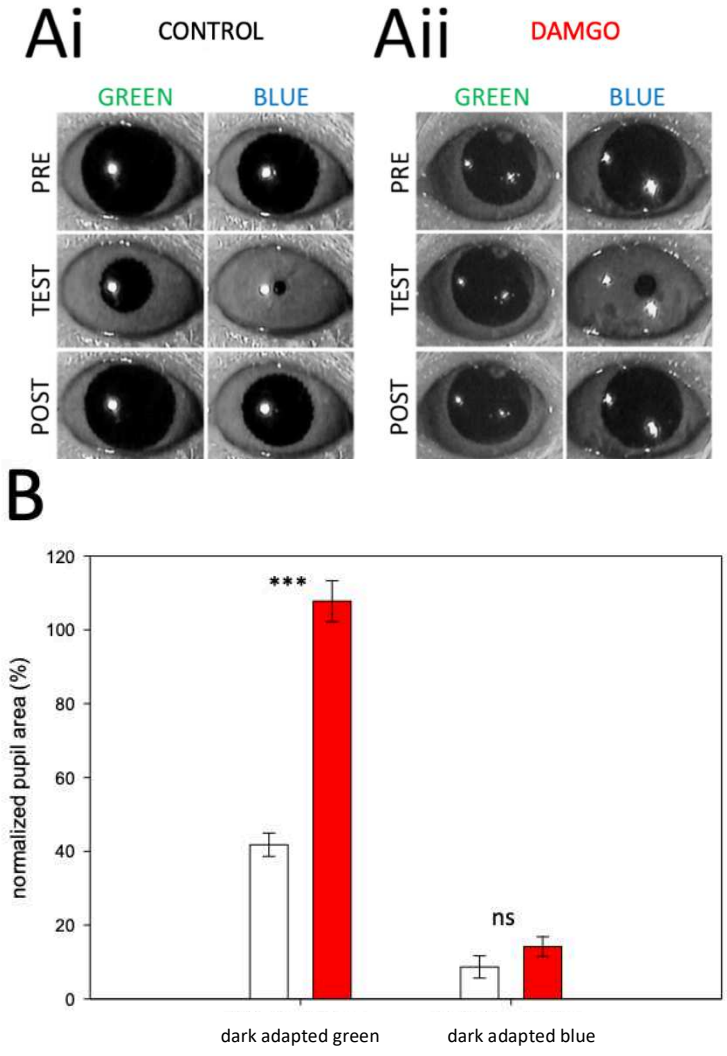

Figure 3.1 MOR specific agonist DAMGO inhibited dark adapted stationary PLR in WT mice. Ai: WT mice had normal PLR in response to green (10^{11} photons/cm^2/s at 525 nm) and blue (10^{14} photons/cm^2/s at 470 nm) light. **Aii:** Unilateral, intraocular injection of DAMGO (1 µl of 2 mg/ml) strongly inhibited contralateral rod/cone driven PLR and partially inhibited melanopsin driven PLR. **B:** Cumulative stationary PLR data under control (white bar, n=16 green light stimulus, n=5 blue light stimulus) and DAMGO (red bar, n=9 green light stimulus, n=5 blue light stimulus) conditions in WT mice. Average ± SEM. ***: p<0.001, Student's t-test.

However, a more detailed analysis of the dynamic PLR showed a marked slowing of the blue light response under DAMGO conditions compared to control, Fig. 3.2.

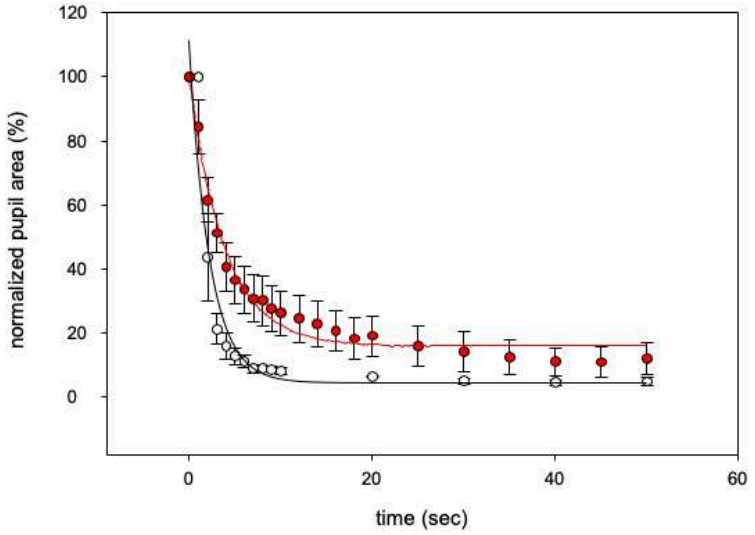

Figure 3.2 MOR specific agonist DAMGO slowed blue light driven dynamic PLR in dark adapted WT mice. Unilateral, intraocular injection of DAMGO (1 µl of 2 mg/ml) slowed PLR stimulated by blue (10^{14} photons/cm^2/s at 470 nm) light (red circles, n=5) compared to control (white circles, n=3). Data points fit with the following sigmoid curve: $f=y_0+a*\exp^{(-b*x)}$

Dark adapted MKO and McKO mice showed normal stationary and dynamic PLR, and DAMGO had no effect on dark adapted PLR

To elucidate whether the intraocular DAMGO effect on the pupillary light reflex is exclusively mediated by MORs expressed by ipRGCs, or whether other retinal cells expressing MORs also contribute, we then performed a parallel series of experiments on MKO and McKO mice.

Control stationary PLR of dark adapted MKO and McKO mice were not significantly different from that of WT mice for any light stimulus, Fig. 3.3 (normalized pupil area of green light WT: 41.78±3.16%, n=16, MKO: 32.74±3.98%, n=21, McKO: 34.08±5.38, n=9, p=0.55; blue light WT: 8.67±3.02%, n=5, MKO: 6.47±0.80%, n=15, McKO: 9.74±1.60%, n=9, p=0.22, one way ANOVA). Detailed analysis of the dynamic PLR of MKO and McKO mice did not show slowing of the blue control response compared to WT mice. MKO and McKO mice are thus valid models for the assessment of acute MOR mediated inhibition of ipRGCs on PLRs.

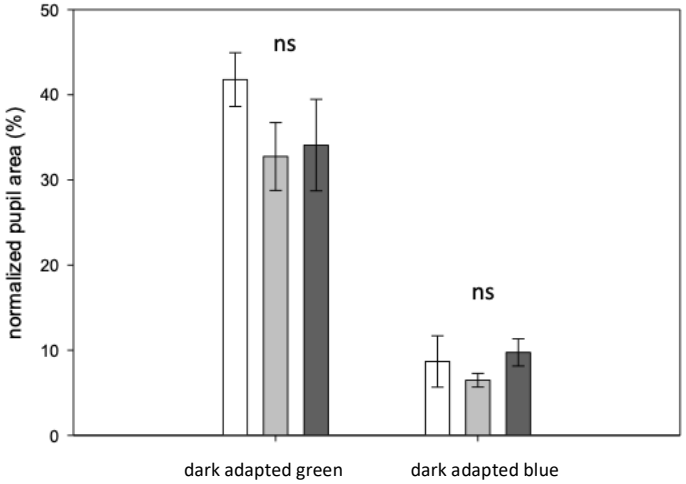

Figure 3.3 Control stationary PLR of dark adapted MKO and McKO mice are comparable to that of WT mice. Cumulative stationary PLR response to green light (10^{11} photons/cm^2/s at 525 nm) (WT: white bar, n=15; MKO: grey bar, n=21; and McKO: black bar, n=9) and blue light (10^{14} photons/cm^2/s at 470 nm) (WT: white bar, n=5; MKO: grey bar, n=16; and McKO: black bar, n=9). Average ± SEM. One way ANOVA.

In dark adapted MKO mice, unilateral, intraocular injection of DAMGO (1 µl of 2 mg/ml) did not inhibit contralateral green or blue light evoked PLR, Fig. 3.4A (normalized pupil area of green light control: 32.74±3.98%, n=21, DAMGO: 24.98±3.08%, n=12, p=0.19; blue light control: 6.47±0.80%, n=15, DAMGO: 3.53±0.30%, n=10, p=0.008, Student's t-test).

Unlike with WT mice, detailed analysis of the dynamic PLR of MKO mice did not show slowing of the blue light response under DAMGO conditions compared to control, Fig. 3.4B.

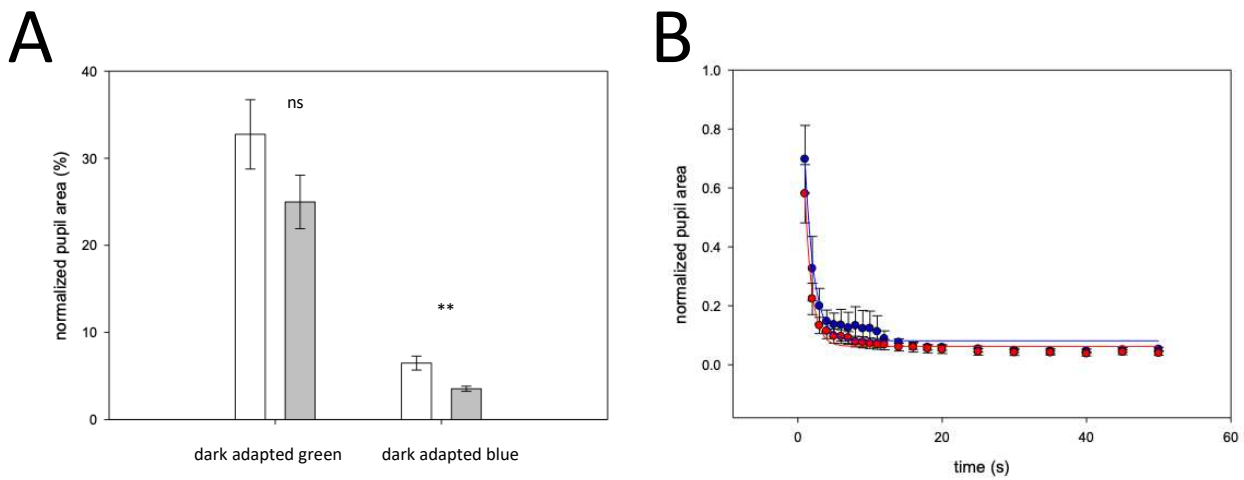

Figure 3.4 MOR specific agonist DAMGO does not inhibit dark adapted stationary or dynamic PLR in MKO mice. Unilateral, intraocular injection of DAMGO (1 µl of 2 mg/ml) did not inhibit contralateral rod/cone driven PLR or melanopsin driven PLR. **A.** Cumulative stationary PLR data under control (white bar, n=21 green light stimulus (10^{11} photons/cm^2/s at 525 nm), n=15 blue light stimulus (10^{14} photons/cm^2/s at 470 nm)) and DAMGO (red bar, n=12 green light stimulus, n=10 blue light stimulus) conditions in MKO mice. Average ± SEM. **:$p<0.01$ Student's t-test. **B.** Unilateral, intraocular injection of DAMGO did not slow PLR stimulated by blue light (red circles) compared to control (blue circles) in MKO mice. Data points fit with the following sigmoid curve:

In dark adapted McKO mice, unilateral, intraocular injection of DAMGO (1 µl of 2 mg/ml) also had no effect on contralateral green or blue light evoked PLR, Fig. 3.5 A (normalized pupil area of green light control: 34.08±5.38%, n=9, DAMGO: 30.38±10.90%, n=6, p=0.94; blue light control: 9.74±1.60%, n=9, DAMGO: 7.27±1.06%, n=11, p=0.20; Student's t-test). As with MKO mice, detailed analysis of the dynamic PLR of McKO mice did not show slowing of the blue light response under DAMGO conditions compared to control, Fig. 3.5 B.

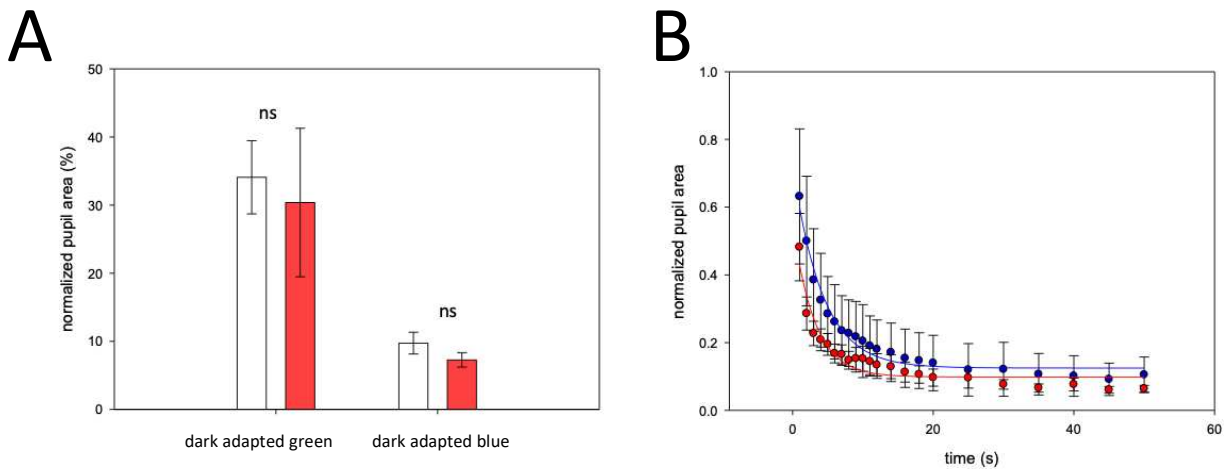

Figure 3.5 MOR specific agonist DAMGO does not inhibit dark adapted stationary or dynamic PLR in McKO mice. Unilateral, intraocular injection of DAMGO (1 µl of 2 mg/ml) did not inhibit contralateral rod/cone driven PLR or melanopsin driven PLR. **A.** Cumulative stationary PLR data under control (white bar, n=9 green light stimulus (10^{11} photons/cm^2/s at 525 nm), n=9 blue light stimulus (10^{14} photons/cm^2/s at 470 nm)) and DAMGO (red bar, n=6 green light stimulus, n=11 blue light stimulus) conditions in McKO mice. Average ± SEM. Student's t-test. **B.** Unilateral, intraocular injection of DAMGO did not slow PLR stimulated by blue light (red circles) compared to control (blue circles) in McKO mice. Data points fit with the following sigmoid curve: $f=y_0+a*\exp^{(-b*x)}$

Importantly, PLRs of dark adapted MKO and McKO mice that received a unilateral, intraocular injection of DAMGO (1 µl of 2 mg/ml) were significantly different from that of WT mice that received a unilateral, intraocular injection of DAMGO (1 µl of 2 mg/ml) for either light stimulus, Fig. 3.6 (normalized pupil area of green light WT: 107.77±5.56%, n=9, MKO: 24.98±3.08%, n=12, McKO: 30.38±10.90%, n=6, $p<0.001$; blue light WT: 14.18±2.67%, n=5, MKO: 3.53±0.30%, n=10, McKO: 7.27±1.06%, n=11, $p<0.001$, one way ANOVA). The greatest relative negative modulatory effect exerted by DAMGO on the PLR was observed with rod-cone mediated PLR. While there was no significant difference in PLRs between the KOs for dark adapted green light conditions, there was a significant difference in PLRs between MKOs and McKOs subject to bright blue irradiance, with greater pupillary constriction in the MKO group vs. the McKO group (MckO vs. MKO difference of mean maximal normalized pupil area for

green light: 5.40%, p=0.53; blue light: 3.74%, p=0.02; Holm-Sidak pairwise multiple comparisons).

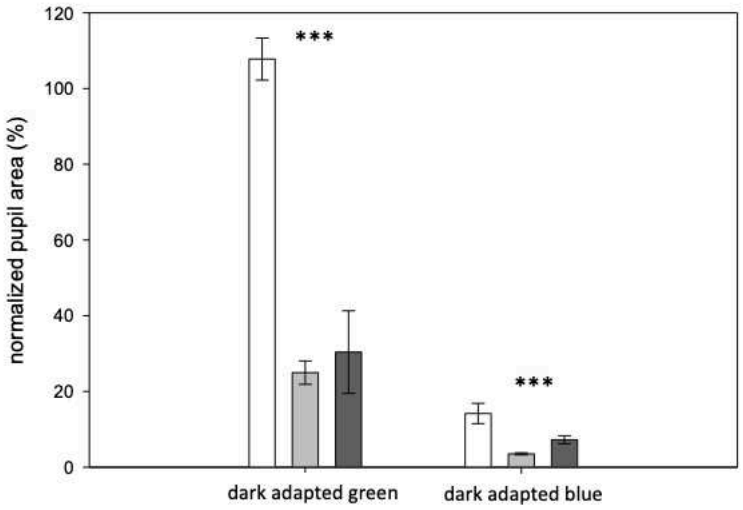

Figure 3.6 MOR specific agonist DAMGO effects on the stationary PLR of dark adapted MKO and McKO mice differ from those of WT mice. Cumulative stationary contralateral PLR response to green light (10^{11} photons/cm^2/s at 525 nm) (WT: white bar, n=9; MKO: grey bar, n=12; and McKO: black bar, n=6) and blue light (10^{14} photons/cm^2/s at 470 nm) (WT: white bar, n=5; MKO: grey bar, n=10; and McKO: black bar, n=11) post unilateral, intraocular injection of DAMGO (1 µl of 2 mg/ml). Average ± SEM. ***:p<0.001. One way ANOVA.

DAMGO injection can be noted to consistently enhance the PLR in both knockout mice. To determine if this was a direct effect of DAMGO or side effect of the intraocular injection itself, we performed unilateral, intraocular injections of 1 µL of saline and compared the saline control to baseline PLRs. The normalized pupil area of green light evoked stationary PLR was smaller after saline injection compared to baseline control (normalized pupil area of green light baseline: 48.70±0.27%, saline control: 18.40±1.67%, n=2, p=0.04, paired t-test, data not shown). While a neurogenic reflex uveitis may result in miosis in the injected eye, the cause of the post-injection enhancement of PLR in the contralateral eye is not known. However, it appears that the negative modulatory effects of DAMGO on the PLR are sufficiently potent to overcome this phenomenon in the WT mouse, given the absence of miosis in response to photic stimulation in the WT mice.

MOR specific antagonist CTAP increased dark adapted PLR triggered by rod-saturating green light in WT mice

Unilateral, intraocular CTAP (1 μl of 2 mg/ml) significantly enhanced the rod-saturating green light-evoked stationary PLR of dark adapted WT mice compared to that of control, Fig. 3.7 (normalized pupil area of control: 41.78±3.16%, n=16, CTAP: 14.77±3.32%, n=6, $p<0.001$, Student's t-test). The CTAP mediated enhancement of PLR was also associated with a slight increase in the velocity of constriction (data not shown). And, while not significant, unilateral, intraocular CTAP similarly enhanced the stationary PLR of WT mice evoked by bright blue light stimulus superimposed on rod-saturating background illumination (normalized pupil area of control: 37.99±4.55%, n=10, CTAP:27.58±2.92%, n=5, p=0.15, Student's t-test).

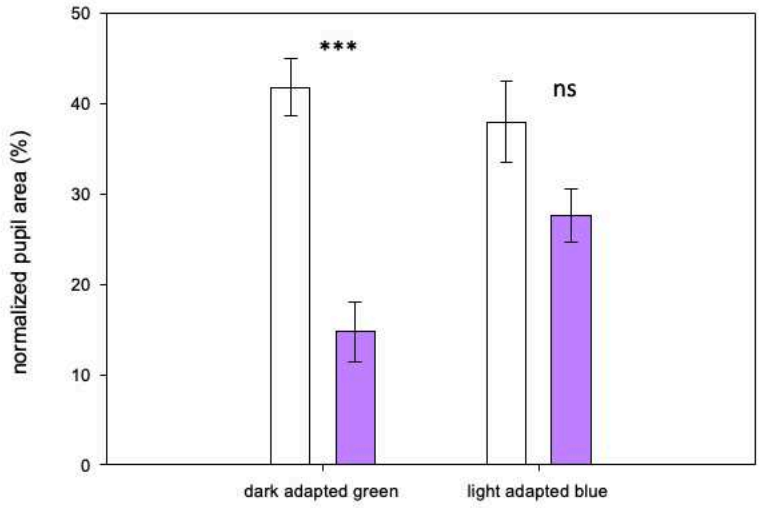

Figure 3.7 MOR specific antagonist CTAP increased dark adapted PLR in WT mice. Unilateral, intraocular injection of CTAP (1 μl of 2 mg/ml) significantly enhanced the green light-evoked stationary PLR of dark adapted WT mice compared to that of control and non-significantly enhanced blue light-evoked stationary PLR of light adapted WT mice compared to that of control. Cumulative stationary PLR data under control (white bar, n=16 green light stimulus (10^{11} photons/cm^2/s at 525 nm), n=10 blue light stimulus (10^{14} photons/cm^2/s at 470 nm on rod saturating background)) and CTAP (purple bar, n=6 green light stimulus, n=5 blue light stimulus) conditions in WT mice. Average ± SEM. ***:$p<0.001$. Student's t-test.

When comparing rod-saturating green light-evoked stationary PLR of dark adapted WT mice, MKO mice, McKO mice, and WT mice given CTAP, there was a significant difference

between only the normalized pupillary area of WT control mice and WT mice given CTAP, Fig. 3.8 (p=0.004, one way ANOVA and Holm-Sidak pairwise multiple comparisons).

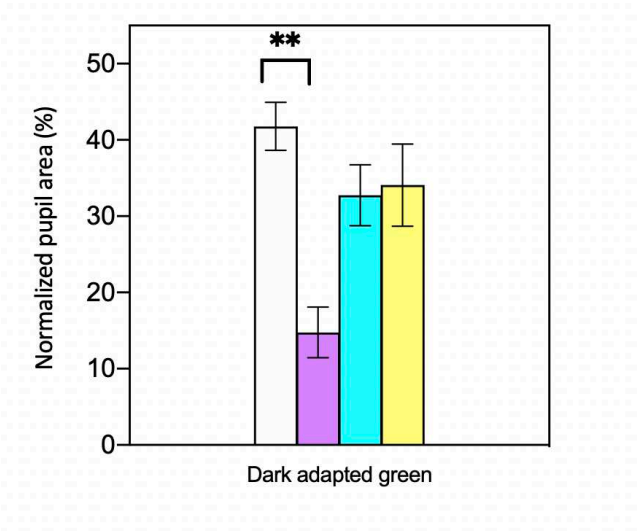

Figure 3.8 Dark adapted stationary green light-evoked PLR of WT control mice and WT mice given the MOR specific antagonist CTAP were significantly different, however, the PLRs of MKO mice, McKO mice, and WT mice injected with CTAP were not significantly different. WT control (white bar), WT with CTAP (purple bar), MKO control (teal bar), and McKO control (yellow bar). Average ± SEM. **:p<0.01. One way ANOVA and Holm-Sidak pairwise multiple comparisons.

3.5 Discussion

Our results show that opioids are negative modulators of the PLR in the WT mouse. It could be argued that opioid inhibition of PLR is secondary to miosis and thus decreased photic stimulation of the retina, however, this seems unlikely as in species where resting miosis is seen secondary to opioids, e.g. in cats (Sharpe, 1991), and man (Pickworth et al., 1991), opioids continue to inhibit the PLR over a wide range of pupil size. And, while intense blue irradiance is still capable of driving the PLR in the face of DAMGO, this is not surprising given prior studies in which elimination of 97% of ipRGCs in the mouse resulted in incomplete PLR in response to low light intensity but did not prevent full pupil constriction in response to high light intensity (Güler et al., 2008). As well, the slowing of the blue light response under DAMGO conditions

compared to control is in accordance with previous studies in man in which opioids decreased the constriction velocity of the PLR (Grace et al., 2010). The absence of DAMGO effect in McKO mice indicates that although MOR expression is not restricted to ipRGCs in the mouse retina (Gallagher et al., 2012), MORs expressed by ipRGCs are necessary and sufficient to mediate opioid action on the bright blue light evoked PLR.

It is of note that the PLR in response to bright blue irradiance was greater in the MKO mice compared to the McKO mice, Fig 3.6. As previously mentioned, synaptic inputs onto ipRGCs downstream of rods and cones, including ON/OFF bipolar cells and amacrine cells, have been shown to extend the dynamic range of ipRGCs in both the intensity and temporal frequency domains (Wong et al., 2007). Given that our prior work showed that MOR action in ipRGCs reduces excitability without affecting phototransduction (Cleymaet et al., 2019), DAMGO is expected to reduce ipRGC signaling both when driven by rod/cone inputs and by the intrinsic melanopsin phototransduction pathway under bright light conditions. The greater pupillary constriction in response to bright blue light in the MKO group vs. the McKO group suggests that in the McKO group, in which MORs are absent from ipRGCs alone, opioids may be exerting a greater inhibitory effect on elements of the retinal circuit downstream of the rod-cone photoreceptors (Gallagher et al., 2012) that are relevant for the integrated rod-cone and melanopsin mediated PLR in response to bright blue irradiance (Güler et al., 2008). Specifically, the inhibitory effects of opioids on the cone circuit mediated PLR are expected to be greater than on the rod circuit mediated PLR. While rod contribution to the PLR is minimal above the melanopsin stimulating light threshold (McDougal and Gamlin, 2010), cones do contribute to maintaining miosis at both low and high irradiances if permitted to dark adapt as per the paradigm used in these experiments (Gooley et al., 2012). Besides the relative contribution of the

different photoreceptor classes to the PLR, previous studies suggest a link between opioids and inhibition of cone mediated retinal events. For example, dopamine release is greater in light adapted retinas vs. dark adapted retinas i.e. the cone circuit drives retinal dopamine release (Dong and McReynolds, 2017). Dopamine stimulates mydriasis (Bartošová et al., 2018), and opiates inhibit retinal dopamine release (Dubocovich and Weiner, 1983); as such, under DAMGO conditions, dopamine antagonism may account for the enhanced effect on cone-circuit mediated PLR in response to bright blue light. Alternatively there may be centrally mediated opioid effects, though this is less likely considering the ~100 μM DAMGO intravitreal concentration in the present study (see Materials and Methods) and that considerably larger concentrations of DAMGO administered directly to CNS are required to produce behavioral effects, with intracerebroventricular application (1-5 μg)(Liang et al., 2015) and direct, bilateral administration of DAMGO to the nucleus accumbens (2.5 μg /site, but not 0.25 μg /site) required for significant effects on behavior using a wheel running assay (Ruegsegger et al., 2015).

The PLRs of MKO mice, McKO mice, and WT control mice were not significantly different; this may be due to compensatory mechanisms developed in the knockout mice from birth.

CTAP's enhancement of the rod/cone driven PLR in the dark-adapted retina and melanopsin driven PLR under photopic conditions in WT mice is consistent with β-endorphin's being released in the dark adapted retina (Morgan and Boelen, 1996). And, given that the PLRs of MKO mice, McKO mice, and WT mice injected with CTAP were not significantly different, the intraocular application of CTAP appears to mimic the loss of opioid effects upon both the retinal circuit downstream of rods/cones and the melanopsin driven PLR achieved via knockout of systemic and ipRGC localized MORs, respectively.

Role for endogenous opioid regulation of the PLR

Is there a physiologic role for endogenous opioid regulation of the pupil? Regarding resting pupil size, systemically applied enkephalins in rats (Tortella et al., 1980) and mice (Korczyn et al., 1980) produce resting mydriasis that is antagonized by naloxone. However, in the mouse, it seems unlikely that endogenous enkephalins have a significant role in the physiologic control of resting pupil size as neither pure naloxone blockade nor prolongation of endogenous enkephalin half-life altered pupil diameter (Korczyn et al., 1980). Nonetheless, given that separate neural mechanisms control pupil size vs. the PLR and that the effect of MORs on each is species-specific, endogenous opioids may yet have a physiologic role in the modulation of PLR.

Enkephalins (Altschuler et al., 1982; Britto and Hamassaki-Britto, 1992; Pan et al., 2008) and β-endorphin (Gallagher et al., 2010) have been detected in the avian and mammalian retina. For these endogenous opioids to regulate the PLR, there must also be receptors for opioids on cells within the retinal circuit relevant for the PLR. Retinal opiate binding sites have been demonstrated in several species, including chick, rabbit, goldfish, rat, mouse, cow, toad, and skate (Howells et al., 1980; Slaughter et al., 1985; Gallagher et al., 2012; Cleymaet et al., 2019). It has been shown that opioid receptor subtypes facilitate different, stereospecific opioid effects on pupil control (Robin et al., 1985). While substrate specificity is not exclusive, of the endogenous opioids, enkaphalins bind preferentially to δ-opioid receptors and β-endorphin to μ-opioid receptors (Kieffer, 1995), and the latter's effects on the PLR are the subject of this study.

In the present study, DAMGO did not significantly impair static PLR stimulated by bright blue light in the dark-adapted retina but did negatively regulate rod-cone mediated PLR. This is not surprising given that the photoisomerization of only a few hundred melanopsin

molecules is all that is necessary to trigger a PLR (Do et al., 2009), and near total ablation of the ipRGC population does not prevent the PLR (Güler et al., 2008). Opioids could thus potentially allow more low-irradiance light through the pupillary aperture to allow for improved vision during night hours. Furthermore, given that CTAP significantly enhanced rod-cone mediated PLR in the dark-adapted retina but not melanopsin-mediated PLR in the light-adapted retina, we suspect that CTAP may well generate a blockage against the regulatory effects of endogenous opioids. In a light adapted retina, there maybe be less of an endogenous opioid tone and thus CTAP's disinhibitory effects are less robust. The data suggests that endogenous opioids are present in the dark-adapted retina and exert a modest inhibition on PLR mediated by the endogenous phototransduction cascade of ipRGCs as well as on PLR triggered by mesopic / dim scoptopic light intensities.

There is evidence for circadian variation in systemic opioid tone, akin to other neuropeptides known to regulate ipRGC signaling such as dopamine and adenosine (Ribelayga et al., 2004; Witkovsky, 2004; Van Hook et al., 2012; Sodhi and Hartwick, 2014). Total opioid levels in murine brains is increased in the late afternoon (Wesche and Frederickson, 1979), and pain-induced plasma β-endorphin levels peak at midnight (Rasmussen and Farr, 2003). In rat, there is also an increased degree of opiate receptor binding at night (Naber et al., 1981). An increase in nighttime retinal opioid levels and binding to MORs on ipRGCs could account for the previously documented nighttime reduction in the ipRGC driven pot-illumination pupil response (PIPR) in man (Zele et al., 2011), in addition to the results observed in the present study. However, in the young rat CNS (specifically the anterior pituitary), POMc mRNA levels are lowest in the afternoon and early evening (Cai et al., 1997), although it is unclear how closely β-endorphin release follows the circadian rhythm of POMC expression.

Might opioids also affect the intrinsic PLR (iPLR), i.e. ipsilateral miosis in response to photic stimulation of the retina without input to the brain? Both melanopsin and MORs are expressed by the ciliary muscles of the iris (Bonfiglio et al., 2006; Wang et al., 2017). Recent studies also showed putative M1 ipRGC processes reach the ciliary muscles and that the iPLR is driven by melanopsin signaling from ipRGCs (Xue et al., 2011; Rupp et al., 2013; Schmidt et al., 2014b; Semo et al., 2014). Together with prior data showing MOR expression on ipRGC processes (Cleymaet et al., 2019), this suggests that opioid action on the ciliary muscles might not be independent of ipRGCs. However, the effect of opioids on the iPLR are beyond the scope of the current study as we were only able to analyze the eye contralateral to the injected eye as reflex uveitis secondary to the injection procedure precluded the analysis of local opioid effects on the iPLR in the injected eye.

Considerations for clinical practice

It is of note that chromatic pupillometry is now utilized for the differentiation of retinal disease (inner vs. outer) and optic nerve disease in both human and veterinary medicine (Park et al., 2011; Rukmini et al., 2015; Yeh et al., 2017). The PLR is utilized in non-ophthalmic applications as well, with melanopsin-mediated PLR deficits considered an indicator for increased vulnerability to major depressive disorder in low light conditions (Laurenzo et al., 2016). Given the prevalence of therapeutic opioid use, opioid modulation of the PLR should be taken into consideration when interpreting the results of diagnostic pupillometry. On the other hand, akin to resting pupillary diameter serving as an indicator of systemic opioid administration, altered PLR dynamics may represent a novel biomarker for response to / efficacy of opioid (ab)use therapy. For example, pupillary unrest under ambient light (PUAL) is depressed by

opioids, and there is a positive correlation between higher levels of post opioid administration PUAL changes and greater analgesia (Neice et al., 2017).

Conclusion

Our results indicate that intraocular opioids acting on MORs of ipRGCs are negative modulators of the PLR and are suggestive of a potential increase in endogenous opioid concentrations in the dark-adapted retina. Future studies should investigate the effect of systemic opioid administration on both the static and dynamic PLR, as this may have significant impact on the interpretation of diagnostic pupillomtery and as well serving as a potential biomarker of systemic opioid effect.

CHAPTER 4. CONCLUSION

The specific aims of the body of this work were to: (1) Analyze the molecular mechanism by which opioids modulate light-evoked signaling of ipRGCs; (2) Determine if acute inhibition of ipRGC signaling via MORs reduces pupillary light reflex (PLR) and (3) alters circadian rhythm of wheel running and the sleep/wake cycle. Chapters 2 and 3 provide support the notion that opioids alter light-evoked activity of ipRGCs and this has behavioral consequences detectable at the reflex level i.e. the PLR. The methods by which aim 3 might be addressed and the translational potential / clinical relevance for this work will be discussed here.

Investigating if acute or chronic stimulation of MORs on ipRGCs triggers wheel running behavior in mouse and/or extended wakefulness

The negative modulatory effects of MOR stimulation on ipRGCs on the PLR provide evidence at the reflex level that opioids can affect downstream functions mediated principally by ipRGCs. There is evidence that ipRGCs are critical for the hypothalamic regulation of sleep and circadian rhythms (see section 1.3.2). It is now important to investigate if the cellular effect noted in M1 ipRGCs is strong enough to facilitate a shift in circadian rhythms of sleep and wakefulness.

Existing evidence for opioids and their role in circadian rhythm and sleep disturbance

Given that the majority of clinically relevant opioid drugs bind to MORs (McDonald and Lambert, 2016), this discussion will focus on that classical opioid receptor subtype. What evidence exists for opioids modulation of circadian rhythms and sleep/wake cycles?

Regarding circadian effects of systemically applied opioids, in mice, high dose morphine injections during the subjective night (the active period of these nocturnal animals) induced

phase shifts, but not when administered during other times. Morphine caused hyperactivity, and when wheel running was prevented, morphine no longer induced a phase shift, suggesting that the action of the opioid was due to behavioral alterations rather than direct pacemaker effects. Furthermore, bilateral enucleation did not alter the results, suggesting that these effects were not mediated through the retina or its input upon the circadian pacemaker (Marchant and Mistlberger, 1995). Subsequently, the same group investigated if morphine could induce behavioral inhibition of photic circadian resetting. They found that pretreatment with morphine caused a 63% attenuation of late night light pulse-induced phase advances; morphine's inhibition of phase advances was prevented by activity restriction (Mistlberger and Holmes, 1999). An investigation of morphine's acute and chronic effects (achieved via continual release of morphine from a pellet implant) on circadian locomotor activity patterns revealed that acutely there was a significant increase in total locomotor activity and moreover the circadian pattern of that activity was markedly altered compared to baseline. Chronically i.e. after three days of morphine administration, the activity had returned to baseline levels. Upon withdrawal, there was again a upswing of locomotor activity and its circadian rhythms were again altered compared to baseline (Glaser et al., 2012).

Multiple studies have also been carried out in the hamster, which in contrast to rats and mice, is a diurnal species (Gattermann et al., 2008). In the hamster, MOR agonism does not increase the animal's activity, allowing for isolation of the effect of opioids on the circadian pacemaker. The injection of fentanyl, a MOR agonist, in the middle of the day induced phase advances (Meijer et al., 2000). A later study demonstrated similar findings (Vansteensel et al., 2005). During the subjective day, light alone did not induce a phase advance but did block that of fentanyl. During the subjective night, the inverse is true; fentanyl alone did not induce a phase

advance but did block that of light. Here, fentanyl appears to be functioning as a blind to light induced circadian alterations. Additionally, naloxone blocked the phase shifts *in vivo*, confirming opioid receptor involvement in the circadian modulations. Fentanyl additionally suppressed SCN firing rate *in vitro* as well as light induced nighttime Period 1 gene expression, suggesting that the effect of opioids on hamster circadian rhythm is mediated by direct modulation of neuronal activity in the SCN as well as regulation of Per genes (Vansteensel et al., 2005).

What can be concluded from the circadian effects of opioids in animals? In some species, opioids can have direct effects on the circadian pacemaker and can functionally blind it to photic stimuli. In mice, it would appear that any circadian effects from opioids are behaviorally mediated; however, additional mechanisms cannot be ruled out as excitation vs. depression of locomotor activity in the mouse is known to be dose, chronicity, and mouse-strain dependent (Babbini and Davis, 1972; Murphy et al., 2008). And, as previously discussed, an organism's circadian rhythms do not directly translate to sleep/wake states but can indirectly affect sleep via circadian phase adjustment.

Regarding effects of systemically applied opioids on the sleep/wake patterns of animals, morphine and/or β-endorphin administrations has been shown to decrease sleep in rabbits (Khazan and Sawyer, 1964), rats in a dose dependent manner (Khazan et al., 1967; Arankowsky-Sandoval and Gold, 1995), and cats (with reversal of opioid effects by nalaxone) (Echols and Jewett, 1972; King et al., 1981; Cronin et al., 1995). In the dog, however, morphine increased the sleep; these effects were antagonized by naloxone (Pickworth and Sharpe, 1979). The authors suggested that the increased somnolence may be drug history dependent i.e. the dogs used in the study were naïve to morphine, however in the above rat and cat studies, the animals were also

opioid naïve and responded with hyposomnolence at the start of their treatment cycles; as such there may be species specific opioid effects.

In man, sleep disorders can be classified as insomnias and circadian rhythm disorders. There are additional disorders such as parasomnias, sleep breathing disorders etc. that are not relevant to this thesis. Insomnia is defined as difficulty falling or staying asleep. Within the classification of circadian rhythm disorders, there exist the following: jet lag, shift work disorders, advanced or delayed sleep phase, and irregular sleep/wake rhythm (no discernable sleep wake pattern) and non-24 sleep/wake rhythm (progressively later sleep time). While opioids have sedating effects, there is significant evidence that they disrupt actual sleep. 87.7% of patients dependent on opium have poor sleep quality (Khazaie et al., 2016). Subjectively, opioid-dependent individuals undergoing methadone detoxification have reported difficulty in initiating and maintain sleep with poor sleep quality and efficiency as well as sleep at inappropriate times. The last category is reported in substance-dependent individuals in general, as they typically adopt nocturnal lifestyle patterns due to perturbations in circadian rhythms. And, while several of these categories have been reported by patients with depression or anxiety, reports of inadequate/poor sleep quality are unique to the opioid-dependent population (Oyefeso et al., 1997). Additional circadian rhythm disruption has been reported in acutely abstinent heroin-dependent individuals; with loss of diurnal rhythmicity in hPER1 and 2 mRNA expressions as well β-endorphin, ACTH, cortisol, leptin, and IL-2 release. These neurobiological changes were protracted, most lasting at least 30 days (Li et al., 2009).

Sleep disruption and increased wakefulness has also been shown in man via studies that objectively examine the effect of opioids on sleep stages using electroencephalograms (EEGs) or polysomnography. In healthy, non-dependent adults, heroin (Lewis et al., 1970), morphine

and/or methadone (Shaw et al., 2005; Dimsdale et al., 2007), morphine and/or methadone (Dimsdale et al., 2007) have been shown to decrease sleep duration and quality. In the opiate-dependent population, similar disruptions of sleep have been found with acute and chronic morphine administration (Kay et al., 1969; Kay, 1975a; Kay et al., 1981) as well as acute methadone administration (Pickworth et al., 1981), though tolerance to methadone's adverse effects on sleep is possible (Kay, 1975b), which may lend support to that opioid's use in replacement therapy. Similar negative effects of sleep are noted with heroin (Kay et al., 1981), with heroin having the strongest effects when compared to those of morphine and methadone (Kay et al., 1979).

Proposed future directions

While opioids may certainly be capable of mediating their sleep disruptive effects via central mechanisms, no consensus has been reached on which specific CNS sites therapeutic or abused opioids act upon to trigger sleep abnormalities (Angarita et al., 2016). Given the importance of ipRGC signaling on the activity of the circadian pacemaker, such centrally mediated opioid effects do not rule out a potential role for opioid modulation of ipRGC signaling and thereby circadian rhythms and the sleep wake state. Given the notion that light can both directly and indirectly impact the sleep/wake state, it is of interest to understand if and how opioids might modulate ipRGC signaling.

In order to use the MKOs and McKOs as models for assessing the effect of acute MOR mediated inhibition of ipRGCs on wheel running behavioral activity, we must first demonstrate if they are (or are not) still capable of photoentrainment. Akin to those experiments performed by (Güler et al., 2008) with *Opn4*$^{aDTA/aDTA}$ mice, MKO and McKO vs. WT wheel running activity should be assessed first under constant dark (DD) to determine if the MKOs and McKOs possess

functional circadian oscillators that determine standard period lengths. If capable of photoentrainment, the MKOs and McKOs should also be capable of responding to (1) advancements / delays of the photoperiod by synchronizing with the shifted cycle as demonstrated by a stable phase relationship with the new photoperiod(s) (2) light pulses as demonstrated by delayed phase onset of activity. Additionally, established effects of sex and potential effect of genotypes on wheel-running activity patterns should be verified in both the MKOs and McKOs, as well as the WT mice (Lightfoot et al., 2004).

Once the MKO and McKO models are validated, bilateral intravitreal injections of DAMGO and morphine can be administered in the middle of the light phase (7 h after light ON) when the homeostatic drive to sleep in mice is minimal. One control group should receive saline and be kept in light conditions identical to the drug injected mice. Wheel running activity should be recorded and compared across groups. If our hypothesis is correct, we would anticipate a larger increase in wheel running in WT mice that receive opioid agonists compared to mice receiving saline. We also expect opioid agonists to trigger more wheel running in WT mice during the day than in MKOs or McKOs. The timing of the intraocular opioid administration/homeostatic drive for sleep should also influence the effect of intraocular opioids; specifically, we expect strong wheel running following opioid agonists administered 7 h into the light phase, when the homeostatic drive for sleep diminishes. The interpretation of such results will be relatively straightforward: in the nocturnal mouse, inhibition of (Brn3b-, M1) ipRGCs via MORs simulates acute dark exposure and triggers wakefulness as well as wheel running activity (Altimus et al., 2008; Lupi et al., 2008). If we see no increase in the wheel running of MKO and McKO mice after DAMGO, the interpretation would be that MORs expressed by ipRGCs are critical in mediating the intraocular DAMGO effect on wheel running.

Although wheel running correlates well with circadian activity (De Visser et al., 2005; Altimus et al., 2008), it is not an exclusive measure of sleep/wake cycle (Novak et al., 2012). As such, to test the notion that systemically applied opioids alter the circadian rhythm of the sleep/wake cycle by inhibiting ipRGC signaling via MORs, WT, MKO, and McKO opioid dependent mice (established via the use of sustained release morphine pellets or osmotic mini pumps) will have their sleep/wake rhythm assessed by analysis of telemetrically transmitted recordings of two implanted biopotentials, i.e. EEG and EMG (Borniger et al., 2013). If our hypothesis is correct, we would anticipate that the circadian activity pattern in control animals receiving chronic opioid treatment will change over time i.e. we expect reduced activity at night and increased activity during the subjective day. In contrast, we expect no change in the MKO and less or no change McKO mice. Our interpretation of such results will be as follows: opioids accumulating in the vitreous inhibit light-evoked ipRGC signaling, therefore simulating darkness, even during the day. This would trigger wakefulness in the nocturnal mouse during the day.

Translational potential / clinical relevance

From a clinical perspective, it is important to note that disrupted sleep directly results in negative modulation of pain thresholds. In the rat, sleep disruption results in hyperalgesia which is reversed by sleep recovery (Onen et al., 2000). In man, total sleep deprivation similarly results in hyperalgesia, with sleep recovery providing an analgesic effect (Onen et al., 2001). Given the sleep disruptive effects of opioids, it may be that opioid administration represents a double-edged sword; while alleviating pain, opioids also decrease the pain threshold – thereby setting patients up for ever increasing opioid requirements and the attendant co-morbidities of excess opioid use. This may also bear relevance on abusers of opioids and risk for recidivism; sleep problems noted

in opioid-dependent patients have a negative impact on substance abuse treatment outcome (Burke et al., 2008). Furthermore, of patients on methadone maintenance treatment, those rated as poor sleepers also had higher levels of psychiatric disease such as anxiety and depression, chronic pain, drug abuse, and unemployment (Stein et al., 2004; Peles et al., 2006, 2009). As such, the translational potential of this project is significant: the results will directly predict if MORs expressed by ipRGCs could be considered as therapeutic targets for focally delivered MOR selective antagonists to reduce the severity and inherent comorbidities of sleep disorders in patients receiving chronic opioid treatment.

Beyond sleep disorders, ipRGCs and the light signals they convey to the central nervous system are important for regulation of mood, learning, and cognitive function. Irregular light, e.g. as a consequence seasonal day length changes, transmeridian travel, and shift work, can negatively impact mental health leading to disorders such as depression, season affective disorder (SAD), and impaired learning / cognition (Legates et al., 2012). Indeed, patients with SAD manifest a reduced melanopsin-mediated post illumination pupil response (PIPR) (Roecklein et al., 2013). Circadian desynchronization has also been shown to promote metabolic pathologies including but not limited to impaired glucose tolerance, systemic blood pressure dysregulation, insulin resistance, obesity, and eating disorders (Albrecht, 2012). In migraneurs, photic signaling of ipRGCs plays an important role in the exacerbation of migraine-type photophobia, wherein headaches are exacerbated by light and there is abnormal sensitivity to light, and also photo-oculodynia, or light-induced ocular pain. The effects are mediated by enhanced activity of relay posterior thalamic trigeminovascular neurons (Noseda and Burnstein, 2011).

Thus, in addition to amelioration of pupillary dysfunction and sleep disorders in chronic opioid users, MORs and modulation of their signaling on ipRGCs suggests a potential new target for therapy of light-mediated disorders. However, therapy for such disorders would need to be specifically directed so as not to disrupt the physiologic and beneficial roles of ipRGCs in non-imaging forming vision.

REFERENCES

Abdul Y, Akhter N, Husain S (2013) Delta-opioid agonist SNC-121 protects retinal ganglion cell function in a chronic ocular hypertensive rat model. Investig Ophthalmol Vis Sci 54:1816–1828.

Adhikari P, Zele AJ, Feigl B (2015) The post-illumination pupil response (PIPR). Investig Ophthalmol Vis Sci 56:3838–3849.

Adler CH, Robin M, Adler MW (1981) Tolerance to morphine-induced mydriasis in the rat pupil. Life Sci 28:2469–2475.

Aghajanian GK (1978) Tolerance of locus coeruleus neurones to morphine and suppression of withdrawal response by clonidine. Nature 276:186–188.

Aghajanian GK, Cedarbaum JM, Wang RY (1977) Evidence for norepinephrine-mediated collateral inhibition of locus coeruleus neurons. Brain Res 136:570–577.

Al-Hasani R, Bruchas MR (2011) Molecular mechanisms of opioid receptor-dependent signaling and behavior. Anesthesiology 115:1363–1381.

Al-Sabi A, Shamotienko O, Dhochartaigh SN, Muniyappa N, Le Berre M, Shaban H, Wang J, Sack JT, Dolly JO (2010) Arrangement of Kv1 α subunits dictates sensitivity to tetraethylammonium. J Gen Physiol 136:273–282.

Albrecht U (2012) Timing to Perfection: The Biology of Central and Peripheral Circadian Clocks. Neuron 74:246–260.

Altimus CM, Güler AD, Villa KL, McNeill DS, LeGates TA, Hattar S (2008) Rods-cones and melanopsin detect light and dark to modulate sleep independent of image formation. Proc Natl Acad Sci 105:19998–20003.

Altschuler RA, Mosinger JL, Hoffman DW, Parakkal MH (1982) Immunocytochemical localization of enkephalin-like immunoreactivity in the retina of the guinea pig. Proc Natl Acad Sci U S A 79:2398–2400.

Angarita GA, Emadi N, Hodges S, Morgan PT (2016) Sleep abnormalities associated with alcohol, cannabis, cocaine, and opiate use: a comprehensive review. Addict Sci Clin Pract 11:1–17.

Arankowsky-Sandoval G, Gold PE (1995) Morphine-Induced Deficits in Sleep Patterns: Attenuation by Glucose. Neurobiol Learn Mem 64:133–138.

Armstrong CM, Gilly WF (1992) Access resistance and space clamp problems associated with whole-cell patch clamping. Methods Enzymol 207:100–122.

Avidor-Reiss T, Nevo I, Levy R, Pfeuffer T, Vogel Z (1996) Chronic opioid treatment induces adenylyl cyclase V superactivation. Involvement of Gbetagamma. J Biol Chem 271:21309–21315.

Babbini M, Davis WM (1972) Time-dose relationships for locomotor activity effects of morphine after acute or repeated treatment. Br J Pharmacol 46:213–224.

Bao Y, Gao Y, Yang L, Kong X, Yu J, Hou W, Hua B (2015) The mechanism of μ-opioid receptor (MOR)-TRPV1 crosstalk in TRPV1 activation involves morphine anti-nociception, tolerance and dependence. Channels 9:235–243.

Bartošová O, Bonnet C, Ulmanová O, Šíma M, Perlík F, Růžička E, Slanař O (2018) Pupillometry as an indicator of l-DOPA dosages in Parkinson's disease patients. J Neural Transm 125:699–703.

Baver SB, Pickard GEGE, Sollars PJ, Pickard GEGE (2008) Two types of melanopsin retinal ganglion cell differentially innervate the hypothalamic suprachiasmatic nucleus and the olivary pretectal nucleus. Eur J Neurosci 27:1763–1770.
Berson DM, Castrucci AM, Provencio I (2010) Morphology and mosaics of melanopsin-expressing retinal ganglion cell types in mice. J Comp Neurol 518:2405–2422.
Berson DM, Dunn FA, Takao M (2002) Phototransduction by retinal ganglion cells that set the circadian clock. Science 295:1070–1073.
Bird SJ, Kuhar MJ (1977) Iontophoretic application of opiates to the locus coeruleus. Brain Res 122:523–533.
Bonfiglio V, Bucolo C, Camillieri G, Drago F (2006) Possible involvement of nitric oxide in morphine-induced miosis and reduction of intraocular pressure in rabbits. Eur J Pharmacol 534:227–232.
Borbe HO, Wollert U, Müller WE (1982) Stereospecific [3H]naloxone binding associated with opiate receptors in bovine retina. Exp Eye Res 34:539–544.
Borbély AA (1982) A two process model of sleep regulation. Hum Neurobiol 1:195–204.
Borniger JC, Weil ZM, Zhang N, Nelson RJ (2013) Dim Light at Night Does Not Disrupt Timing or Quality of Sleep in Mice. Chronobiol Int 30:1016–1023.
Bosma MM, Allen ML, Martin TM, Tempel BL (1993) PKA-dependent regulation of mKv1.1, a mouse Shaker-like potassium channel gene, when stably expressed in CHO cells. J Neurosci 13:5242–5250.
Bourinet E, Soong TW, Stea A, Snutch TP (1996) Determinants of the G protein-dependent opioid modulation of neuronal calcium channels. Proc Natl Acad Sci U S A 93:1486–1491.
Brainard GC, Hanifin JP, Greeson JM, Byrne B, Glickman G, Gerner E, Rollag MD (2001) Action spectrum for melatonin regulation in humans: evidence for a novel circadian photoreceptor. J Neurosci 21:6405–6412.
Brew HM, Gittelman JX, Silverstein RS, Hanks TD, Demas VP, Robinson LC, Robbins CA, McKee-Johnson J, Chiu SY, Messing A, Tempel BL (2007) Seizures and reduced life span in mice lacking the potassium channel subunit Kv1.2, but hypoexcitability and enlarged Kv1 currents in auditory neurons. J Neurophysiol 98:1501–1525.
Brew HM, Hallows JL, Tempel BL (2003) Hyperexcitability and reduced low threshold potassium currents in auditory neurons of mice lacking the channel subunit Kv1.1. J Physiol 548:1–20.
Britto LRG, Hamassaki-Britto DE (1992) Enkephalin-immunoreactive ganglion cells in the pigeon retina. Vis Neurosci 9:389–398.
Bullitt E (1990) Expression ofC-fos-like protein as a marker for neuronal activity following noxious stimulation in the rat. J Comp Neurol 296:517–530.
Burke CK, Peirce JM, Kidorf MS, Neubauer D, Punjabi NM, Stoller KB, Hursh S, Brooner RK (2008) Sleep problems reported by patients entering opioid agonist treatment. J Subst Abuse Treat 35:328–333.
Cachero TG, Morielli AD, Peralta EG (1998) The Small GTP-Binding Protein RhoA Regulates a Delayed Rectifier Potassium Channel. Cell 93:1077–1085.
Cagnacci A, Kräuchi K, Wirz-Justice A, Volpe A (1997) Homeostatic versus Circadian Effects of Melatonin on Core Body Temperature in Humans. J Biol Rhythms 12:509–517.
Cagnacci A, Soldani R, Yen SS (2017) Contemporaneous melatonin administration modifies the circadian response to nocturnal bright light stimuli. Am J Physiol Integr Comp Physiol 272:R482–R486.

Cai A, Scarbrough K, Hinkle DA, Wise PM (1997) Fetal grafts containing suprachiasmatic nuclei restore the diurnal rhythm of CRH and POMC mRNA in aging rats. Am J Physiol Integr Comp Physiol 273:R1764–R1770.
Cassone VM, Chesworth MJ, Armstrong SM (1986) Entrainment of rat circadian rhythms by daily injection of melatonin depends upon the hypothalamic suprachiasmatic nuclei. Physiol Behav 36:1111–1121.
Centers for Disease Control and Prevention (2018) 2018 Annual Surveillance Report of Drug-Related Risks and Outcomes — United States. Surveillance Special Report 2.
Chastrette N, Cespuglio R, Jouvet M (1990) Proopiomelanocortin (POMC)-derived peptides and sleep in the rat Part 1 — Hypnogenic properties of ACTH derivatives. Neuropeptides 15:61–74.
Chen SK, Badea TC, Hattar S (2011) Photoentrainment and pupillary light reflex are mediated by distinct populations of ipRGCs. Nature 476:92–96.
Chen Y, Stevens B, Chang J, Milbrandt J, Barres BA, Hell JW (2008) NS21 : Re-defined and modified supplement B27 for neuronal cultures. 171:239–247.
Clark JD, Tempel BL (1998) Hyperalgesia in mice lacking the Kv1.1 potassium channel gene. Neurosci Lett 251:121–124.
Cleymaet AM, Gallagher SK, Tooker RE, Lipin MY, Renna JM, Sodhi P, Berg D, Hartwick ATE, Berson DM, Vigh J (2019) μ-Opioid Receptor Activation Directly Modulates Intrinsically Photosensitive Retinal Ganglion Cells. Neuroscience 408:400–417.
Cobaugh DJ, Gainor C, Gaston CL, Kwong TC, Magnani B, Mcpherson ML, Painter JT, Krenzelok EP (2014) The opioid abuse and misuse epidemic: Implications for pharmacists in hospitals and health systems. Am J Heal Pharm 71:1539–1554.
Coleman SK, Newcombe J, Pryke J, Dolly JO (1999) Subunit composition of Kv1 channels in human CNS. J Neurochem 73:849–858.
Connors EC, Ballif BA, Morielli AD (2008) Homeostatic regulation of Kv1.2 potassium channel trafficking by cyclic AMP. J Biol Chem 283:3445–3453.
Cox RH (2005) Molecular determinants of voltage-gated potassium currents in vascular smooth muscle. Cell Biochem Biophys 42:167–195.
Cronin A, Keifer JC, Baghdoyan HA, Lydic R (1995) Opioid inhibition of rapid eye movement sleep by a specific mu receptor agonist. Br J Anaesth 74:188–192.
Czeisler CA, Shanahan TL, Klerman EB, Martens H, Brotman DJ, Emens JS, Klein T, Rizzo JF (1995) Suppression of Melatonin Secretion in Some Blind Patients by Exposure to Bright Light. N Engl J Med 332:6–11.
Dang VC, Christie MJ (2012) Mechanisms of rapid opioid receptor desensitization, resensitization and tolerance in brain neurons. Br J Pharmacol 165:1704–1716.
De Visser L, Van Den Bos R, Spruijt BM (2005) Automated home cage observations as a tool to measure the effects of wheel running on cage floor locomotion. Behav Brain Res 160:382–388.
De Wied D, Jolles J (1982) Neuropeptides derived from pro-opiocortin: behavioral, physiological, and neurochemical effects. Physiol Rev 62:976–1059.
DiFrancesco D, Ferroni A, Mazzanti M, Tromba C (1986) Properties of the hyperpolarizing-activated current (if) in cells isolated from the rabbit sino-atrial node. J Physiol 377:61–88.
Dijk DJ, Cajochen C (1997) Melatonin and the Circadian Regulation of Sleep Initiation, Consolidation, Structure, and the Sleep EEG. J Biol Rhythms 12:627–635.
Dimsdale JE, Norman D, DeJardin D, Wallace MS (2007) The Effect of Opioids on Sleep

Architecture Joel. J Clin Sleep Med 3:33–36.
Djamgoz MB, Stell WK, Chin CA, Lam DM (1981) An opiate system in the goldfish retina. Nature 292:620–623.
Do MTH, Kang SH, Xue T, Zhong H, Liao H, Bergles DE, Yau K-W (2009) Photon capture and signalling by melanopsin retinal ganglion cells. Nature 457:281–287.
Dong CJ, McReynolds JS (2017) Comparison of the effects of flickering and steady light on dopamine release and horizontal cell coupling in the mudpuppy retina. J Neurophysiol 67:364–372.
Douglas RM, Alam NM, Silver BD, McGill TJ, Tschetter WW, Prusky GT (2005) Independent visual threshold measurements in the two eyes of freely moving rats and mice using a virtual-reality optokinetic system. Vis Neurosci 22:677–684.
Doyle SE, Castrucci AM, McCall M, Provencio I, Menaker M (2006) Nonvisual light responses in the Rpe65 knockout mouse: rod loss restores sensitivity to the melanopsin system. Proc Natl Acad Sci U S A 103:10432–10437.
Drago F, Gorgone G, Spina F, Panissidi G, Bello AD, Moro F, Scapagnini U (1980) Opiate receptors in the rabbit iris. Naunyn Schmiedebergs Arch Pharmacol 315:1–4.
Dubocovich ML, Weiner N (1983) Enkephalins modulate [3H]dopamine release from rabbit retina in vitro. J Pharmacol Exp Ther 224:634–639.
Dumitrescu ON, Pucci FG, Wong KY, Berson DM (2009) Ectopic retinal ON bipolar cell synapses in the OFF inner plexiform layer: Contacts with dopaminergic amacrine cells and melanopsin ganglion cells. J Comp Neurol 517:226–244.
Echols SD, Jewett RE (1972) Effects of morphine on sleep in the cat. Psychopharmacologia 24:435–448.
Ecker JL, Dumitrescu ON, Wong KY, Alam NM, Chen S-KK, LeGates T, Renna JM, Prusky GT, Berson DM, Hattar S (2010) Melanopsin-expressing retinal ganglion-cell photoreceptors: Cellular diversity and role in pattern vision. Neuron 67:49–60.
Ecker JL, Hattar S (2010) Understanding the Complexity of ipRGCs Targeting and Functions. Invest Ophthalmol Vis Sci 51:664.
Edgar DM, Dement WC, Fuller CA (1993) Effect of SCN lesions on sleep in squirrel monkeys: evidence for opponent processes in sleep-wake regulation. J Neurosci 13:1065–1079.
Emanuel AJ, Do MTH (2015) Melanopsin tristability for sustained and broadband phototransduction. Neuron 85:1043–1055.
Engelund A, Fahrenkrug J, Harrison A, Hannibal J (2010) Vesicular glutamate transporter 2 (VGLUT2) is co-stored with PACAP in projections from the rat melanopsin-containing retinal ganglion cells. Cell Tissue Res 340:243–255.
Estevez ME, Fogerson PM, Ilardi MC, Borghuis BG, Chan E, Weng S, Auferkorte ON, Demb JB, Berson DM (2012) Form and Function of the M4 Cell , an Intrinsically Photosensitive Retinal Ganglion Cell Type Contributing to Geniculocortical Vision. 32:13608–13620.
Faber ESL, Sah P (2004) Opioids Inhibit Lateral Amygdala Pyramidal Neurons by Enhancing a Dendritic Potassium Current. J Neurosci 24:3031–3039.
Fanciullacci M, Boccuni M, Pietrini U, F S (1981) Search for opiate receptors in human pupil. Int J Clin Pharmacol Res 1:139–143.
Fernandez DC, Chang Y-T, Hattar S, Chen S-K (2016) Architecture of retinal projections to the central circadian pacemaker. Proc Natl Acad Sci 113:6047–6052.
Fernández P, Seoane S, Vázquez C, Tabernero MJ, Carro AM, Lorenzo RA (2013) Chromatographic determination of drugs of abuse in vitreous humor using solid-phase

extraction. J Appl Toxicol 33:740–745.
Finnegan TF, Chen S, Pan H, Thomas F, Chen S, Opioid HP (2006) Mu-Opioid Receptor Activation Inhibits GABAergic Inputs to Basolateral Amygdala Neurons Through Kv1.1/1.2 Channels. j n 95:2032–2041.
Foster RG (1998) Shedding Light on the Biological Clock. Neuron 20:829–832.
Foster RG, Provencio I, Hudson D, Fiske S, De Grip W, Menaker M (1991) Circadian photoreception in the retinally degenerate mouse (rd/rd). J Comp Physiol A 169:39–50.
Fox PD, Hentges ST (2017) Differential Desensitization Observed at Multiple Effectors of Somatic μ-Opioid Receptors Underlies Sustained Agonist-Mediated Inhibition of Proopiomelanocortin Neuron Activity. J Neurosci Off J Soc Neurosci 37:8667–8677.
Freedman MS, Lucas R, Soni B, von Schantz M, Muñoz M, David-Gray Z, Foster R (1999) Regulation of Mammalian Circadian Behavior by Non-rod, Non-cone, Ocular Photoreceptors. Science 284:502–504.
Fuller PM, Gooley JJ, Saper CB (2006) Neurobiology of the sleep-wake cycle: Sleep architecture, circadian regulation, and regulatory feedback. J Biol Rhythms 21:482–493.
Galeotti N, Ghelardini C, Papucci L, Capaccioli S, Quattrone A, Morgagni VGB, Florence I- (1997) An Antisense Oligonucleotide on the Mouse Shaker -like Potassium Channel Kv1 .1 Gene Prevents Antinociception Induced by Morphine and Baclofen 1. 281:941–949.
Galeotti N, Ghelardini C, Vinci MC, Bartolini A (1999) Role of potassium channels in the antinociception induced by agonists of α2-adrenoceptors. Br J Pharmacol 126:1214–1220.
Gallagher SK (2013) Mu-opioid system in the mammalian retina.
Gallagher SK, Anglen JN, Mower JM, Vigh J (2012) Dopaminergic amacrine cells express opioid receptors in the mouse retina. Vis Neurosci 29:203–209.
Gallagher SK, Witkovsky P, Roux MJ, Low MJ, Otero-corchon V, Hentges ST, Vigh J (2010) B-Endorphin Expression in the Mouse Retina. J Comp Neurol 3148:3130–3148.
Gamlin PDR, McDougal DH, Pokorny J, Smith VC, Yau KW, Dacey DM (2007) Human and macaque pupil responses driven by melanopsin-containing retinal ganglion cells. Vision Res 47:946–954.
Gattermann R, Johnston RE, Yigit N, Fritzsche P, Larimer S, Ozkurt S, Neumann K, Song Z, Colak E, Johnston J, McPhee ME (2008) Golden hamsters are nocturnal in captivity but diurnal in nature. Biol Lett 4:253–255.
Glaser AM, Reyes-Vázquez C, Prieto-Gómez B, Burau K, Dafny N (2012) Morphine administration and abrupt cessation alter the behavioral diurnal activity pattern. Pharmacol Biochem Behav 101:544–552.
Glazebrook PA, Ramirez AN, Schild JH, Shieh CC, Doan T, Wible BA, Kunze DL (2002) Potassium channels Kv1.1, Kv1.2 and Kv1.6 influence excitability of rat visceral sensory neurons. J Physiol 541:467–482.
Goldstein A, Fischli W, Lowney LI, Hunkapiller M, Hood L (1981) Porcine pituitary dynorphin: complete amino acid sequence of the biologically active heptadecapeptide. Proc Natl Acad Sci U S A 78:7219–7223.
Gooley JJ, Ho Mien I, St. Hilaire MA, Yeo S-C, Chua EC-P, van Reen E, Hanley CJ, Hull JT, Czeisler CA, Lockley SW (2012) Melanopsin and Rod-Cone Photoreceptors Play Different Roles in Mediating Pupillary Light Responses during Exposure to Continuous Light in Humans. J Neurosci 32:14242–14253.
Gooley JJ, Lu J, Fischer D, Saper CB (2003) A broad role for melanopsin in nonvisual photoreception. J Neurosci 23:7093–7106.

Gordon E, Stang B V., Heidel J, Poulsen KP, Cebra CK, Schlipf JW (2018) Pharmacokinetic evaluation and safety of topical 1% morphine sulfate application on the healthy equine eye. Vet Ophthalmol 21:516–523.

Grace PM, Stanford T, Gentgall M, Rolan PE (2010) Utility of saccadic eye movement analysis as an objective biomarker to detect the sedative interaction between opioids and sleep deprivation in opioid-naive and opioid-tolerant populations. J Psychopharmacol 24:1631–1640.

Gracitelli CPB, Duque-Chica GL, Moura AL de A, Roizenblatt M, Nagy B V., de Melo GR, Borba PD, Teixeira SH, Tufik S, Ventura DF, Paranhos A (2016) Relationship between Daytime Sleepiness and Intrinsically Photosensitive Retinal Ganglion Cells in Glaucomatous Disease. J Ophthalmol 2016:1–9.

Gracitelli CPB, Duque-Chica GL, Roizenblatt M, Moura AL de A, Nagy B V., Ragot de Melo G, Borba PD, Teixeira SH, Tufik S, Ventura DF, Paranhos A (2015) Intrinsically Photosensitive Retinal Ganglion Cell Activity Is Associated with Decreased Sleep Quality in Patients with Glaucoma. Ophthalmology 122:1139–1148.

Graham DM, Wong KY, Shapiro P, Frederick C, Pattabiraman K, Berson DM (2008) Melanopsin ganglion cells use a membrane-associated rhabdomeric phototransduction cascade. J Neurophysiol 99:2522–2532.

Grissmer S, Nguyen N, Hanson C, Mather J, Gutman A, Karmilowicz J, Auperin D, George K (1994) Pharmacological Characterization of Five Cloned Voltage-Gated Expressed in Mammalian Cell Lines. Mol Pharmacol 45:1227–1234.

Güler AD, Ecker JL, Lall GS, Haq S, Altimus CM, Liao W, Barnard AR, Cahill H, Badea TC, Zhao H, Mark W, Berson DM, Lucas RJ, Yau K, Hattar S (2008) Melanopsin cells are the principal conduits for rod/cone input to non-image forming vision. Nature 453:102–105.

Gutman GA, Chandy KG, Grissmer S, Lazdunski M, McKinnon D, Pardo LA, Robertson GA, Rudy B, Sanguinetti MC, Stühmer W, Wang X (2005) International Union of Pharmacology. LIII. Nomenclature and molecular relationships of voltage-gated potassium channels. Pharmacol Rev 57:473–508.

Hall CA, Chilcott RP, Hall CA, Chilcott RP (2018) Eyeing up the Future of the Pupillary Light Reflex in Neurodiagnostics. Diagnostics 8:1–20.

Hankins MW, Peirson SN, Foster RG (2007) Melanopsin : an exciting photopigment. Trends Neurosci 31:27–36.

Hannibal J (2006) Roles of PACAP-Containing Retinal Ganglion Cells in Circadian Timing. Int Rev Cytol 251:1–39.

Harrington ME (1997) The ventral lateral geniculate nucleus and the intergeniculate leaflet: Interrelated structures in the visual and circadian systems. Neurosci Biobehav Rev 21:705–727.

Hartwick ATE, Bramley JR, Yu J, Stevens KT, Allen CN, Baldridge WH, Sollars PJ, Pickard GE (2007) Light-Evoked Calcium Responses of Isolated Melanopsin- Expressing Retinal Ganglion Cells. J Neurosci 27:13468–13480.

Hatori M, Le H, Vollmers C, Keding SR, Tanaka N, Schmedt C, Jegla T, Panda S (2008) Inducible ablation of melanopsin-expressing retinal ganglion cells reveals their central role in non-image forming visual responses. PLoS One 3.

Hattan D, Nesti E, Cachero TG, Morielli AD (2002) Tyrosine phosphorylation of Kv1.2 Modulates its interaction with the actin-binding protein cortactin. J Biol Chem 277:38596–38606.

Hattar S, Liao HW, Takao M, Berson DM, Yau KW, America N, Dee P (2002) Melanopsin-containing retinal ganglion cells: Architecture, projections, and intrinsic photosensitivity. Science 295:1065–1070.
Hattar S, Lucas RJ, Mrosovsky N, Thompson S, Douglas RH, Hankins MW, Lem J, Biel M, Hofmann F, Foster RG, Yau KW (2003) Melanopsin and rod—cone photoreceptive systems account for all major accessory visual functions in mice. Nature 424:76–81.
Hattar SS, Kumar M, Park A, Tong P, Tung J, Yau K-W, Berson DM (2006) Central Projections of Melanopsin- Expressing Retinal Ganglion Cells in the Mouse. J Comp Neurol 497:326–349.
Haverkamp S, Wassle H (2000) Immunocytochemical analysis of the mouse retina. J Comp Neurol 424:1–23.
Hoshi H, Liu W-L, Massey SC, Mills SL (2009) ON Inputs to the OFF Layer: Bipolar Cells That Break the Stratification Rules of the Retina. J Neurosci 29:8875– 8883.
Hosoya K, Tomi M, Tachikawa M (2011) Strategies for therapy of retinal diseases using systemic drug delivery: relevance of transporters at the blood–retinal barrier. Expert Opin Drug Deliv 8:1571–1578.
Howells R, Gorth J, Hiller J, Simon E (1980) Opiate binding sites in the retina: properties and distribution. J Pharmacol Exp Ther 215:60–64.
Hsia JA, Moss J, Hewlett EL, Vaughan M (1984) ADP-ribosylation of adenylate cyclase by pertussis toxin. Effects on inhibitory agonist binding. J Biol Chem 259:1086–1090.
Hu C, Hill DD, Wong KY (2013) Intrinsic physiological properties of the five types of mouse ganglion-cell photoreceptors. J Neurophysiol 109:1876–1889.
Huang X-Y, Morielli AD, Peralta EG (1993) Tyrosine Kinase-Dependent Suppression of a Potassium Channel by the G Protein-Coupled ml Muscarinic Acetylcholine Receptor. Cell 75:1145–1156.
Hughes J, Smith TW, Kosterlitz HW, Fothergill LA, Morgan BA, Morris HR (1975) Identification of two related pentapeptides from the brain with potent opiate agonist activity. Nature 258:577–580.
Husain S, Abdul Y, Potter DE (2012) Non-analgesic effects of opioids: neuroprotection in the retina. Curr Pharm Des 18:6101–6108.
Husain S, Potter DE, Crosson CE (2009) Opioid Receptor-Activation: Retina Protected from Ischemic Injury. Investig Opthalmology Vis Sci 50:3853–3859.
Ingram SL, Williams JT (1994) Opioid inhibition of Ih via adenylyl cyclase. Neuron 13:179–186.
Isayama T, Zagon IS (1991) Localization of preproenkephalin a mRNA in the neonatal rat retina. Brain Res Bull 27:805–808.
Jackson IM, Bolaffi JL, Guillemin R (1980) Presence of immunoreactive beta-endorphin and enkephalin-like material in the retina and other tissues of the frog, Rana pipiens. Gen Comp Endocrinol 42:505–508.
Jerng HH, Pfaffinger PJ, Covarrubias M (2004) Molecular physiology and modulation of somatodendritic A-type potassium channels. Mol Cell Neurosci 27:343–369.
Johnson J, Wu V, Donovan M, Majumdar S, Renteria RC, Porco T, Van Gelder RN, Copenhagen DR (2010) Melanopsin-dependent light avoidance in neonatal mice. Proc Natl Acad Sci 107:17374–17378.
Jones K a, Hatori M, Mure LS, Bramley JR, Artymyshyn R, Hong S-P, Marzabadi M, Zhong H, Sprouse J, Zhu Q, Hartwick ATE, Sollars PJ, Pickard GE, Panda S (2013) Small-molecule

antagonists of melanopsin-mediated phototransduction. Nat Chem Biol 9:630–635.
Kakidani H, Furutani Y, Takahashi H, Noda M, Morimoto Y, Hirose T, Asai M, Inayama S, Nakanishi S, Numa S (1982) Cloning and sequence analysis of cDNA for porcine beta-neo-endorphin/dynorphin precursor. Nature 298:245–249.
Kalsbeek A, Garidou ML, Palm IF, Van Vliet J Der, Simonneaux V, Pevet P, Buijs RM (2000) Melatonin sees the light: Blocking GABA-ergic transmission in the paraventricular nucleus induces daytime secretion of melatonin. Eur J Neurosci 12:3146–3154.
Kanakin T (2009) Biased agonism. Biol Reports 1:1–5.
Kangawa K, Matsuo H, Igarashi M (1979) α-Neo-endorphin: A “big” leu-enkephalin with potent opiate activity from porcine hypothalami. Biochem Biophys Res Commun 86:153–160.
Kankipati L, Girkin CA, Gamlin PD (2011) The post-illumination pupil response is reduced in glaucoma patients. Investig Ophthalmol Vis Sci 52:2287–2292.
Kay D, Pickworth W, Neider G (1981) Morphine-like insomnia from heroin in nondependent human addicts. Br J Clin Pharmacol 11:159–169.
Kay DC (1975a) Human sleep during chronic morphine intoxication. Psychopharmacologia 44:117–124.
Kay DC (1975b) Human sleep and EEG through a cycle of methadone dependence. Electroencephalogr Clin Neurophysiol 38:35–43.
Kay DC, Eisenstein RB, Jasinski DR (1969) Morphine effects on human REM state, waking state and NREM sleep. Psychopharmacologia 14:404–416.
Kay DC, Pickworth WB, Neidert GL, Falcone D, Fishman PM, Othmer E (1979) Opioid effects on computer-derived sleep and EEG parameters in nondependent human addicts. Sleep 2:175–191.
Keenan WT, Rupp AC, Ross RA, Somasundaram P, Hiriyanna S, Wu Z, Badea TC, Robinson PR, Lowell BB, Hattar SS (2016) A visual circuit uses complementary mechanisms to support transient and sustained pupil constriction. Elife 5:e15392.
Kelly E, Bailey CP, Henderson G (2009) Agonist-selective mechanisms of GPCR desensitization. Br J Pharmacol 153:S379–S388.
Kew JN, Davies CH eds. (2010) Ion Channels: From Structure to Function, 2nd ed. New York: Oxford University Press.
Khazaie H, Najafi F, Ghadami MR, Azami A, Ms MN, Tahmasian M, Khaledi-paveh B (2016) Sleep Disorders in Methadone Maintenance Treatment Volunteers and Opium-dependent Patients. Addict Heal Spring 8:84–89.
Khazan K, Weeks JR, Schroeder LA (1967) Electroencephalographic, electromyographic and behavioral correlates during a cycle of selfmaintained morphine addiction in the rat. J Pharmacol Exp Ther 155:521–531.
Khazan N, Sawyer CH (1964) Mechanisms of paradoxical sleep as revealed by neurophysiologic and pharmacologic approaches in the rabbit. Psychopharmacologia 5:457–466.
Kieffer BL (1995) Recent advances in molecular recognition and signal transduction of active peptides: Receptors for opioid peptides. Cell Mol Neurobiol 15:615–635.
King C, Masserano JM, Codd E, Byrne WL (1981) Effects of β-endorphin and morphine on the sleep-wakefulness behavior of cats. Sleep 4:259–262.
Kirkpatrick SL, Bryant CD (2015) Behavioral architecture of opioid reward and aversion in C57BL/6 substrains. Front Behav Neurosci 8:1–11.
Kolb H, Fernandez E, Nelson R (2007) Inner Plexiform Layer. Webvision Organ Retin Vis Syst Available at: https://www.ncbi.nlm.nih.gov/books/NBK11536/ [Accessed January 26,

2019].
Korczyn AD, Eshel Y, Keren O (1980) Enkephalin mydriasis in mice. Eur J Pharmacol 65:285–287.
Korczyn AD, Maor D (1982) Central and peripheral components of morphine mydriasis in mice. Pharmacol Biochem Behav 17:897–899.
Korf J, Bunney BS, Aghajanian GK (1974) Noradrenergic neurons: Morphine inhibition of spontaneous activity. Eur J Pharmacol 25:165–169.
Kostic C, Crippa S V, Martin C, Kardon RH, Biel M, Arsenijevic Y, Kawasaki A (2016) Determination of Rod and Cone Influence to the Early and Late Dynamic of the Pupillary Light Response. Invest Ophthalmol Vis Sci 57:2501–2508.
Kräuchi K, Cajochen C, Wirz-Justice A (1997) A relationship between heat loss and sleepiness: effects of postural change and melatonin administration. J Appl Physiol 83:134–139.
Krieger DT (1983) Brain Peptides: What, Where, and Why? Science 222:9750985.
Laurenzo SA, Kardon R, Ledolter J, Poolman P, Schumacher AM, Potash JB, Full JM, Rice O, Ketcham A, Starkey C, Fiedorowicz JG (2016) Pupillary response abnormalities in depressive disorders. Psychiatry Res 246:492–499.
Lee CWS, Yan JY, Chiang YC, Hung TW, Wang HL, Chiou LC, Ho IK (2011) Differential pharmacological actions of methadone and buprenorphine in human embryonic kidney 293 cells coexpressing human μ-opioid and opioid receptor-like 1 receptors. Neurochem Res 36:2008–2021.
Lee HK, Wang SC (1975) Mechanism of morphine-induced miosis in the dog. J Pharmacol Exp Ther 192:415–431.
Legates TA, Altimus CM, Wang H, Lee H, Yang S, Zhao H, Kirkwood A, Weber ET, Hattar S (2012) Aberrant light directly impairs mood and learning through melanopsin-expressing neurons. Nature 491:594–598.
Lehman MN, Silver R, Gladstone WR, Kahn RM, Gibson M, Bittman EL (1987) Circadian rhythmicity restored by neural transplant. Immunocytochemical characterization of the graft and its integration with the host brain. J Neurosci 7:1626–1638.
Levitt ES, Purington LC, Traynor JR (2010) Gi/o-Coupled Receptors Compete for Signaling to Adenylyl Cyclase in SH-SY5Y Cells and Reduce Opioid-Mediated cAMP Overshoot. Mol Pharmacol 79:461–471.
Lewis SA, Oswald I, Evans JI, Akindele MO, Tompsett SL (1970) Heroin and human sleep. Electroencephalogr Clin Neurophysiol 28:374–381.
Lewy AJ, Ahmed S, Jackson JM, Sack RL (1992) Melatonin shifts human circadian rhythms according to a phase-response curve. Chronobiol Int 9:380–392.
Li CH, Chung D (1976) Isolation and structure of an untriakontapeptide with opiate activity from camel pituitary glands. Proc Natl Acad Sci U S A 73:1145–1148.
Li S xia, Shi J, Epstein DH, Wang X, Zhang X li, Bao Y ping, Zhang D, Zhang X yang, Kosten TR, Lu L (2009) Circadian Alteration in Neurobiology During 30 Days of Abstinence in Heroin Users. Biol Psychiatry 65:905–912.
Liang NC, Bello NT, Moran TH (2015) Wheel running reduces high-fat diet intake, preference and mu-opioid agonist stimulated intake. Behav Brain Res 284:1–10.
Lightfoot JT, Turner MJ, Daves M, Vordermark A, Kleeberger SR (2004) Genetic influence on daily wheel running activity level. Physiol Genomics 19:270–276.
Lucas RJ, Douglas RH, Foster RG (2001) Characterization of an ocular photopigment capable of driving pupillary constriction in mice. Nat Neurosci 4:621–626.

Lucas RJ, Hattar SS, Takao M, Berson DM, Foster RG, Yau K-W (2003) Diminished Pupillary Light Reflex at High Irradiances in Melanopsin-Knockout Mice. Science 299:245–247.
Lupi D, Oster H, Thompson S, Foster RG (2008) The acute light-induction of sleep is mediated by OPN4-based photoreception. Nat Neurosci 11:1068–1073.
Lydic R, Keifer JC, Baghdoyan HA, Becker BS (1993) Microdialysis of the Pontine Reticular Formation Revels Inhibition of Acetylcholine Release by Morphine. Anesthesiol J Am Soc Anesthesiol 79:1003–1012.
Lynch TJ, Siminoff R, Podolsky R, Adler MW (1985) Morphine-induced pupillary fluctuations in the rat: correlations with EEG and respiratory changes. J Ocul Pharmacol 1:255–261.
Lynch TJ, Tiseo PJ, Adler MW (1990) Morphine-induced pupillary fluctuation: physiological evidence against selective action on the Edinger-Westphal nucleus. J OculPharmacol 6:165–174.
Manchikanti L, Helm II S, Fellow B, Janata JW, Pampati V, Grider JS, Boswell M V (2012) Opioid Epidemic in the United States. Pain Physician 15:ES9–ES38.
Mansour A, Hoversten MT, Taylor LP, Watson SJ, Akil H (1995) The cloned μ, δ and κ receptors and their endogenous ligands: Evidence for two opioid peptide recognition cores. Brain Res 700:89–98.
Marchant EG, Mistlberger RE (1995) Morphine phase-shifts circadian rhythms in mice: role of behavioural activation. Neuroreport 7:209–212.
Maynard ML, Zele AJ, Kwan AS, Feigl B (2017) Intrinsically photosensitive retinal ganglion cell function, sleep efficiency and depression in advanced age-related macular degeneration. Investig Ophthalmol Vis Sci 58:990–996.
McDonald J, Lambert DG (2016) Opioid mechanisms and opioid drugs. Anaesth Intensive Care Med 17:464–468.
McDougal DH, Gamlin PD (2010) The influence of intrinsically-photosensitive retinal ganglion cells on the spectral sensitivity and response dynamics of the human pupillary light reflex. Vision Res 50:72–87.
Medzihradsky F (1976) Stereospecific binding of etorphine in isolated neural cells and in retina determined by a sensitive microassay. Brain Res 108:212–219.
Meijer JH, Ruijs ACJ, Albus H, Van De Geest B, Duindam H, Zwinderman AH, Dahan A (2000) Fentanyl, a μ-opioid receptor agonist, phase shifts the hamster circadian pacemaker. Brain Res 868:135–140.
Meijer JH, Schwartz WJ (2003) In Search of the Pathways for Light-Induced Pacemaker Resetting in the Suprachiasmatic Nucleus. J Biol Rhythms 18:235–249.
Meunier J-C, Mollereau C, Toll L, Suaudeau C, Moisand C, Alvinerie P, Butour J-L, Guillemot J-C, Ferrara P, Monsarrat B, Mazarguil H, Vassart G, Parmentier M, Costentin J (1995) Isolation and structure of the endogenous agonist of opioid receptor-like ORL1 receptor. Nature 377:532–535.
Meyer-Franke A, Kaplan MR, Pfieger FW, Barres BA (1995) Characterization of the signaling interactions that promote the survival and growth of developing retinal ganglion cells in culture. Neuron 15:805–819.
Minami M, Satoh M (1995) Molecular biology of the opioid receptors: structures, functions and distributions. Neurosci Res 23:121–145.
Minamino N, Kangawa K, Chino N, Sakakibara S, Matsuo H (1981) Beta-neo-endorphin, a new hypothalamic "big" Leu-enkephalin of porcine origin: its purification and the complete amino acid sequence. Biochem Biophys Res Commun 99:864–870.

Minamino N, Kangawa K, Fukuda A, Matsuo H, Iagarashi M (1980) A new opioid octapeptide related to dynorphin from porcine hypothalamus. Biochem Biophys Res Commun 95:1475–1481.
Mistlberger RE, Holmes MM (1999) Morphine-induced activity attenuates phase shifts to light in C57BLr6J mice. Brain Res 829:113–119.
Mohan K, Harper MM, Kecova H, Ye E-A, Lazic T, Sakaguchi DS, Kardon RH, Grozdanic SD (2012) Characterization of structure and function of the mouse retina using pattern electroretinography, pupil light reflex, and optical coherence tomography. Vet Ophthalmol 15:94–104.
Mojumder DK, Qian Y, Wensel TG (2009) Two R7 Regulator of G-Protein Signaling Proteins Shape Retinal Bipolar Cell Signaling. J Neurosci 29:7753–7765.
Moore RY (1995) Neural control of the pineal gland. Behav Brain Res 73:125–130.
Moore RY, Eichler VB (1972) Loss of a circadian adrenal corticosterone rhythm following suprachiasmatic lesions in the rat. Brain Res 42:201–206.
Morgan IG, Boelen MK (1996) A retinal dark-light switch: a review of the evidence. Vis Neurosci 13:399–409.
Murphy NP, Lam HA, Maidment NT (2008) A comparison of morphine-induced locomotor activity and mesolimbic dopamine release in C57BL6, 129Sv and DBA2 mice. J Neurochem 79:626–635.
Murray RB, Adler MW, Korczyn AD (1983) The pupillary effects of opioids. Life Sci 33:495–509.
Murray RB, Loughnane MH (1981) Infrared video pupillometry: A method used to measure the pupillary effects of drugs in small laboratory animals in real time. J Neurosci Methods 3:365–375.
Naber D, Wirz-Justice A, Kafka MS (1981) Circadian rhythm in rat brain opiate receptor. Neurosci Lett 21:45–50.
Neice AE, Behrends M, Bokoch MP, Seligman KM, Conrad NM, Larson MD (2017) Prediction of Opioid Analgesic Efficacy by Measurement of Pupillary Unrest. Anesth Analg 124:915–921.
Nelson AM, Battersby AS, Baghdoyan HA, Lydic R (2009) Opioid-induced decreases in rat brain adenosine levels are reversed by inhibiting adenosine deaminase. Anesthesiology 111:1327–1333.
Nelson DE, Takahashi JS (1991) Sensitivity and integration in a visual pathway for circadian entrainment in the hamster (Mesocricetus auratus). J Physiol 439:115–145.
Nesti E, Everill B, Morielli AD (2004) Endocytosis as a Mechanism for Tyrosine Kinase-dependent Suppression of a Voltage-gated Potassium Channel. Mol Biol Cell 15:4073–4088.
Nestler EJ, Tallman JF, E.J. N (1988) Chronic morphine treatment increases cyclic AMP-dependent protein kinase activity in the rat locus coeruleus. Mol Pharmacol 33:127–132.
NHLBI (2018) Sleep Deprivation and Deficiency. Natl Hear Lung,and Blood Inst Available at: https://www.nhlbi.nih.gov/health-topics/sleep-deprivation-and-deficiency [Accessed October 16, 2018].
NIH: National Institute on Drug Abuse (NIDA) (2019) Opioids. Available at: https://www.drugabuse.gov/drugs-abuse/opioids [Accessed March 24, 2019].
Nisida I, Okada H (1959) The activity of the pupillo-constrictory centers. Jpn J Physiol 10:64–72.

Noseda R, Burnstein R (2011) Advances in understanding the mechanisms of migraine-type photophobia. Curr Opin Neurol 24:197–202.
Noseda R, Kainz V, Jakubowski M, Gooley JJ, Saper CB, Digre K, Burstein R (2010) A neural mechanism for exacerbation of headache by light. Nat Neurosci 11:239–246.
Novak CM, Burghardt PR, Levine JA (2012) The use of a running wheel to measure activity in rodents: Relationship to energy balance, general activity, and reward. Neurosci Biobehav Rev 36:1001–1014.
Ocaña M, Cendán CM, Cobos EJ, Entrena JM, Baeyens JM (2004) Potassium channels and pain: Present realities and future opportunities. Eur J Pharmacol 500:203–219.
Ohayon MM (2005) Relationship between chronic painful physical condition and insomnia. J Psychiatr Res 39:151–159.
Okuda–Ashitaka E, Ito S (2000) Nocistatin: a novel neuropeptide encoded by the gene for the nociceptin/orphanin FQ precursor. Peptides 21:1101–1109.
Onen SH, Alloui A, Eschalier A, Dubray C (2000) Vocalization thresholds related to noxious paw pressure are decreased by paradoxical sleep deprivation and increased after sleep recovery in rat. Neurosci Lett 291:25–28.
Onen SH, Alloui A, Gross A, Eschallier A, Dubray C (2001) The effects of total sleep deprivation, selective sleep interruption and sleep recovery on pain tolerance thresholds in healthy subjects. J Sleep Res 10:35–42.
Oyefeso A, Sedgwick P, Ghodse H (1997) Subjective sleep-wake parameters in treatment-seeking opiate addicts. Drug Alcohol Depend 48:9–16.
Pan HL, Wu ZZ, Zhou HY, Chen SR, Zhang HM, Li DP (2008) Modulation of pain transmission by G-protein-coupled receptors. Pharmacol Ther 117:141–161.
Panda S, Nayak SK, Campo B, Wlkaer JR, Hogenesch JB, Jegla T (2005) Illumination of the Melanopsin Signaling Pathway. Science 307:600–604.
Panda S, Provencio I, Tu DC, Pires SS, Rollag MD, Castrucci AM, Pletcher MT, Sato TK, Wiltshire T, Andahazy M, Kay SA, Van Gelder RN, Bogenesch JB (2003) Melanopsin Is Required for Non–Image-Forming Photic Responses in Blind Mice. Science 301:1488–1490.
Park JC, Moura AL, Raza AS, Rhee DW, Kardon RH, Hood DC (2011) Toward a clinical protocol for assessing rod, cone, and melanopsin contributions to the human pupil response. Investig Ophthalmol Vis Sci 52:6624–6635.
Pasternak GW ed. (2010) The Opiate Receptors, second. New York: Humana Press.
Peirson S, Foster RG (2006) Melanopsin: Another Way of Signaling Light. Neuron 49:331–339.
Peirson SN, Oster H, Jones SL, Leitges M, Hankins MW, Foster RG (2007) Microarray Analysis and Functional Genomics Identify Novel Components of Melanopsin Signaling. Curr Biol 17:1363–1372.
Peles E, Schreiber S, Adelson M (2006) Variables associated with perceived sleep disorders in methadone maintenance treatment (MMT) patients. 82:103–110.
Peles E, Schreiber S, Adelson M (2009) Documented poor sleep among methadone-maintained patients is associated with chronic pain and benzodiazepine abuse , but not with methadone dose. Eur Neuropsychopharmacol 19:581–588.
Peng P-H, Huang H-S, Lee Y-J, Chen Y-S, Ma M-C (2008) Novel role for the δ-opioid receptor in hypoxic preconditioning in rat retinas. J Neurochem 108:741–754.
Pennartz CMA, de Jeu MTG, Bos NPA, Schaap J, Geurtsen AMS (2002) Diurnal modulation of pacemaker potentials and calcium current in the mammalian circadian clock. Nature

416:286–290.
Pennock RL, Hentges ST (2011) Differential Expression and Sensitivity of Presynaptic and Postsynaptic Opioid Receptors Regulating Hypothalamic Proopiomelanocortin Neurons. J Neurosci 31:281–288.
Perez-Leighton CE, Schmidt TM, Abramowitz J, Birnbaumer L, Kofuji P (2011) Intrinsic phototransduction persists in melanopsin-expressing ganglion cells lacking diacylglycerol-sensitive TRPC subunits. Eur J Neurosci 33:856–867.
Perez-leon JA, Warren EJ, Allen CN, Robinson DW, Brown RL (2006) Synaptic inputs to retinal ganglion cells that set the circadian clock. 24:1117–1123.
Perreau-Lenz S, Kalsbeek A, Pévet P, Buijs RM (2004) Glutamatergic clock output stimulates melatonin synthesis at night. Eur J Neurosci 19:318–324.
Pert CB, Kuhar MJ, Snyder SH (1976) Opiate receptor: autoradiographic localization in rat brain. Proc Natl Acad Sci U S A 73:3729–3733.
Pickard GE, Sollars PJ, Schmidt TM, Chen SK, Hattar S (2011) Intrinsically photosensitive retinal ganglion cells: Many subtypes, diverse functions. Trends Neurosci 34:572–580.
Pickworth WB, Bunker E, Welch P, Cone E (1991) Intravenous buprenorphine reduces pupil size and the light reflex in humans. Life Sci 49:129–138.
Pickworth WB, Lee H, Fudala PJ (1990) Buprenorphine-induced pupillary effects in human volunteers. Life Sci 47:1269–1277.
Pickworth WB, Neidert GL, Kay DC (1981) Morphine like arousal by methadone during sleep. Clin Pharmacol Ther 30:796–804.
Pickworth WB, Sharpe LG (1979) Eeg-behavioral dissociation after morphine- and cyclazocine-like drugs in the dog: further evidence for two opiate receptors. Neuropharmacology 18:617–622.
Pickworth WB, Sharpe LG (1985) Morphine-induced mydriasis and inhibition of pupillary light reflex and fluctuations in the cat. J Pharmacol Exp Ther 234:603–606.
Pickworth WB, Welch P, Henningfield JE, Cone EJ (1989) Opiate-Induced Pupllary Effects in Humans. Methods Find Exp Clin Pharmacol 11:759–763.
Pivik RT, McCarley RW, Hobson JA (1977) Eye movement-associated discharge in brain stem neurons during desynchronized sleep. Brain Res 121:59–76.
Poon SJ, Greenwood-Ericksen MB (2014) The Opioid Prescription Epidemic and the Role of Emergency Medicine. Ann Emerg Med 64:490–495.
Proft J, Weiss N (2015) G protein regulation of neuronal calcium channels: back to the future. MolPharmacol 87:890–906.
Provencio I, Cooper HM, Foster RG (1998) Retinal projections in mice with inherited retinal degeneration: Implications for circadian photoentrainment. J Comp Neurol 395:417–439.
Provencio I, Rodriguez IR, Jiang G, Hayes WP, Moreira EF, Rollag MD (2000) A Novel Human Opsin in the Inner Retina. J Neurosci 20:600–605.
Purves D, Augustine G, FItzpatrick D eds. (2001) The Circadian Cycle of Sleep and Wakefulness. In: Neuroscience, 2nd edition, 2nd ed. Sunderland, MA: Sinauer Associates.
Qu C-L, Huo F-Q, Huang F-S, Tang J-S (2015) Activation of mu-opioid receptors in the ventrolateral orbital cortex inhibits the GABAergic miniature inhibitory postsynaptic currents in rats. Neurosci Lett 592:64–69.
Quattrochi LE, Stabio ME, Kim I, Ilardi MC, Michelle Fogerson P, Leyrer ML, Berson DM (2019) The M6 cell: A small-field bistratified photosensitive retinal ganglion cell. J Comp Neurol 527:297–311.

Rajaratnam SMW, Middleton B, Stone BM, Arendt J, Dijk D-J (2004) Melatonin advances the circadian timing of EEG sleep and directly facilitates sleep without altering its duration in extended sleep opportunities in humans. J Physiol 561:339–351.
Rappoport D, Morzaev D, Weiss S, Vieyra M, Nicholson JD, Leiba H, Goldenberg-Cohen N (2013) Effect of intravitreal injection of bevacizumab on optic nerve head leakage and retinal ganglion cell survival in a mouse model of optic nerve crush. Invest Ophthalmol Vis Sci 54:8160–8171.
Rasmussen NA, Farr LA (2003) Effects of morphine and time of day on pain and beta-endorphin. Biol Res Nurs 5:105–116.
Reinscheid RK, Nothacker HP, Bourson A, Ardati A, Henningsen RA, Bunzow JR, Grandy DK, Langen H, Monsma FJ, Civelli O (1995) Orphanin FQ: a neuropeptide that activates an opioidlike G protein-coupled receptor. Science 270:792–794.
Reiter RJ (2003) Melatonin: Clinical relevance. Best Pract Res Clin Endocrinol Metab 17:273–285.
Renna JM, Weng S, Berson DM (2011) Light acts through melanopsin to alter retinal waves and segregation of retinogeniculate afferents. Nat Neurosci 14:827–829.
Reppert SM, Weaver DR (2002) Coordination of circadian timing in mammals. 418:935–941.
Riazi-Esfahani M, Kiumehr S, Asadi-Amoli F, Dehpour AR (2009) Effects of intravitreal morphine administered at different time points after reperfusion in a rabbit model of ischemic retinopathy. Retina 29:262–268.
Ribelayga C, Wang Y, Mangel SC (2004) A circadian clock in the fish retina regulates dopamine release via activation of melatonin receptors. J Physiol 5542:467–482.
Robin M, Kirby A, Messner S, Geller EB, Adler MW (1985) Differentiating opioids by their pupillary effects in the rat. Life Sci 36:1669–1677.
Roecklein K, Wong P, Ernecoff N, Miller M, Donofry S, Kamarck M, Wood-Vasey WM, Franzen P (2013) The post illumination pupil response is reduced in seasonal affective disorder. Psychiatry Res 210.
Ruegsegger GN, Toedebusch RG, Will MJ, Booth FW (2015) Mu opioid receptor modulation in the nucleus accumbens lowers voluntary wheel running in rats bred for high running motivation. Neuropharmacology 97:171–181.
Rukmini A V, Milea D, Baskaran M, How AC, Perera SA, Aung T, Gooley JJ (2015) Pupillary Responses to High-Irradiance Blue Light Correlate with Glaucoma Severity. Ophthalmology 122:1777–1785.
Rupp A, Schmidt T, Chew K, Yungher B, Park K, Hattar S (2013) ipRGCs mediate ipsilateral pupil constriction. In: ARVO Annual Meeting 2013 -Investigative Ophthalmology & Visual Science, pp 310.
Rusin KI, Giovannucci DR, Stuenkel EL, Moises HC (1997) Kappa-opioid receptor activation modulates Ca2+ currents and secretion in isolated neuroendocrine nerve terminals. J Neurosci 17:6565–6574.
Sand A, Schmidt TM, Kofuji P (2012) Diverse types of ganglion cell photoreceptors in the mammalian retina. Prog Retin Eye Res 31:287–302.
Saper CB, Scammell TE, Lu J (2005) Hypothalamic regulation of sleep and circadian rhythms. Nature 437:1257–1263.
Saszik SM, Robson JG, Frishman LJ (2002) The Scotopic Threshold Response of the Dark-Adapted Electroretinogram of the Mouse. J Physiol 543:899–916.
Sawynok J (1998) Adenosine receptor activation and nociception. Eur J Pharmacol 347:1–11.

Schmidt TM, Alam NM, Chen S, Kofuji P, Li W, Prusky GT, Hattar S (2014a) A Role for Melanopsin in Alpha Retinal Ganglion Cells and Contrast Detection. Neuron 82:781–788.
Schmidt TM, Kofuji P (2009) Functional and Morphological Differences among Intrinsically Photosensitive Retinal Ganglion Cells. J Neurosci 29:476–482.
Schmidt TM, Kofuji P (2010) Differential Cone Pathway Influence on Intrinsically Photosensitive Retinal Ganglion Cell Subtypes. J Neurosci 30:16262–16271.
Schmidt TM, Kofuji P (2011) Structure and function of bistratified intrinsically photosensitive retinal ganglion cells in the mouse. J Comp Neurol 519:1492–1504.
Schmidt TM, Rupp AC, Yungher B, Cui Y, Wess J, Park K, Hattar S (2014b) A retinal projection to the iris mediates pupil constriction. In: ARVO Annual Meeting 2014 - Investigative Ophthalmology & Visual Science, pp 1231. C.V. Mosby Co.
Schmidt TM, Taniguchi K, Kofuji P (2008) Intrinsic and Extrinsic Light Responses in Melanopsin-Expressing Ganglion Cells During Mouse Development. J Neurophysiol 100:371–384.
Selley DE, Cao CC, Sexton T, Schwegel JA, Martin TJ, Childers SR (2001) μ Opioid receptor-mediated G-protein activation by heroin metabolites: Evidence for greater efficacy of 6-monoacetylmorphine compared with morphine. Biochem Pharmacol 62:447–455.
Semo M, Gias C, Ahmado A, Vugler A (2014) A role for the ciliary marginal zone in the melanopsin-dependent intrinsic pupillary light reflex. Exp Eye Res 119:8–18.
Sernagor E, Eglen SJ, Wong ROL (2001) Development of Retinal Ganglion Cell Structure and Function. 20.
Sexton TJ, Golczak M, Palczewski K, Van Gelder RN (2012) Melanopsin is highly resistant to light and chemical bleaching in vivo. J Biol Chem 287:20888–20897.
Shamotienko OG, Parcej DN, Dolly JO (1997) Channel Kv1 Subtypes in Synaptic Membranes from Bovine Brain. Biochemistry 36:8195–8201.
Sharpe LG (1991) Separate neural mechanisms mediate sufentanil-induced pupillary responses in the cat. J Pharmacol Exp Ther 256:845–849.
Sharpe LG, Pickworth WB (1981) Pharmacologic evidence for a tonic muscarinic inhibitory input to the Edinger-Westphal nucleus in the dog. Exp Neurol 71:176–190.
Sharpe LG, Pickworth WB (1985) Opposite Pupillary Size Effects in the Cat and Dog After Microinjections of Morphine, Normorphine and Clonidine in the Edinger-Westphal Nucleus. Brain Res Bull 15:329–333.
Shaw IR, Lavigne G, Mayer P, Choinière M (2005) Acute intravenous administration of morphine perturbs sleep architecture in healthy pain-free young adults: a preliminary study. Sleep 28:677–682.
Shi G, Nakahira K, Hammond S, Rhodes KJ, Schechter LE, Trimmer JS (1996) Beta Subunits promote K+ channel surface expression through effects early in biosynthesis. Neuron 16:843–852.
Simantov R, Kuhar MJ, Uhl GR, Snyder SH (1977) Opioid peptide enkephalin: immunohistochemical mapping in rat central nervous system. Proc Natl Acad Sci U S A 74:2167–2171.
Slaughter MM, Mattler JA, Gottlieb DI (1985) Opiate binding sites in the chick, rabbit and goldfish retina. Brain Res 339:39–47.
Smart SL, Lopantsev V, Zhang CL, Robbins CA, Wang H, Chiu SY, Schwartzkroin PA, Messing A, Tempel BL (1998) Deletion of the K(v)1.1 Potassium channel causes epilepsy in mice. Neuron 20:809–819.

Sodhi P, Hartwick ATE (2014) Adenosine modulates light responses of rat retinal ganglion cell photoreceptors througha cAMP-mediated pathway. J Physiol 592:4201–4220.
Sodhi P, Hartwick ATE (2016) Muscarinic acetylcholine receptor-mediated stimulation of retinal ganglion cell photoreceptors. Neuropharmacology 108:305–315.
Solessio E, Vigh J, Cuenca N, Rapp K, Lasater EM (2002) Membrane properties of an unusual intrinsically oscillating, wide-field teleost retinal amacrine cell. J Physiol 544:831–847.
Sollars PJ, Pickard GE (2015) The Neurobiology of Circadian Rhythms. Psychiatr Clin North Am 38:645–665.
Sollars PJ, Smeraski CA, Kaufman JD, Ogilvie MD, Provencio I, Pickard GE (2003) Melanopsin and non-melanopsin expressing retinal ganglion cells innervate the hypothalamic suprachiasmatic nucleus. Vis Neurosci 20:601–610.
Stabio ME, Sabbah S, Quattrochi LE, Ilardi MC, Fogerson PM, Leyrer ML, Kim MT, Kim I, Schiel M, Renna JM, Briggman KL, Berson DM (2018) The M5 Cell: A Color-Opponent Intrinsically Photosensitive Retinal Ganglion Cell. Neuron 97:150-163.e4.
Stein MD, Herman DS, Bishop S, Lassor JA, Weinstock M, Anthony J, Anderson BJ (2004) Sleep disturbances among methadone maintained patients. J Subst Abuse Treat 26:175–180.
Stephan FK, Zucker I (1972) Circadian rhythms in drinking behavior and locomotor activity of rats are eliminated by hypothalamic lesions. Proc Natl Acad Sci U S A 69:1583–1586.
Stirling L, Williams MR, Morielli AD (2009) Dual Roles for RHOA/RHO-Kinase In the Regulated Trafficking of a Voltage-sensitive Potassium Channel. Mol Biol Cell 20:2991–3002.
Substance Abuse and Mental Health Services Administration (2017) Key substance use and mental health indicators in the United States: Results from the 2016 National Survey on Drug Use and Health (HHS Publication No. SMA 17-5044, NSDUH Series H-52). Rockville, MD.
Suh B-C, Inoue T, Meyer T, Hille B (2006) Rapid chemically induced changes of PtdIns(4,5)P2 gate KCNQ ion channels. Science 314:1454–1457.
Takahashi JS, Decoursey PJ, Bauman L, Menaker M (1984) Spectral sensitivity of a novel photoreceptive system mediating entrainment of mammalian circadian rhythms. Nature 308:186–188.
Talbot MJ, Sayer RJ (1996) Intracellular QX-314 inhibits calcium currents in hippocampal CA1 pyramidal neurons. J Neurophysiol 76:2120–2124.
Tooker RE, Lipin MY, Leuranguer V, Rozsa E, Bramley JR, Harding JL, Reynolds MM, Vigh J (2013) Nitric oxide mediates activity-dependent plasticity of retinal bipolar cell output via S-nitrosylation. J Neurosci 33:19176–19193.
Torrecilla M, Marker CL, Cintora SC, Stoffel M, Williams JT, Wickman K (2002) G-protein-gated potassium channels containing Kir3.2 and Kir3.3 subunits mediate the acute inhibitory effects of opioids on locus ceruleus neurons. J Neurosci 22:4328–4334.
Torrecilla M, Quillinan N, Williams JT, Wickman K (2008) Pre- and postsynaptic regulation of locus coeruleus neurons after chronic morphine treatment: A study of GIRK-knockout mice. Eur J Neurosci 28:618–624.
Tortella FC, Cowan A, Adler MW (1980) Pupillary effects of leucine and methionine enkephalin in rats after intraperitoneal administration. Peptides 1:237–241.
Tsai JW, Hannibal J, Hagiwara G, Colas D, Ruppert E, Ruby NF, Heller HC, Franken P, Bourgin P (2009) Melanopsin as a Sleep Modulator: Circadian Gating of the Direct Effects of Light on Sleep and Altered Sleep Homeostasis in Opn4−/− Mice Foster RG, ed. PLoS Biol

7:e1000125.
Tu DC, Owens LA, Anderson L, Golczak M, Doyle SE, McCall M, Menaker M, Palczewski K, Van Gelder RN (2006) Inner retinal photoreception independent of the visual retinoid cycle. Proc Natl Acad Sci 103:10426–10431.
Uebele VN, England SK, Chaudhary A, Tamkun MM, Snyders D (1996) Functional Differences in Kv1.5 Currents Expressed in Mammalian Cell Lines Are Due to the Presence of Endogenous Kvbeta2.1 Subunits. J Biol Chem 271:2406–2412.
Ueda H, Inoue M, Takeshima H, Iwasawa Y (2000) Enhanced Spinal Nociceptin Receptor Expression Develops Morphine Tolerance and Dependence. J Neurosci 20:7640–7647.
Van Hook MJ, Berson DM (2010) Hyperpolarization-activated current (Ih) in ganglion-cell photoreceptors. PLoS One 5.
Van Hook MJ, Wong KY, Berson DM (2012) Dopaminergic modulation of ganglion-cell photoreceptors in rat. Eur J Neurosci 35:507–518.
Vaněček J, Pavlík A, Illnerová H (1987) Hypothalamic melatonin receptor sites revealed by autoradiography. Brain Res 435:359–362.
Vansteensel MJ, Magnone MC, van Oosterhout F, Baeriswyl S, Albrecht U, Albus H, Dahan A, Meijer JH (2005) The opioid fentanyl affects light input, electrical activity and Per gene expression in the hamster suprachiasmatic nuclei. Eur J Neurosci 21:2958–2966.
Verster JC, Veldhuijzen DS, Volkerts ER (2006) Effects of an opioid (oxycodone/paracetamol) and an NSAID (bromfenac) on driving ability, memory functioning, psychomotor performance, pupil size, and mood. Clin J Pain 22:499–504.
Vuong HE, Hardi CN, Barnes S, Brecha NC (2015) Parallel Inhibition of Dopamine Amacrine Cells and Intrinsically Photosensitive Retinal Ganglion Cells in a Non-Image-Forming Visual Circuit of the Mouse Retina. J Neurosci 35:15955–15970.
Wamsley JK, Palacios JM, Kuhar MJ (1981) Autoradiographic localization of opioid receptors in the mammalian retina. Neurosci Lett 27:19–24.
Wang H, Kunkel DD, Martin TM, Schwartzkroin PA, Tempel BL (1993) Heteromultimeric K+ channels in terminal and juxtaparanodal regions of neurons. Nature 365:75–79.
Wang J-S, Kefalov VJ (2011) The Cone-specific visual cycle. Prog Retin Eye Res 30:115–128.
Wang Q, Wing W, Yue S, Jiang Z, Mikoshiba K, Offermanns S, Yau Correspondence K-W, Xue T, Kang SH, Bergles DE, Yau K-W (2017) Synergistic Signaling by Light and Acetylcholine in Mouse Iris Sphincter Muscle. Curr Biol 27:1791-1799.e5.
Warman VL, Dijk DJ, Warman GR, Arendt J, Skene DJ (2003) Phase advancing human circadian rhythms with short wavelength light. Neurosci Lett 342:37–40.
Warren EJ, Allen CN, Brown RL, Robinson DW (2006) The light-activated signaling pathway in SCN-projecting rat retinal ganglion cells. Eur J Neurosci 23:2477–2487.
Wässle H (2004) Parallel processing in the mammalian retina. Nat Rev Neurosci 5:1–11.
Watts VJ (2002) Molecular mechanisms for heterologous sensitization of adenylate cyclase. J Pharmacol Exp Ther 302:1–7.
Welch SP, Dunlow LD (1993) Antinociceptive activity of intrathecally administered potassium channel openers and opioid agonists: a common mechanism of action? JPharmacolExpTher 267:390–399.
Wesche DL, Frederickson RCA (1979) Diurnal differences in opioid peptide levels correlated with nociceptive sensitivity. Life Sci 24:1861–1867.
Williams JT, Christie MJ, Manzoni O (2001) Cellular and synaptic adaptations mediating opioid dependence. Physiol Rev 81:299–343.

Williams JT, Ingram SL, Henderson G, Chavkin C, von Zastrow M, Schulz S, Koch T, Evans CJ, Christie MJ (2013) Regulation of μ-Opioid Receptors: Desensitization, Phosphorylation, Internalization, and Tolerance. Pharmacol Rev 65:223–254.
Williams MR, Fuchs JR, Green JT, Morielli AD (2012) Cellular Mechanisms and Behavioral Consequences of Kv1.2 Regulation in the Rat Cerebellum. J Neurosci 32:9228–9237.
Williams MR, Markey JC, Doczi MA, Morielli AD (2007) An essential role for cortactin in the modulation of the potassium channel Kv1.2. PNAS 104:17412–17417.
Witkovsky P (2004) Dopamine and retinal function. Doc Ophthalmol 108:17–40.
Wong KY, Dunn FA, Graham DM, Berson DM (2007) Synaptic influences on rat ganglion-cell photoreceptors. J Physiol 582:279–296.
Wyman J, Bultman S (2004) Postmortem distribution of heroin metabolites in femoral blood, liver, cerebrospinal fluid, and vitreous humor. J Anal Toxicol 28:260–263.
Xue T, Do MTH, Riccio A, Jiang Z, Hsieh J, Wang HC, Merbs SL, Welsbie DS, Yoshioka T, Weissgerber P, Stolz S, Flockerzi V, Freichel M, Simon MI, Clapham DE, Yau KW (2011) Melanopsin signalling in mammalian iris and retina. Nature 479:67–72.
Yatani A, Codina J, Brown A, Birnbaumer L (1987) Direct activation of mammalian atrial muscarinic potassium channels by GTP regulatory protein Gk. Science 235:207–211.
Yeh CY, Koehl KL, Harman CD, Iwabe S, Guzman JM, Petersen-Jones SM, Kardon RH, Komáromy AM (2017) Assessment of rod, cone, and intrinsically photosensitive retinal ganglion cell contributions to the canine chromatic pupillary response. Investig Ophthalmol Vis Sci 58:65–78.
Yoshikawa K, Williams C, Sabol SL (1984) Rat brain preproenkephalin mRNA. cDNA cloning, primary structure, and distribution in the central nervous system. J Biol Chem.
Young MJ, Lund RD (1994) The anatomical substrates subserving the pupillary light reflex in rats: Origin of the consensual pupillary response. Neuroscience 62:481–496.
Young WS, Uhl GR, Kuhar MJ (1978) Iontophoresis of neurotensin in the area of the locus coeruleus. Brain Res.
Zacny JP, Goldman RE (2004) Characterizing the subjective, psychomotor, and physiological effects of oral propoxyphene in non-drug-abusing volunteers. Drug Alcohol Depend 73:133–140.
Zamponi GW, Snutch TP (1998) Modulation of voltage-dependent calcium channels by G proteins. Curr Opin Neurobiol 8:351–356.
Zele AJ, Feigl B, Smith SS, Markwell EL (2011) The circadian response of intrinsically photosensitive retinal ganglion cells Dryer S, ed. PLoS One 6:e17860.